UNIVERSITY OF
BIRMINGHAM

Pyrococcus furiosus α-amylase as a Candidate Sterilisation Time-Temperature Integrator

by

IAN BROWN

A thesis submitted to
The University of Birmingham
for the degree of
DOCTOR OF PHILOSOPHY

Department of Chemical Engineering
School of Engineering
The University of Birmingham
October 2009

Abstract

Thermal treatment is the most common method used by industry to ensure food is safe for consumption and to increase storage life. To ensure safety, food is often over processed, which can significantly affect its nutritional value as well as taste and flavour attributes. In this study a candidate sterilisation time-temperature integrator (TTI) from the hyperthermophilic *Pyrococcus furiosus* α-amylase is investigated.

Reliability and accuracy of the TTIs was determined by exposure to various isothermal and non-isothermal industrially relevant temperature profiles. The integrated temperature history obtained by the TTIs correlated generally well with the data obtained from thermocouples installed, although the error increased with hold time of heat treatment. The work showed that the TTIs can be used reliably over a range (3-25 minutes at 121°C) which is relevant for conditions of thermal sterilisation. This was measured by developing a new assay technique for assaying the activity of hyperthermophilic α-amylase within the food industry. The assay was calibrated against more laboratory relevant assays and computational models.

The kinetics and mechanism of thermal denaturation of *Pyrococcus furiosus* α-amylase was determined through FT-IR, DSC and CD techniques. It was found that through thermal denaturation after the melting temperature (T_m), the enzyme unfolded by first order kinetics from a α-helical structure, through β-sheet structure to aggregation of the enzyme.

Acknowledgments

I would like to express my gratitude to my supervisors, Prof. Peter Fryer and Dr Philip Cox, for their invaluable guidance and advice throughout my project. I would like to thank them for their patience and kindness which helped me achieve this work. A thank you goes to Dr Serafim Bakalis for his help and advice. Also for his help with the computer programming and modelling within this work.

I would also like to thank Gary Tucker for his industrial knowledge and help and use of the equipment at Campden BRI. James Chong (University of York) for his guidance in growing extremophilic organisms. Prof. Robert Kelly and Inci Ozdemi (North Carolina State University) for supplying the amylopullanase used.

I would like to thank Hazel Jennings, Elaine Mitchell, David Adams and Christine Fletcher and the people in my laboratory for their support.

I am grateful to Benjamin Le Reverend and Karin Mehauden for their time, help, support and discussions in relation to my project.

I would like to make a special thank you to my family for their patience and support while I completed this work.

Table of Contents

List of Figures

List of Tables

Nomenclature

$A_{initial}$ / A_{final}	Ratio of the enzyme activities before and after heat treatment
a_w	Water activity
c	Amylase concentration (mg/ml)
C_p	Heat capacity ($Jkg^{-1}K^{-1}$)
d	Depth of RED plate
D	Diffusion rate (m^2s^{-1})
Dn	Dilution rate (ls^{-1})
D_T	Decimal Reduction Time (min)
Ea	Activation Energy ($Jmol^{-1}$)
F	Sterilisation value (min)
G	Gibbs Free Energy ($Jmol^{-1}$)
H	Enthalpy (J)
I	Inactive form of protein
k	Rate constant (s^{-1})
N	Natured form of protein
$N_{initial}$ and N_{final}	Initial and final number of micro organism
P	Pasteurisation value (min)
r	Halo radius (mm)
R	Well radius (mm)
R^2	Coefficient of determination
S	Entropy ($Jkg^{-1}K^{-1}$)
t	Duration of the heat treatment (min)
T_m	Melting temperature (°C)
T_{opt}	Optimal activity/growth temperature
$T(t)$	Product temperature (°C)
T_{ref}	Reference temperature (°C)
U	Reversible form of protein
z	z value (number of degrees Celsius to bring about a ten-fold change in Decimal reduction time) (°C)

Greek symbols

μ	Dynamic viscosity (Pa.s)
μ_m	Maximum growth rate
ρ	Density (kgm^{-3}).
μ_{app}	Apparent viscosity (Pa s)
$\dot{\gamma}$	Shear rate (s^{-1})
μ_0 and μ_∞	Viscosities at shear rate ($\dot{\gamma}$) = 0 and $\dot{\gamma} = \infty$ respectively

Abbreviations

3-D	Three dimensional

ASW	Artificial Sea Water
BAA	*Bacillus amyloliquefaciens* α-amylase
BLA	*Bacillus licheniformis* α-amylase
CCFRA	Campden and Chorleywood Food Research Association
CD	Circular Dichroism
CSTR	Continuous StirredTank Reactor
DCW	Dry Cell Weight
DNS	Dinitrosalicilic acid
DSC	Differential Scanning Calorimetry
EDTA	ethylenediaminetetraacetic acid
FDP	Freeze-Dried Protein
FT-IR	Fourier Transform Infrared Spectroscopy
HACCP	Hazard Analysis Critical Control Point
HPLC	High Performance Liquid Chromatography
HT	High Tension
PCR	Polymerase Chain Reaction
PFA	*Pyrococcys furiosus* -amylase
RED	Radial Enzymatic Diffusion
SDS-PAGE	Sodiumdodecylsulphate polyacrylamide gel electropheresis
SEM	Scanning Electron Microscopy
SSE	Sum of Squares
TEM	Transmission Scanning Microscopy
TTI	Time Temperature Integrators

Chapter 1

Introduction

Sterilisation and preservation procedures have been known from ancient times. It is likely that pre-historic and early man discovered preserving foods by drying the meat, fish and fruits they hunted and gathered. Foods that had been exposed to salt solutions as well as high sugar solutions (such as honey) were also discovered to putrefy at a slower rate than foods that were not treated (Hugo, 1995). These early preservation methods are now known to work by reducing the water activity of the product to a low level. Bacterial growth at low ambient temperatures was well known to be slowed by placing foods in environments where the ambient environmental temperatures were low and the stability of perishable foods in cold conditions would have been recognised. For example ice houses to chill food were dug deep into the ground and constructed with ice transported from the mountains which could then be used to chill the food.

Direct chemical methods have also been used to preserve food; e.g. smoking of meats. In about 450 BC the Persians knew that water stored in earthenware containers became foul (Hugo, 1995) but if it was placed in copper or silver containers then the water remained ‘sweet’ for longer. However the beginnings of true sterilisation techniques came when Aristotle recommended the ancient Greek army boil their drinking water before they consume it. In 1809 the French government offered a prize for a method of preserving food for long sea voyages for the navy. The application of heat as a preservative was at the forefront of the entries. Nicholas Appert’s

method of sealing vegetables and fruit in glass jars and then heating them by boiling the jars in water won the prize. 50 years later, Pasteur found that, with the spoilage of wine, micro-organisms other than yeast were present in the sour wine and deduced they were responsible for the spoilage, and he recommended that new wine be heated at 55°C in the absence of air (Hugo, 1995).

Pasteur and Appert both gave their names to the two types of heating process which are commonly applied to destroy micro-organisms in food: pasteurisation and appertisation. The main difference between pasteurisation and appertisation (sterilisation) is the temperature for thermal treatment. Pasteurisation uses temperatures applied at 60-80°C for the elimination of key pathogens (*Salmonella*) and spoilage organisms. Appertisation is used to eliminate micro-organisms to achieve 'commercial sterility' by applying temperatures of greater than 100°C.

Observations involving the use of heat by Tyndall (1897) found that while vegetative micro-organisms were destroyed by boiling, the spores produced by some species were resistant. If these spores were allowed to germinate, micro-organisms would be killed by a repeat of the heating process. Successive thermal treatments over 3-5 days were commonplace for sterilisation before the invention of the autoclave. The autoclave allowed higher temperatures and pressures for sterilisation and could remove the spores of micro-organisms in a single step.

According to the temperature of the thermal treatment, the effect on the destruction of the micro organism will be different. Table 1-1 shows the impact of the various temperatures on the food product.

Table 1-1Common heat processes applied to foods (Moss, 2000)

Heat process	Temperature	Objective
Cooking Baking Boiling Frying Grilling	≤ 100°C	Improvement of digestibility Improvement of flavour Destruction of pathogenic micro-organisms
Blanching	<100°C	Expulsion of oxygen from tissues Inactivation of enzymes
Drying/Concentration	<100°C	Removal of water to enhance keeping quality
Pasteurisation	60-80°C	Elimination of key pathogens and spoilage organisms
Appertisation, Sterilisation	>100°C	Elimination of micro-organisms to achieve 'commercial sterility'

Manufacturers are legally responsible for the food they produce and so have to supply safe food for the consumer. As such, thermal treatment of food is the normal practice within industry to eliminate micro-organisms and spores from the product (DoH, 1994; FDA, 2005).

Thermal treatments are generally directly applied to foods, so as to cook and thermally treat the product at the same time in order to preserve it. This stage needs accurate monitoring as too little thermal processing makes the food unsafe to the consumer, whereas if the thermal processing is too high the product may be safe at the expense of food quality with a possible decrease in flavour and consumer acceptance. An option for monitoring and assessing the time-temperature history of an applied thermal process, which has been used in this study, is the use of enzymatic time-temperature integrators (TTIs). Enzymatic TTIs are based on the quantification of activity of an enzyme before and after thermal processing, providing evidence for the thermal processing they have received expressed in terms of *D* and *z* values. These are properly defined in Chapter 5.

For use in sterilisation TTIs, i.e. for validating processes in the range 110-140°C, a highly thermostable enzyme is needed, showing measurable residual activity at 121°C, so the TTI could assess the relative time-temperature history of a sterilisation process. The work reported here concerns an enzyme (*Pyrococcus furiosus* α-amylase referred to as PFA: PF0478) extracted from cultures of a native strain of *Pyrococcus furiosus*.

In general (especially in the UK) the food industry regards any 'genetically modified' products as undesirable and they are not used due to the conservative nature of the customer and thus of the industry. This restricts the creation of a TTI by the obvious route of overproduction of thermostable enzymes in *Escherichia coli* and yeasts.

Here the accuracy of PFA TTIs has been assessed using isothermal and non-isothermal heating profiles, with the results compared to values measured using more traditional methods of time-temperature history profiles i.e. thermocouples and data-loggers. The time-temperature profiles were also altered by changing the specific heat capacities of the food-stuff measured. The PFA TTIs have been applied to pilot scale canning retorts with real foods and the results have then been compared to the responses of fixed thermocouple time-temperature profiles.

Enzymatic TTIs work on the basis of denaturation of the enzyme due to heat, and show lower residual activity after sterilisation compared to the enzyme in its non-thermal processed state. For its effective use as a TTI, the mechanism of denaturation of *Pyrococcus furiosus* α-amylase should be known, and this has been examined in a thermal processing context. The effects of a range of temperatures (20-130°C) on the stability and folding characteristics of the α-amylase were studied, and related to how heat affects the activity of the enzyme.

The overall aim of the study was to identify engineering conditions where sterilisation TTIs can be used in confidence within an industrial, commercial setting.

1.1 Aims and objectives

The aims and objectives of this investigation can be summarised as

- Cultivation of *Pyrococcus furiosus* and extraction of α-amylase for use within sterilisation TTIs (Chapter 3).

- The development and use of a quick and reliable assay, which is industrially applicable, for the highly thermostable α-amylases (Chapter 4).

- Determining the accuracy of TTIs over a range of sterilisation time-temperature profiles, and the evaluation of TTIs within the sterilisation based canning industry as compared to traditional monitoring techniques for thermal processing (Chapter 5).

- Assess the mechanisms of unfolding of *Pyrococcus furiosus* α-amylase, investigating the stages of denaturation, and the kinetics of each step (Chapter 6).

1.2 Thesis plan

Beyond this chapter, chapter 2 gives a review of the published literature in the field and provides an overview of thermal treatment methods. These methods of food preservation and the theory behind sterilisation include descriptions of traditional monitoring techniques. The use of TTIs within the food industry and their applicability for pasteurisation treatments are also reviewed.

The second part of the chapter then focuses on thermostable enzymes, their sources and their possible inclusion as a thermally liable substance inside a candidate TTI.

Chapter 3 details the cultivation and purification techniques for batch and continuous fermentation of *Pyrococcus furiosus* for α-amylase for the maximum yield of α-amylase.

Chapter 4 details the development of a new industry-relevant method for analysing highly thermostable α-amylases. This assay uses radial diffusion behaviour of the enzyme as an indicator of activity; a process which can be implemented at factory floor level. The assay has been modelled and then calibrated against more accurate laboratory assays.

Chapter 5 then details the validation work performed on TTIs to investigate their accuracy and reliability for evaluating thermal treatments. Their reliability is assessed in terms of the likely ranges of operation for sterilisation processes and a process engineering context through isothermal and non-isothermal processing. The study will include results from pilot scale canning trials with the sterilisation TTIs.

Finally in chapter 6 the mechanisms for the denaturing of *Pyrococcus furiosus* α-amylase were examined using FT-IR, CD and DSC analysis. This indicated the fate of the enzyme when thermally processed, and hence may be used to improve its use as a candidate sterilisation time-temperature integrator

The main findings and recommendations for future work are summarised in chapter 7.

Chapter 2

Literature review

In the food industry, preservation of foods is commonly achieved by thermal processing i.e. pasteurisation and sterilisation. These processes would seem easy to evaluate, but industrial canning is done on a massive scale and rate, with food sterilised in large sterilisation vessels known as retorts. In retort processing, the food to be sterilised is first filled and hermetically sealed in rigid or flexible enclosures, such as metal cans, glass jars, or retortable pouches. The retort is then filled with containers stacked either randomly or in trays. Once the retorts are full of containers, the retort doors are closed tightly and the air is replaced by steam under pressure to achieve temperatures above the atmospheric boiling point of water. The common retort temperature for sterilising canned foods is 121^{o}C, at one atmosphere of internal over pressure. After the containers have been exposed to the sterilising temperature for sufficient time to achieve the desired level of sterilization, the steam is shut off and cooling water is introduced to cool the containers and controllably reduce the pressure, thus ending the process. This is known as a batch retort operation which can become very labour-intensive for large scale production.

Modern food canning plants that produce large volumes of canned foods operate with great efficiency by using continuous retort systems. In continuous rotary retort systems, filled and sealed containers travel in single file along automated conveying tracks into a series of

continuous retorts operating at different temperatures. They enter through a rotating pressure-seal valve to maintain the steam pressure inside the retort while introducing container after container from the outside atmosphere at speeds approaching 500 units per minute. Once inside the continuous retort, the containers travel slowly along a rotating helical path until they exit the opposite end of the retort through a similar rotating pressure-seal valve directly from the high pressure steam retort into a cooling retort which is filled with cooling water instead of hot steam to accomplish the cool-down portion of the process.

Within these processes it is very hard to evaluate the temperature profile inside the retort and whether each can has received the minimum safe cook. Moreover if excessive thermal processing is given in batch retorts to ensure the central cans are safe from harmful contaminants, the cans towards the edge of the retort may suffer quality degradation in nutrients or colour loss (Adams and Moss, 2000). Too little thermal processing is disastrous for the food industry; it is likely that the outside cans will still be safe from micro-organisms but the central, inside cans will not have received enough thermal processing to ensure sterility. This must be avoided, to ensure that consumers are not endangered. Such limits of undercook, cook and overcook are complicated by the can contents which can be solid, liquid, or a mixture of particulates in liquor, with all forms showing different heating profiles (Tucker *et al*., 2007).

The following section will detail the current state of work on determination of heat treatment efficiency and the applications of extremophiles, and the apparent relevance for use within sterilisation TTIs of *Pyrococcus furiosus* α-amylase.

2.1 Methods of food safety and preservation

2.1.1 Existing techniques

Micro-organism growth in food can make it unfit for consumption. *Listeria monocytogenes* (milk, vegetables and poultry), *Staphylococcus aureus* (meat, poultry and eggs) and *Clostridium botulinum* (any non-low acidic foods) are three pathogenic micro-organisms which can all become a public heath concern when in foods (Frazier and Westhoff, 1978). *Clostridium botulinum* especially can be a problem in canning as it grows in anaerobic conditions and has highly heat resistant spores. Enzyme production due to micro-organism growth may not be pathogenic for the consumer but does cause unwanted changes in the foodstuff attributes by degrading lipids, proteins and low molecular weight organosulphur compounds (Adams and Moss, 2000).

Micro-organisms can grow rapidly in most foodstuffs as there is sufficient moisture, suitable pH and temperature levels and the food is also high in nutrients. Elimination of one or a combination of these elements without causing excess degradation to the product is the basis for food preservation techniques, and reduction of the ability of micro-organisms to grow. Eliminating pathogenic micro-organisms which could be present remains the preserve of thermal treatments.

2.1.1.1 Non Thermal Treatments

Biological fermentation. One of the oldest methods of food preservation is to increase the population of desirable micro-organisms which causes competitive inhibition and disappearance of micro-organisms which are non-desirable (Goff, 1999). This can be seen within brewing

where the desirable micro-organism is brewers yeast (*Saccharomyces cerevisiae*), and which provides storable water by producing alcohol as a by-product. Within minced meat *Lactobacillus sake* Lb706 can be used (Schillinger *et al*., 1991) as competitive inhibition of harmful organisms forming products. Other biological fermentation treatments include *Lactobacillus* and *Aspergillus oryzae* which are used to make foods such as sauerkraut and miso.

Chemical preservation. As mentioned in chapter 1, chemicals such as salt and high sugar concentrations (jams and preservatives) reduce the water activity (Hugo, 1995). Acid such as vinegar, in the case of pickling, decrease the pH, limiting the growth of the micro-organism (Goff, 1999). Smoking is also a common method of preserving foods, especially meats. Smoking reduces water activity and impregnates the tissue with chemical preservatives such as formaldehyde and phenols which inhibit bacterial growth.

Low temperature storage. Low temperature methods of preservation are commonplace in the home; these include refrigeration and freezing. At low temperatures micro-organism growth is not eradicated, only retarded. The lower the storage temperature is from the optimal growth temperature of the organism the greater the retardation of growth. For example Griffiths *et al*. (1987) studied storage of raw milk with an initial preservation temperature of 2°C rather than 6°C and saw preservation greatly increased.

Active packaging. Also known as ‘smart packaging’, active packaging uses the container of the food stuff to control and prolong the shelf life of the product. Active packaging interacts with the product or the headspace between the package and food, to obtain a desired outcome (Labuza and Breene, 1989; Rooney, 1995). Packaging may be termed ‘active’ when it performs some role

in food preservation other than providing an inert barrier to external conditions (Hutton, 2003). Packaging may take the form of oxygen scavengers, carbon dioxide scavengers and emitters, moisture control agents, or anti-microbial agents (Kerry *et al*., 2006). In recent studies compounds that are active against Gram-negative bacteria (nisin or lysozyme) have been combined with chelating agents (EDTA) to target *E.coli* (Padgett *et al*., 2000) and *Salmonella typhimurium* (Natrajan and Sheldon, 2000).

Irradiation. Appertisation can be achieved by using electromagnetic radiation where X-rays, β-rays, or γ-radiation are used. Irradiation damages the microbial DNA and causes potentially lethal DNA lesions to the bacteria. Within foods Fuld *et al*. (1957) demonstrated irradiation sterilisation of *E.coli*, *B.subtilis* and *B.thermoacidurans* in milk, pea puree and tomato juice. Sterilisation by irradiation is an effective method; but applications in the food industry are limited due to public concerns (Hendrickx *et al*., 1998).

Pulsed electric field. In this process short duration (1-100μs) high electric field pulses (10-50kV cm^{-1}) are applied to food between two electrodes. The structure of the membrane of the micro organism is generally damaged during the exposure at high voltage field. This technique can only be applied to liquid foods such as orange juice and liquid eggs (Manas and Pagan, 2005; Stewart, 2004; Devlieghere *et al*., 2004; De Haan *et al*., 2002; Lado and Yousef, 2002). The effectiveness of pulsed electric fields on enzyme inactivation has been considered debatable (Hendrickx *et al*., 1995).

High pressure. Damage to the micro-organism cell membrane and protein denaturation is caused by high pressure processing, in which pressures of 100-1000 MPa are applied to the food. High

pressure processing can cause minimal effects on sensory qualities (Arroyo *et al*., 1999) while a number of studies including ones on orange juice (Bull *et al*., 2005) found a significant increase in shelf-life of the product.

2.1.1.2 Heat treatment techniques

Despite the emergence of promising 'non-thermal' technologies (§2.1.1.1), thermal processes remain by far the most used techniques to preserve food-stuffs between the moment of production and the moment of consumption (Guiavarc'h *et al*., 2004). Heat treatment techniques are commonly used by food manufactures applying high temperatures to foods to reduce the number of micro-organisms and spores present (Fryer *et al*., 1997).

Pasteurisation applies heat to destroy all or most of those organisms in a vegetative state which would produce illnesses, or produce spoilage in certain foods (Gaze, 2006). Pasteurisation commonly involves heating the food to temperatures between 70°C and 90°C for 3 to 30 minutes. This does not sterilise the material; pasteurisation only reduces the number of micro-organisms. It is considered a mild treatment and the food product must be kept refrigerated to retard the re-growth of any surviving micro-organism or spores. It also inactivates most of the enzymes which, as shown in Table 2-1, cause degradation of the food product upon storage.

Sterilisation processes such as canning are still widespread; for example, H.J. Heinz Company Limited sells 300 million cans of soup per year in the UK (www.heinzsoup.co.uk). Sterilisation is a high temperature treatment using temperatures in the range 115-125°C to destroy pathogenic micro-organisms and their spores (Lopez, 1987). As such the sterilised products can be stored at ambient conditions for years. A heat resistant pathogen that might survive the thermal processing

of low-acid foods (pH > 4.5) enabling growth in anaerobic packaged and canned foods is the anaerobic spore-forming micro-organism *Clostridium botulinum* (Valentas *et al*., 1997). Sterilisation treatments are based on the probable destruction of *C.botulinum*, and the elimination of this micro-organism and its spores is the industry's standard reference to ensure safety in the products (Tucker *et al*., 2006). Thus a commercialised food sterilisation process must reduce the probability of a single *C.botulinum* spore surviving in a low-acid product to one in 10^{12}. This is called a '*botulinum* cook', and the standard process to achieve this level of spore reduction is equivalent to holding the food at a minimum of 3 minutes at 121.1°C (DoH, 1994; FDA, 2005).

Table 2-1 Enzyme activity and quality of foods (Adams and Moss, 2000)

Quality attribute changed	Enzyme	Reaction catalysed	Perceived quality change
Flavour	Lipase / phospholipase	Lipid hydrolysis	Soapy/rancid (dairy products)
	Sulphydryl oxidase	Thiol oxidation	Elimination of cooked flavours (milk)
Colouring	Polyphenol oxidase	Phenol oxidation	Browning (fruit, vegetables)
	Lipoxygenase	Pigment co-oxidation	Decolourisation (bread, vegetables)
Texture	Amylase	Starch hydrolysis	Viscosity reduction
	Protease	Protein hydrolysis	Softening (meat, cheese)

2.1.2 Quantification of thermal processes

Quantification of the impact of any thermal process on the relative safety and quality attributes of food products is indispensible in design, evaluation, control and optimisation and in obtaining a safe food with maximal quality retention (Guiavarc'h *et al.*, 2004). The kinetics of thermal death of the micro-organisms is the basis for all rational design of sterilisation equipment. There are two methods commonly used for this quantification of thermal processing:

- *In situ* method
- Physical-mathematical approach

The *in situ* method is widely applied and uses judgement of nutritional quality of the food after sterilization such as taste, colour, texture etc to measure the amount of thermal processing. The advantage of the *in situ* method is that the impact of the thermal process on the parameters of interest can be directly and accurately known (Van Loey *et al.*, 1996b). The disadvantages of the *in situ* method as expressed by Hendrickx *et al.*, (1995) is that it is time consuming and hence expensive.

The physical mathematical approach (Bigelow, 1921; Esty and Meyer, 1922; Lund, 1975; Ball and Olsen, 1957) uses a combination of knowledge of the temperature history imposed on the food combined with knowledge of the kinetic parameters of the safety or quality attributes to calculate the impact of treatment. This can either be constructed theoretically or empirically from knowledge of characteristics of the food physical heating (Van Loey *et al.*, 1996a; Holdsworth, 1985). The downside to this method is that it is often impossible to obtain, by direct recording /

heat transfer simulations, the necessary time-temperature data of the product during the process, such as cold spots, which will invariably happen due to incomplete mixing of the material (Hendrickx *et al*., 1995).

The classical thermo-bacteriological/ thermal death time (TDT) approach was deduced by Bigelow (1921) and Ball and Olsen (1957). Assuming a first order process, at a constant temperature *T*, the death of the micro-organism is given by:

$$\frac{N_{final}}{N_{initial}} = 10^{\frac{-t}{D}} \qquad (2.1)$$

where $N_{initial}$ and N_{final} are the initial and final numbers of micro-organisms, t is the heat treatment duration, and *D* is the decimal reduction time, i.e. the time needed to reduce the number of micro-organisms by 1 log cycle (90%) at temperature, *T*. This is shown in Figure 2-1; the *D* value varies with organism and also with temperature (Valentas *et al*., 1997).

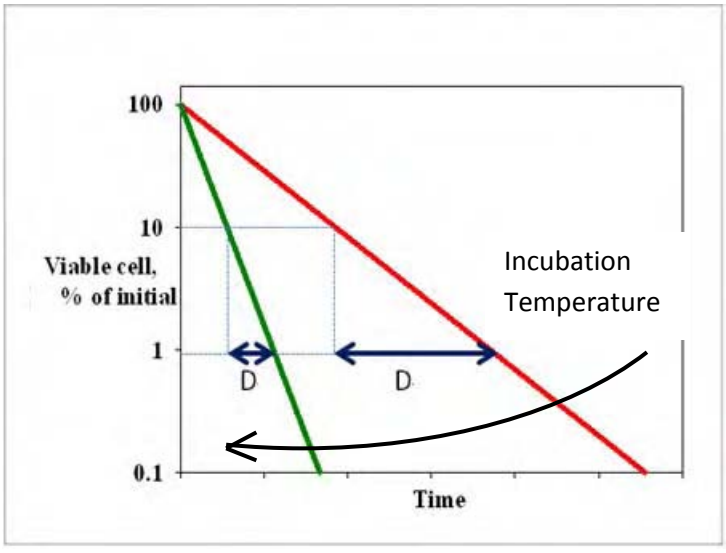

Figure 2-1 The survivor curve showing the decimal reduction time, and the effect of increasing temperature

Thermal processes can be compared even though the temperature of thermal processing may be different, the time for a given process can be expressed as a parameter of *D*. Thus, rearranging equation (2.1) ensures that it can be compared with the *in situ* method by using the equation:

$$P \text{ or } F = D_{(ref)} \cdot log\left(\frac{N_{initial}}{N_{final}}\right) \qquad (2.2)$$

where *F* or *P* are the process values, expressed as time (commonly written as *F* for sterilisation and *P* for pasteurisation) and with the units of time. In order to calculate the process value, the organism should follow the thermal death time model (Bigelow, 1921; Guiavarc'h *et al.*, 2005). The *F* or *P* value can also be calculated from the time-temperature history of the product upon which the heat treatment is applied. The product time-temperature history of a particular thermal process can be translated into an equivalent time at a chosen reference temperature i.e. the time that the material would have to be held at the reference temperature to generate the same effect as the process (Ball and Olson, 1957; Hendrickx *et al.*, 1995; Holdsworth, 1985). This allows the comparison between different thermal processes using the physical-mathematical approach. Thus for sterilisation:

$$F = \int_0^t 10^{\frac{T(t)-T_{ref}}{z}} \cdot dt \qquad (2.3)$$

where *T(t)* is the product temperature (°C), T_{ref} is the reference temperature at which the *D* value (°C) is calculated, t is the process time (min) while *z* is the temperature change needed to bring about a 1 log cycle (90%) change in decimal reduction time (Figure 2-2). The z value represents the temperature sensitivity of the system; the whole approach is a local linearization of the Arrhenius expression

for decimal kinetics, but works because of the relatively small temperature differences found in food processing.

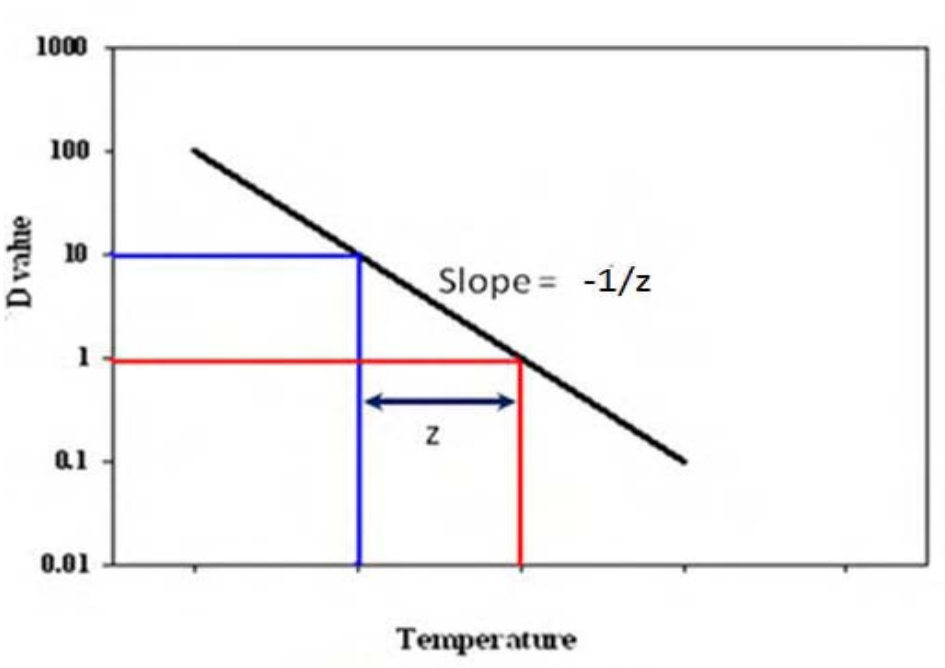

Figure 2-2 The thermal resistance curve showing the method for calculation of thermal sensitivity

The *z* value is important as it represents the temperature sensitivity of the system and for a TTI should be ideally the same or very close to the targeted micro-organism (Hendrickx *et al*., 1995; Richardson, 2001). *Clostridium botulinum* the target micro-organism in the canning industry has a *z* value of approximately 10°C (Hendrickx *et al*., 1995; Richardson, 2001), meaning there is a 90% increase in the rate of destruction of *C.botulinum* spores every 10°C increase in temperature. This also depends on the food stuff, and so it has also been variably measured as 8.3°C in puree peas (Stumbo *et al*., 1950) and 9.8°C in vegetables (Perkin *et al*., 1975).

The *F* value is a measure of the thermal processing received by the food at a reference temperature, which allows different thermal processes to be compared against each other. To obtain the *F* value in an industrial context, thermocouples and data-loggers are commonly used, which then supply temperature history data into the physical-mathematical method of Ball and Olson (1957) (Equation 2.3) to integrate the time-temperature history. Validation is straight forward and data analysis is relatively fast so that the calculation of *F* can take place whilst the process is acquiring. However thermocouples and data-loggers are not always convenient for every thermal process. It is generally not possible to use thermocouples in rotating retorts as they are impractical, or when the product is semi-convective (solid particulates in a liquid) i.e. the fluid in the can is able to move. Also Hendrickx *et al*, (1995) and Weng *et al*, (1991) found thermocouples impractical for agitated vessels where surface scraped heat exchangers were used because the thermocouple would become damaged. In continuous sterilisation processes, where the liquid is processed before packaging, it is often impossible to infer the correct time-temperature history of the bulk fluid as thermocouples are static devices in a complex flowing fluid. In addition the size (may take up most of the content space) and density (sink to the bottom of the can) of data-loggers is an issue (Hendrickx *et al*., 1995; Marra and Romano, 2003), interfering with the movement of the fluid and it may be either impossible to put them at the coldest point of a container or they maybe placed inadvertently in a local ‘hot’ or ‘cold spot’ (Hendrickx *et al*., 1995; Marra and Romano, 2003).

Therefore there needs to be an alternative to the approach of thermocouples, data-loggers and the *in situ* method, for a more comprehensive analysis of the thermal destruction of micro-organisms

within heat preservation. One technique, the use of time-temperature integrators, will be explored in this study.

2.2 Time-Temperature Integrators

TTIs can be defined as small, inexpensive, wireless sensors, placed in the product before heating and recovered from the product after heating, that shows a precisely, easily and correctly, measurable and irreversible change that allows the quantification of that target attribute undergoing the same variable temperature exposure, without the need for information on the actual time-temperature history in the product during the heating process (Decordt *et al.*, 1994; Taoukis and Labuza, 1989b; Taoukis and Labuza, 1989a; Weng *et al.*, 1991; Fu and Labuza, 1995; Guiavarc'h *et al.*, 2004). The kinetics of a TTI should be describable by an equation analogous to that of the target organism, i.e

$$F_{TTI} = D_{ref} \cdot \log\left(\frac{A_{initial}}{A_{final}}\right) \qquad (2.4)$$

where F_{TTI} is the process value derived from the TTI (min), D_{ref} is the decimal reduction time at a reference temperature, T_{ref} (min), $A_{initial}$ is the initial level of the target attribute, A_{final} is the level of the attribute after thermal processing. It should be noted that for this equation to be correct, and the use of a decimal reduction time be acceptable, the rate of loss of activity both of the TTI and the corresponding target should follow a first-order reaction. For further discussion see chapter 6.

By definition all TTI's are *post factum* indicators of the impact of the thermal process (Van Loey *et al.*, 1996a) because the calculations are based on the change in the TTI after thermal treatment compared to their initial status and are thus *in situ* measurement devices.

The criteria set by Van Loey *et al.*, (1996a) are that TTIs should be:

- Inexpensive, quickly and easily prepared, easy to recover, accurate and a have user friendly readout.

- Can be incorporated into food without disturbing heat transfer and therefore experience the same time-temperature profile as the food and not change it, whilst as mentioned previously this is not done by thermocouples and data-loggers.

- Have an equivalent temperature sensitivity of the rate constants (z values) of the TTIs and the target attributes i.e. ca. 10°C for the target of *C.botulinum*.

Thus TTIs can quantify the integrated temperature impact on the target attribute without the need to know the actual temperature history of the system; this is the TTIs major advantage over the *in situ* and physical mathematical methods.

TTIs can be made neutrally buoyant using materials with the same thermal conductivity as the food. They do not interfere with the fluid motion in the product. Analysis can be fast and relatively simple (Guiavarc'h *et al*., 2005); Van Loey *et al*., 1996b).

2.2.1 Types of TTI

TTIs are generalised and classified in terms shown in Figure 2-3, using the approach of Hendrickx *et al.*, (1993) in terms of working principle, response, origin, application and location. The factors shown in Figure 2-3 are discussed in this section.

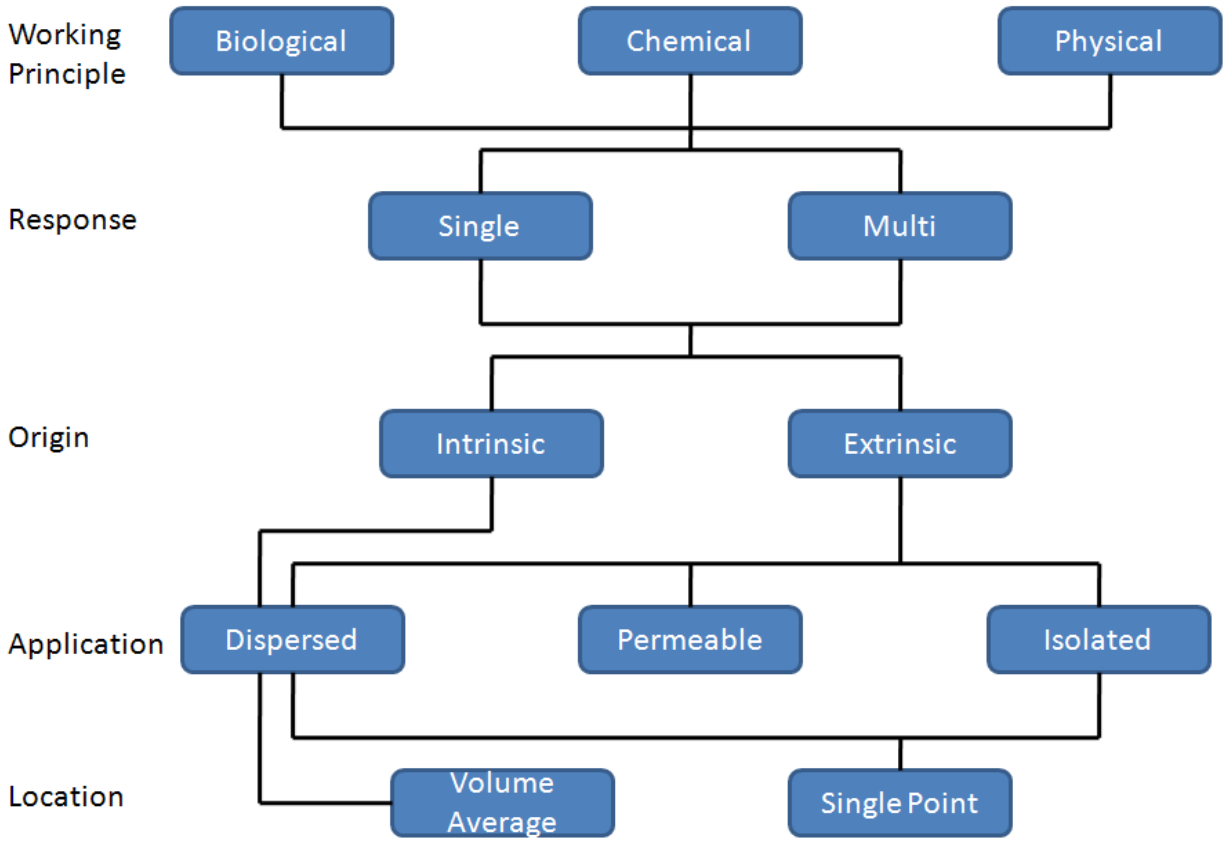

Figure 2-3 General classification of TTIs examining the factors of suitability for a thermal process (Hendrickx *et al.*, 1993)

Intrinsic TTIs are naturally present in food and the efficiency can be evaluated and quantified before and after thermal processing. Intrinsic TTIs are homogeneously dispersed in the food; for example Claeys *et al*, (2002) used the proteins naturally occurring in milk as the TTI to study the heat treatment the milk has received.

Extrinsic TTIs are artificial to the food and are added before the thermal process (Claeys *et al*., 2002). As shown in Figure 2-3 extrinsic TTIs can be sub-divided further into 3 groups (Hendrickx et al., 1995; Van Loey *et al*., 1996a).

- *Dispersed TTIs* are added and mixed into the food directly, and have direct contact with the food. This gives an accurate time-temperature profile but it is difficult to recover a known concentration to measure after processing.

- *Permeable TTIs* are located in separate units with a permeable barrier to allow exchange of heat between food and the TTIs.

- *Isolated TTIs* are located in separate units with non-permeable barriers and so do not allow exchange with food materials. Isolated TTIs have a slightly different time-temperature profile to the food, because of the need to conduct heat into the TTI, but are easily recovered and uniform in concentration and used in this study.

Chemical TTIs detect a change in concentration of a chemical extrinsically added to the food. These are analytically accurate and fast, but cannot be used for food safety monitoring due to the possibility of contamination into the food (Adams and Langley, 1998). Their use is rare and specialised as most micro organisms, vegetative cells and spores have a *z* value ranging from 5˚C to 12˚C while the *z* value for the destruction of thermal labile chemical substances start from 25˚C to 30˚C (Adams and Langley, 1998). The destruction of nutrients is less temperature sensitive than the destruction of micro organisms.

Physical TTIs generally use a diffusion method of a coloured compound in a paper wick. Physical TTIs have limited applications (Hendrickx *et al*., 1995) as the system is activated by steam so no other heating system can be used. Physical TTIs are however easy to calibrate, fast to analyse and easy to recover from the product.

Biological TTIs are by far the most widely used and researched area in TTI development. These TTIs are advantageous but the targeted attribute must be sensitive to heat in the same temperature range as the process i.e. a measurable output can be identified after the process. Biological TTIs can be divided, not only by their response to the time-temperature profile, but by whether they use whole micro-organisms or just the biological components e.g. enzymes they produce to predict this impact, so the biological TTIs can be divided to microbiological TTIs and enzymatic TTIs. These can be either intrinsic or extrinsic.

Microbiological TTIs such as spore beads are the most popular type of TTI within industry and have two types of response. The impact of the process can either be quantified by (i) the number of micro-organisms that survive the process or (ii) showing if there is growth or no growth of the organism depending on the organism and / or the temperature of treatment. For example TTIs containing *Bacillus stearothermophilus* spores have been used in pasteurisation processes (Hendrickx *et al*., 1995). The disadvantage of microbiological TTIs is the length of the assay, of hours or days, as long incubation times between the process and readouts do not allow for rapid intervention. There is also inherent variability of organisms (Hendrickx *et al*., 1995; Van Loey *et al*., 1996a) which affects the linearity of response, which is non-desirable.

Enzyme TTIs form the majority of those used in practice, and are reviewed in detail below.

2.2.2 Enzymatic TTIs

Enzymatic TTIs are used by quantifying the activity of a thermally labile enzyme that retains some activity after heat treatment. The residual activity can be related to the amount of thermal processing. The advantage of using TTIs with enzymes which are thermostable has been described by Van Loey *et al*, (1997) in that they are small, cheap and easy to prepare, can be used at relatively high temperatures, heat inactivation kinetics can be manipulated to the desired values while the response properties of activation and enthalpy can be measured accurately and rapidly (Haentjens *et al.*, 1998). The isothermal inactivation of the enzymes must however follow known order kinetics to calibrate the TTIs *F* value with processing time (Welt *et al*., 2003). Since capsules containing the TTI enzyme are commonly very small, such as the 10mm length of 3mm tubing used by Mehauden *et al*., (2006), TTIs can be difficult to retrieve after processing. A typical enzymatic TTI used by Mehauden *et al*., (2006) can be seen in Figure 2-4. Another limitation of TTIs is the need to know accurately the *D* and *z* values in order to process the data. Preliminary experiments are needed before it is possible to use them and each batch of enzyme has to be calibrated because there can be significant batch-to-batch variation (Maesmans *et al*., 2005; Van Loey *et al*., 1996a; b).

Figure 2-4 Capsule enzymatic TTIs (10mm length, 3mm tubing)

A *z* value of 10°C is the minimal process requirement for low acid foods which is the *z* value for *Clostridium botulinum* spore destruction so the enzyme used should have a *z* value close to 10°C to be used as a food safety tool e.g. amylases (Van Loey et al., 1996).

Studies on candidate enzymatic TTIs have been undertaken using various enzymes. Tomato and cucumber pectinmethylesterase (Guiavarc'h *et al*., 2003), peroxidase (Hendrickx *et al*., 1992), and carrot and potato peroxidase, polygalacturonase and lipoxygenase (Anthon and Barrett, 2002) have all had the kinetic parameters of thermal inactivation studied and were not applicable for pasteurisation or sterilisation TTIs because the *z* values did not match those of *Clostridium botulinum*. The effects of not matching the TTI *z* value with the target organism *z* value can be seen in chapter 5.

A novel TTI based on an amperometric glucose oxidase biosensor (Reyes De Corcuers *et al*., 2005) was used for the fast assessment for the effects of pasteurisation on *Salmonella* and *Listeria monocytogenes*. The glucose oxidase enzyme was trapped within a poly-o-phenylenediamine film coating the interior wall of the can. The TTI could be rapidly analysed by

an amperometer to measure the thickness of the film, although this has not been developed for higher pasteurisation or sterilisation temperatures where the target organism is *Clostridium botulinum*.

Most studies into TTIs have been focused on the use of α-amylase from *Bacillus spp*., which has a *z* value close to that of *Clostridium botulinum* and its denaturation follows first order kinetics (Van Loey et al., 1996; Tucker *et al*., 2002). Several studies have been undertaken in which amylases from different micro-organisms have been used (Guiavarc'h *et al*., 2004a and b; Haentjens *et al*., 1998; Van Loey *et al*., 1996). Guiavarc'h *et al*. (2003) showed that the D_{ref} and *z* could be changed by immobilising the enzyme, or changing the enzyme environment (pH, [NaCl], etc.).

Pasteurisation Enzymatic TTIs have been developed successfully using α-amylase from *Bacillus spp.* (Decordt *et al.*, 1992; Maesmans *et al.*, 1994; Van Loey *et al.*, 1996a; b; Mehauden *et al*., 2006). This previous work and that of Van Loey *et al.* (1997) and Mehauden *et al*. (2006; 2007) show that amylases can display kinetic parameters that make them applicable for estimating microbial thermal death treatment. TTIs were used to quantify effective thermal processing in comparing ohmic columns and a tubular heat exchanger for the pasteurisation of fruit as thermocouples could not be used (Tucker *et al.*, 2002) (Table 2-2). TTIs have also been used to measure pasteurisation on mushroom quiches (Tucker *et al*., 2005a) to analyse the thermal kill of *Salmonella* and *Listeria monocytogens*. Tucker *et al*. (2005a) made pasteurisation TTIs from a *Bacillus amyloliquefaciens* α-amylase. By using multiple TTIs in a single pack, TTIs could distinguish and find the cold spots in the centre of quiches. Pasteurisation TTIs were shown to

work well in comparison to thermocouple data (Mehauden *et al*., 2006; 2007) and are now not just a novel technique for measurement of process parameters, but a reliable process tool.

Sterilisation Enzymatic TTIs have mainly been seen as a progression of pasteurisation TTIs. Several studies have been published on sterilisation TTIs made from the α-amylase from *Bacillus subtilis* and *Bacillus licheniformis* which have been at the forefront of pasteurisation enzymatic TTIs (De Cordt *et al*., 1994; Van Loey *et al*., 1997; Guiavarc'h *et al.*, 2003). This α-amylase was used at reduced water content and was immobilised on glass beads. Under isothermal conditions, these TTIs were thermally stable at temperatures ranging from 100 to 132°C. TTIs (*z* value of 9.4°C) that were equilibrated at a_w = 4.8 could monitor process values at 121.1°C in the range of 0-30 min under non isothermal conditions. Although difficult to measure the results nevertheless showed that this TTI can be used to determine the heat treatment efficiency of sterilisation processes (De Cordt *et al*., 1994; Van Loey *et al*., 1997; Guiavarc'h *et al.*, 2003). The method used a Differential Scanning Calorimeter (DSC) to measure the change in enthalpy resulting from processing of dried amylases. Using this approach canned ravioli was processed with TTIs (Guiavarc'h *et al*., 2005) (Table 2-2). The *z* values of both enzymes were seen to be significantly higher to that which was measured previously (13.9°C and 16.4°C respectively). The study showed that measuring the temperature in the sauce overestimated the effect of the process by 30%. This overestimation is a problem for the safety of the food as it has not received as much thermal processing as it is believed.

The drawback to this technique for sterilisation TTIs is the complicated preparation and the need for technical skills to analyse the TTIs. Tucker and Wolf (2003) found issues in sealing the DSC pans from moisture ingress within industrial trials, and the high pan density prevents this method

from being used for liquid flowing systems This made the approach commercially impractical. Therefore a different method for sterilisation TTIs was required.

Investigations have been undertaken on the reliability of pasteurisation TTIs under non isothermal conditions (Taoukis and Labuza, 1989). Non isothermal experiments of two types were performed: the first experiment was performed using high temperature for a long time followed by storage at low temperature to investigate the 'history effect' and the second experiment was done by storage at controlled sinusoidally varying temperatures. The results of this research shows that there is a direct correlation between the TTIs' responses and the quality of the food under variable time temperature profiles. Guiavarc'h *et al.* (2002b) used TTIs to monitor thermal impact inside a solid/liquid model food and showed that incorrect conclusions could be drawn using *F* values for solid pieces obtained just by using temperatures recorded at the centre of the solid at the tip of a thermocouple. Nevertheless, these results show the potential of TTIs in the evaluation of the thermal process efficiency. Yet, currently published literature on their use is limited. In general, there is a lack of knowledge on their accuracy and efficiency. Errors in the measurement arise from a number of factors, including variability in the manufacture of the TTIs, errors in determining the final and initial value of activity, as well as non-linearities and variations in the kinetics of the enzyme (Mehauden *et al*., 2007). Some understanding of the inherent accuracy of the devices is needed in order to develop TTIs as effective process probes. TTIs have been used for various industrial applications as described in Table 2-2.

Table 2-2 Examples of applications for TTIs

	Study 1	Study 2	Study 3
Application	*P*-values for fruits processed in a tubular heat exchanger	*F* values for Raviolis inside cans processed in a spiral retort (Sterilmatic, Belgium)	*P* values in a stirred vessel (250l) – 200l batch of 5% Colflo 67 starch
Number of TTIs used	70	7 cans with 10 TTIs in each	50
Mean *P* value or *F* value	$P_{85°C}$~ 60 min	$F_{121.1°C}$~ 18.8 min	$P_{85°C}$~ 3.9 min
Variability	$P_{85°C}$ vary from 33 min to 109 min	$F_{121.1°C}$ vary from 10 min to 29.1 min	$P_{85°C}$ vary from 1.2 min to 11.3 min
Reference	Tucker *et al.*, 2002	Guiavarc'h *et al.*, 2005	Lambourne et Tucker, 2001

Previous work with amylases (Van Loey et al., 1997a; b) found their thermal stabilities (*z*) to be in the range 9 to 10°C, ideal for bacterial spore destruction. The next target was to find an amylase heat stable enough at sterilisation temperatures to work as an enzymatic time-temperature integrator.

Tucker *et al*, (2005b; 2007) determined that the hyperthermophile *Pyrococcus furiosus* (§ 2.3) produced thermostable α-amylase which was possibly suitable for use in sterilisation TTIs, as the enzyme had a decimal reduction time (*D*) high enough for residual amylase activity to be measured following a typical full commercial sterilisation process (24 minutes), but also a *z* value close to 10°C (9.9°C). Theoretically *F*=3 minutes is acceptable for food sterilisation processes (DoH, 1994; FDA, 2005), but in practice food industrially is thermally processed for *F*=24-30 minutes and sometimes more.

Tucker *et al.*, (2005b) used the same TTI casing as that of pasteurization TTI's to give a high physical robustness, where silicon tube capped with a silicon elastomeric compound was used to encapsulate the α-amylase solution. In this case the TTI was close to neutral density in water and

had heat transfer characteristics the same as water content in foods. It was capable of surviving sterilisation temperatures of 115-135°C and up to 4 bar with rapid pressure changes. The TTI casing is defined in chapter 4.

The hyperthermophile α-amylase sterilisation TTI seems to be a better alternative to using pasteurisation TTIs and making them more thermostable by changing their water content. Preparation and use of the sterilisation TTI might be similar to pasteurisation TTIs which now have a relatively long history of successful industrial use such as Mehauden *et al*. (2006). However, the previous trials by Tucker *et al*, (2005b; 2007) were limited due to the small amount of *Pyrococcus furiosus* α-amylase available and were able to establish that the method might be feasible.

2.3 Extremophilic organisms and enzymes for TTIs development

In §2.2.2 are reasons for use of hyperthermophilic enzymes for use in a sterilisation time-temperature integrator. This section will briefly outline the research on hyperthermophiles, hyperthermophilic enzymes, and culturing techniques, especially those associated with *Pyrococcus furiosus* and the product / extraction of its extracellular α-amylase.

2.3.1 Extremophiles and Extremozymes

Extremozymes are enzymes found in micro-organisms that, in comparison to the majority of species, are capable of surviving in extreme conditions. These micro-organisms are termed extremophiles. Extremophiles can be hyperthermophilic, where the growth environmental temperatures routinely exceed 70°C. Halophiles are micro-organisms which survive and grow in

conditions of high salt concentrations of up to 20% NaCl (Schiraldi and De Rosa, 2002), and alkophiles have adapted to grow in high alkalinity conditions, plus other microbes may grow in areas of high pressure and / or acidity or low a_w.

Studies of extremophiles have helped to redraw the evolutionary tree of life by Woese *et al.* (1990) and shown in Figure 2-5; because of their adaptation to extreme environments for primitive life and study for the last common ancestor.

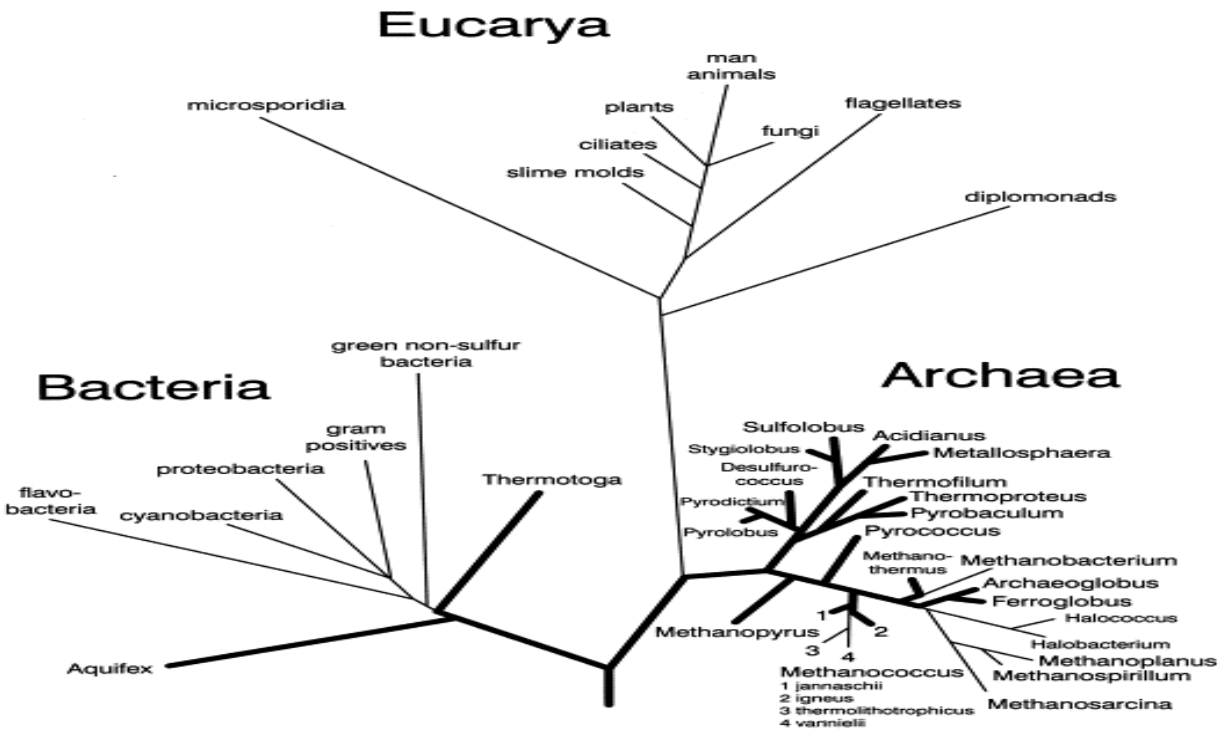

Figure 2-5 Evolutionary phylogenic tree (hyperthermophiles within the phylogenetic tree are in bold) (Woese *et al*., 1990)

Most extremophiles belong to the group known as Archaebacterium. For example, more than 70 species, 29 genera, 10 orders of hyperthermophiles have been discovered (Vieille and Zeikus, 2001), while only two, Thermotogales and Aquificales are true bacteria based hyperthermophiles.

Archaea morphologically resemble true bacteria in many ways (e.g. no nuclear envelope) but a large quantity of archaea genes appear to be unique, for example archaea (unlike bacteria), have no peptidloglycan in their cell walls, and archaea also have some unusual lipids in their cell membranes in comparison to bacteria (Madigan and Marrs, 1997).

As inferred by Figure 2-5, hyperthermophiles appear to be the most primitive organisms still existing but work on extremophiles is relatively new, with the first thermophilic extremophile being found approximately only 30 years ago in Yellowstone National Park, Wyoming. *Sulfolobus acidocaldarius* was found living at 85°C in a hot spring (Brock, 1978). Since then there has been limited work on the exploration of extremophiles due to the difficulty in cultivating them.

2.3.2 Hyperthermophiles and their Enzymes

Thermophilic and hyperthermophilic enzymes, as a result of the growth conditions of the micro-organism they come from, for example Solfataric fields which consist of solids, mud holes and surface waters heated by volcanic exhaustion to 90°C from magma chambers below, have to be intrinsically stable and active at high temperatures. Their advantages in industrial processes over mesophilic counterparts are discussed by Vieille and Zeikus, (2001) and Krahe *et al.*, (1996);

- Expressed in mesophilic hosts they are easier to purify by heat treatment (personal communications with Prof. R.Kelly (NCSU) on *P.furiosus* β-galactosidase expressed in *E.coli*) because the mesophilic host will be destroyed by the high temperatures leaving the unaffected thermophilic enzyme in one purification step.

- Thermostability is associated with a higher resistance to chemical denaturants and so can be used in more industrial processes, without being denatured chemically than their mesophilic counterparts

- Reactions at a higher temperature allows higher substrate concentrations due to higher solubility, lower viscosity, fewer risks of microbial contaminations and often higher reaction rates (Q_{10} rule).

Thermophilic enzymes have been used in the bioconversion of *n*-alkanes and wax degradation in the oil industry, and for hydrogen production from *Thermoanaerobacterium thermosaccharolyticum* fermentation (Liu *et al*., 2008). Novel thermophilic transaminase and dehalogenase enzymes from *Sulfolobus* spp. are used in applications for industrial biocatalysis. (Littlechild, 2002). Not many publications have been produced describing the applications of thermophilic and hyperthermophilic enzymes.

Typically above 110°C molecules such as amino acids and metabolites become highly unstable (ATP spontaneously hydrolyses in aqueous solution at temperatures above 140°C) and hydrophobic interactions weaken significantly so the upper level in which any life can be sustained is likely to be around 110°C (Jaenicke, 1998). Indeed a central question that remains amongst extremophilic biologists is how these organisms actually manage to grow.

The thermostability exhibited by these enzymes is maintained without any components unique to thermophiles (Vieille and Zeikus, 2001), suggesting that the increase in molecular stability is

accomplished through some stereochemical interactions which are not found in their mesophilic counterparts.

2.3.2.1 Ecological Basis of Hyperthermophilic Growth

Baross and Holden, (1996) found hyperthermophiles employ original strategies to enable protein stability, such as thermostable histone-like proteins, DNA super-coiling and tetra-ether membranes, for stabilizing nucleic acids and macromolecules within their environment. Through the Q_{10} rule, where the reaction rate doubles with each 10°C increase in temperature, one would expect that a hyperthermophilic enzyme would have a specific activity of 50-100 times higher than that of a mesophilic enzyme. Some observations, including those done by Zhao and Arnold (1999) showed that both hyperthermophilic and mesophilic enzymes have approximately the same reaction rates and efficiencies. This was believed to be due to the absence of selection pressure and so not being catalytically optimised (Vieille and Zeikus, 2001).

Due to the low concentration of organic matter in submarine environments, energy and a carbon source are obtained from complex mixtures of peptides obtained from decomposition of primary producers, while a few hyperthermophiles (including *P.furiosus*) are capable of exploiting avaliable polysaccharides (starch, pectin, glycogen etc.).

2.3.2.2 Hyperthermophilic Fermentation

Hyperthemophiles are primary producers and decomposers of organic matter in their communities. All hyperthermophilic primary producers are chemolithoautotrophs (Fischer *et al.*, 1983) i.e. they are sulphur oxidisers, reducers or methanogens and so do not use oxygen as a terminal electron acceptor. Chemolithoautotrophs are either facultative or obligate depending on

whether the organism is aerobic or anaerobic respectively. Facultative organisms oxidise the sulphur to produce sulphuric acid, whereas obligate (anaerobic) organisms reduce the sulphur to produce hydrogen sulphide. *Pyrococcus furiosus* reduces sulphur to produce hydrogen sulphide.

Thermophilic and hyperthermophilic fermentations have many advantages over mesophilic fermentations within industry. The advantages in the applications of hyperthermophiles are shown below (adapted from Sharp and Munster (1987)), i.e. in comparision to a fermentation at 37°C, one at 98°C has the advantage that;

1. Costs of cooling large scale thermophilic fermentations are reduced;
2. Reduced viscosity of media increases efficiency of mixing and harvesting rate;
3. Increases in solubility of reactants allows higher concentrations of less soluble components to be used;
4. Volatile and inhibitory products may be removed through a mild vacuum;
5. Reactor operation at elevated temperatures greatly reduces contamination by mesophilic micro-organisms;
6. Decreased solubility of oxygen aids cultivation of anaerobic organisms;
7. Thermophilic enzymes are more resistant to detergents or solvents;
8. Higher enzyme recoveries are possible due to enhanced protein stability;

Points 2 and 3 result from the increased mass transfer between the micro-organism and the fermentation broth.

The disadvantage of archaebacterial fermentations is however the typical low biomass yields associated with them (0.1 – 1g/l wet weight) compared to a typical eubacterial fermentation (> 30g/l wet weight) (Cowan, 1992).

One of the most studied hyperthermophilic archaebacterium is *Pyrococcus furiosus* which is studied here because of the reported heat stability of the organisms proteins.

2.4 *Pyrococcus furiosus*

P.furiosus was isolated by Fiala and Stetter (1986) in marine, shallow hydrothermal solfataric fields off Volcano Island, Italy, where the environmental conditions and hence the evolved optimal growth conditions are 100°C, pH 6 and 2% NaCl. Although Malik *et al.* (1989) found growth in the laboratory between pH 5-9 and 70-103°C with optimal conditions of pH 7 and 98-100°C. *P.furiosus* has a doubling time of 37 minutes (Fiala and Stetter, 1986).

P.furiosus is an obligate heterotrophic anaerobe which grows on peptides or carbohydrates with elemental sulphur (S^o) stimulating growth (Fiala and Stetter, 1986). With S° *P.furiosus* synthesises several new proteins that are different from those produced in sulphur free media (Kelly and Deming, 1988) indicating that there may be several membrane-associated proteins that are involved in the metabolism of S°, so there are inducible responses to the environment.

Hydrogen ions are seen to inhibit growth of *P.furiosus* (Fiala and Stetter, 1986; Rudiger *et al.*, 1992). Therefore S° added to the fermentation broths is then utilised to remove the inhibitory

hydrogen and produce hydrogen sulphide. Stripping / gassing has been used to remove rapidly the hydrogen with an inert gas (Krahe *et al.*, 1996). Complete oxidation was never observed, even in the presence of S^o, with acetate being the predominate end product (Schicho *et al.*, 1993) so there was always slight inhibition to growth by hydrogen.

Holst *et al.* (1997) stated that as the hydrogen sulphide is produced, which is reasonably soluble in water (especially at high temperatures), it will react with transition metals present that are freely available in natural or artificial seawater, forming insoluble sulphides. These sulphides will precipitate and are believed to inhibit growth of *P.furiosus* (Holst *et al.*, 1997). The inhibition is thought to be due to the toxicity of the metal sulphides and / or the reduced metal ion concentration in the media for cell growth. This forms a complex environment in which the *Pyrococcus furiosus* grows, and will be discussed in chapter 3. For all the reasons stated above, it has been noted by a number of workers that extremophiles are notoriously difficult to grow (Raven *et al.*, 1992; Scott, 2003; J. Chong, University of York personal communications).

2.4.1 Morphology of *Pyrococcus furiosus*

P.furiosus morphology was characterised by Fiala and Stetter (1986) and can be seen in Figure 2-6. The typical morphology is slight irregular cocci, 0.8-2.5 μm diameter which can often be found in pairs, the cocci are surrounded by an envelope 50 nm thick. Each coccus has about 50 monopolar polytrichous flagella, each of 7 nm width and 7 μm length (Figure 2-6).

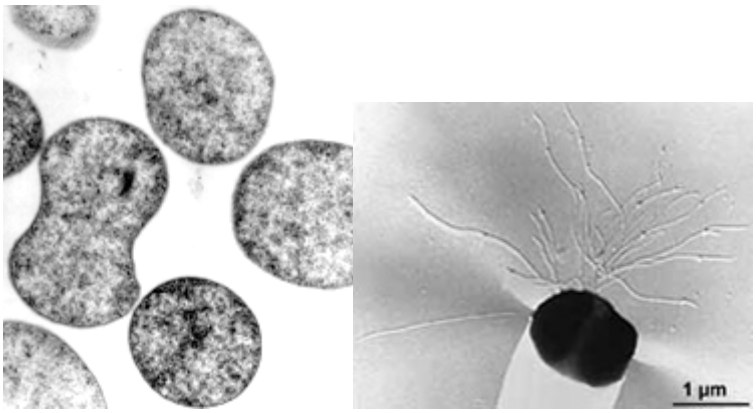

Figure 2-6 Morphology of *Pyrococcus furiosus* (commtechlab.msu.edu, 2005; microbeworld.org, 2005)

2.4.2 Cultivation of *Pyrococcus furiosus*

Techniques for growth of hyperthermophile micro-organisms range from glass serum and Wheaten bottles, to larger scale continuous fermentations (2-70 l operational volume) (Holst *et al.*, 1997) and dialysis membrane reactors (Markl *et al.*, 1990). Hyperthermophiles have even had genes of interest expressed in a mesophilic host such as *E.coli* (Adams and Kelly, 1998; Laderman *et al.*, 1993), *B.subtilis* and yeasts (Ito, 1997; Niehaus *et al.*, 1999; Lim *et al.*, 2001). However to obtain a sufficient amount of recombinant enzyme, *E.coli* is recommended (Schiraldi *et al.*, 2001; Schiraldi *et al.*, 2000) because this host is easily grown and the vectors are well characterised. This though can not be done for enzymatic TTIs in this project as the application of the work is in food processing and '*E.coli*' and 'gene expression' are terms that can not be readily associated with the UK food industry! This remains a central tenet throughout this work.

Some of the general challenges associated with the cultivation of extremophiles are that they are notoriously difficult to pre-culture and grow, plus only liquid media can usually be used with hyperthermophile organisms due to the high temperatures melting the solid media (Robb, 1995).

High temperatures may also cause the nutrients in the media to react, as Maillard reactions, with amino acids and sugars which can inhibit growth (Krahe *et al.*, 1996) reducing availability for growth as well as toxic products from reactions possibly being formed. Thus the majority of basic microbiological preparative steps either hae to be changed or not used at all.

2.4.2.1 Batch Cultivation of Pyrococcus furiosus

Batch cultivation is generally the preferred method for cultivation of *Pyrococcus furiosus*. *P.furiosus* was firstly, and is still, grown on a small batch scale either in serum bottles (Fiala and Stetter, 1986) or Wheaton bottles (Brown *et al.*, 1990) on complex medium. The advantages of using batch cultivation over continuous are first the ease at which the experiment can be run as all nutrients are in place at the start and then the organism can be allowed to grow until a limiting substrate has stopped growth and batch extraction is used. Another advantage to running batch cultivation, especially for an anaerobe such as *P.furiosus*, is that with continuous cultivation it is more difficult to maintain an anaerobic environment as fresh substrates have to be added continuously and an anaerobic barrier maintained. However, a problem with batch cultivation is in pre-culture and start up. If a large amount of *P.furiosus* was required then this would mean a large batch volume or lots of small batches with all the associated problems in start up and pre-culture associated with it. Examples of fermentations of *Pyrococcus furiosus* are summarised in Table 2-3.

In the case of Fiala and Stetter (1986), without elemental sulphur present, a cell density of up to $3x10^8$ cells/ml in Wheaton bottles was achieved. In the presence of sulphur Bonchosmolovskaya and Stetter (1991) found cell densities more than doubled to 7.8×10^8 cells ml^{-1}. This is comparable and even better than cell densities obtained in fermenters which are poorly gassed

and mixed gently with a magnetic stirrer (1 x 10^8 cells ml^{-1} (Schafer and Schonheit, 1992) and 2 x 10^8 cells ml^{-1} (Snowden *et al.*, 1992)). As previously stated in this section, the hydrogen sulphide being produced limits the hydrogen ions and thus growth of cells.

Table 2-3 Examples of fermentations of *Pyrococcus furiosus*

	Study 1	Study 2	Study 3	Study 4
Fermentation Type	Batch Wheton Bottle	Batch Wheton Bottle	Batch fermentation 2litre	Continuous operation at log phase
Cell Concentration (cells ml^{-1})	$3x10^8$	$7.8x10^8$	$3x10^9$	$3.5x10^9$
Detail	-S°	+S°	1800rpm agitation and gassing at 0.2vvm	
Reference	Fiala and Stetter (1986)	Bonchosmolovskaya and Stetter (1991)	Rudiger et al., (1992)	Krahe et al., (1996)

2.4.2.2 Continuous Cultivation of Pyrococcus furiosus

The aim of continuous culture is to grow organisms to produce the highest amount per volume time, and in effect produce high cell density cultures based on maintaining a maximal growth rate (Riesenberg and Guthke, 1999). The best way for this is continuous cultivation in smaller vessels. Continuous cultivation of *P.furiosus* is problematic as mentioned above but as there is no growth limiting substrate associated with the process then much higher cell densities can be obtained per unit time than in batch fermentations. Growth of microbial organisms often takes place in continuously stirred tank reactors (CSTR) due to their ease of use.

Brown and Kelly (1989) like Pysz *et al.* (2001) grew their culture in a batch phase until the culture reached a late-log phase, and then moved into continuous fermentation, in a 2 litre fermenter for 1 litre of broth. Brown and Kelly (1989) saw an increase in cell densities as the dilution rate was increased up to 0.8 hr^{-1} where it then decreased. This was concluded to be due to either incomplete mixing occurring or a manifestation of some metabolic change. Although it is believed by this author the decrease was due to washout of the organism.

Rudiger *et al.* (1992) used inert gas (N_2/CO_2 95:05) at 0.2vvm and found a 30% increase in growth rate and a 3.5 fold increase in cell density over non-gassed cultures. This was because the hydrogen was being gassed out by the N_2/CO_2 gas. This gas also kept the pressure higher than the external environment and helped keep an anaerobic environment inside the growth area. The maximal cell densities were found to increase proportionally with increased stirrer speed. Rudiger *et al.* (1992) reached a maximal cell density of 3×10^9 cell ml^{-1} when a stirrer speed of 1800rpm was used. This showed that product inhibition of *P.furiosus* can be reduced by gassing and agitation. Growth was however negatively influenced approaching 2400rpm; where cell density and amylase activity diminished probably due to the shear stress of the mixing acting on the cells. This apparent critical value of the hydrodynamic stress for the cells of *P.furiosus*, suggests a maximal growth rate that can be achieved from a commercial standpoint given a set volume of fermentation vessel.

Once grown, cells could be separated from the culture broth in continuous culture, ideally with cells being returned to the medium to maintain long term, steady state operation. Conversely removing both the cells and the broth keeps the remaining cells in a continuous log-phase, and as such can increase the amount of cells produced over a given time period which has implications

for removal of first and second degree metabolites (extracellular α-amylase). Krahe *et al.* (1996) reported cell densities of 3.5 x 10^9 cells ml^{-1} corresponding to 2.6 gl^{-1} dry cell weight (DCW) thus represents a 100-fold increase when compared to fermentations performed in static serum bottles. Rudiger *et al.* (1992) found an over-production of extracellular α-amylase of 5.2-fold (2500-13000 U/l) when using dialysis fermentation for the removal of inhibitory substrates in the growth chamber.

The Raven *et al.* (1992) method has become an attractive method for growth of hyperthermophiles when using a gas-lift bioreactor. The influence of several inert gases and flow rates was measured during a continuous fermentation of *P.furiosus*, finding nitrogen at a flow rate of 0.5 vvm to achieve a cell density of 3 x 10^9 cells ml^{-1} under chemostatic conditions. Above 0.5 vvm the flowrate of gas caused excessive foaming from the extracellular proteins, implying that the proteins are denatured before they can be removed and purified. A greatly reduced surface area is, therefore, available for gas transfer which reduces the capacity for hydrogen removal. For *Thermococcus hydrothermalis* gassing rates > 0.3 vvm caused severe build up of surface foam (Postec *et al.*, 2005).

2.4.3 *Pyrococcus furiosus* growth media

Raven and Sharp (1997) established a defined medium for the cultivation of *P.furiosus*, and replaced complex nutrients with defined amino acids and vitamins and could achieve a 5-10 fold increase in cell density to 3x10^9 cells ml^{-1} in fermentation in comparison to Fiala and Stetter (1986).

Koch *et al.* (1990) found a maximal cell density of 6.2 x 10^9 cells ml^{-1} producing 200 U/l of α-amylase after 8 hours, on a modified medium with soluble starch and elemental sulphur. The conditions were 98°C, pH 6.6 and an anaerobic atmosphere of 80:20 H_2/CO_2. Rapid growth of high cell density *P.furiosus* gave a significant production of α-amylase if grown correctly and reducing proteases present in the media.

2.4.4 *Pyrococcus furiosus* α-amylase

α-amylase cleaves α-1, 4-glycosidic linkages in polysaccharides (Figure 2-7) in a random fashion to form branched oligosaccharides. α-amylase does not posses de-branching activity and, therefore, is not able to hydrolyse α-1, 6-linkages in branched polysaccharides such as amylopectin and glycogen.

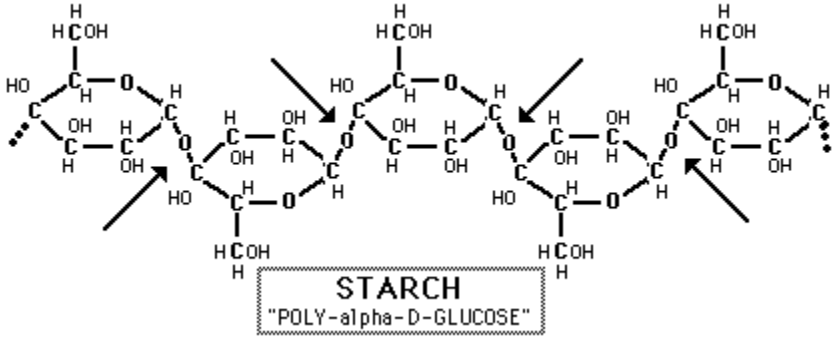

Figure 2-7 Points where the starch molecules are broken down by α-amylase (as indicated by the arrows)

Thermophilic and hyperthermophilic anaerobic bacteria and archaea have developed efficient enzyme systems to produce absorbable sugars from branched polysaccharides; as free maltose is scarce in the natural environment. In most cases of extracellular enzymes, enzymes production

parallels first degree metabolite product and reaches its maximum at the end of the logarithmic growth period (Antranikian, 1990).

α-amylase is an important industrial enzyme, demonstrated by Shaw *et al.* (1995), as an additive in detergents, the removal of starch sizing from textiles, liquefaction of starch or in the formation of dextrin in baking, to name a few uses. The most widely used α-amylase in industry is from the "relatively" thermostable microbe *B.licheniformis*, but as mentioned in §2.2.2 *B.licheniformis* is still not thermostable enough for use in sterilisation processes at 121°C.

Thermophiles have shown themselves to be a source of heat stable α-amylase and have been successfully produced from various micro organisms including *Thermotoga maritime* (Leuschner and Antranikian, 1995), *Clostridium thermohydrosulfuricum* (Melasniemi, 1987), *Desulfurcoccus fermentans* (Perevalova *et al.*, 2005), *Geobacillus thermolevorans* (Rao and Satyanarayana, 2004) and *Sofolobus solfataficus* (Worthington *et al.*, 2003), but most of literature has been produced on *Pyrococcus furiosus* amylases, therefore this is used as a logical starting point.

The ability of the thermostable amylase from *P.furiosus* to degrade native starch efficiently at 100°C in the absence of metal ions makes this enzyme of great interest for the industrial applications mentioned above. The *P.furiosus* α-amylase has a molecular mass of 129kDa (Laderman et al., 1993). It has been reported that α-amylase from *P.furiosus* is active between 40 and 140°C at a range of pH 3.5-8 (Brown *et al.*, 1990; Koch *et al.*, 1991; Laderman *et al.*, 1993). Whereas the optimal temperature for activity is generally agreed to be approximately 100°C; but the pH is more subjective. Koch *et al.* (1990) found an optimum pH of 5, and Brown *et al.*

(1990) a pH optimal of 5.6, and Laderman *et al.* (1993) discovered a pH optimal in the range 6.5-7.5. In this study it was found to replicate the findings of Koch *et al*., (1990) and Brown *et al*., (1990).

While reviewing the thermal stability of α-amylase from *P.furiosus,* Koch *et al.* (1990) found that after 6 hours of incubation at various temperatures (90-120°C), the enzyme was extremely thermostable with no loss of activity at 90°C, 20% loss at 100°C and 90% loss at 120°C after 6 hours incubation. Also Laderman *et al.* (1993) found the amylase to have a half life of 2 hours at 120°C which makes it potentially ideal for food industry applications to withstand a typical process of 30 minutes at 121 °C. Koch *et al.* (1990) also showed that the α-amylase from *P.furiosus* is primarily extracellular (approximately 80%) which was also verified by Tucker *et al.* (2005).

Calcium (Ca^{2+}) ions were found to stabilize the α-amylase enzyme (Laderman *et al.*, 1993). Co^{2+}, Ni^{2+}, Fe^{2+} were seen though to give a slight inhibition and the addition of 2 mM of Cr^{3+}, Zn^{2+} or Cu^{2+} gave almost complete inhibition to the enzymatic activity of the α-amylase, most of these ions though are present in defined media. Within the cultivation media many metal ions are available for stabilisation of the extracellular α-amylase at high environmental temperatures and are needed in the defined media.

2.5 Conclusion

TTIs, although not as accurate as data-loggers or thermocouples, are the best way of validating thermal treatments where data-loggers and thermocouples are impractical for use, such as within the food sterilisation and canning industries. α-amylases from *Bacillus sp.* have been used for

pasteurisation processes with great effect, and now an integral tool in the measurement of food safety. Some work has been focused on using the moderately thermophilic *Bacillus sp.* α-amylase for sterilisation TTIs, but limited work has been focused on using native hyperthermophilic enzymes for use in sterilisation TTIs. It is therefore essential to understand the enzyme's thermal degradation kinetics and particularly the unfolding characteristics, as well as the parameters associated with TTI use at sterilisation temperatures.

This work will begin by examining the growth conditions of *Pyrococcus furiosus* and purification techniques for the greatest yield of extracellular α-amylase. Then the effects of iso- and non-isothermal processing on amylase will be explored along with the variability of TTIs. To complete this work, the kinetics and mechanism of unfolding due to thermal processing will be examined.

The constraints of this work are that the enzyme should come from a non-GMO source, because it could be used within the food industry. This should then be GRAS approved (generally recognised as safe). The *z* value should match that of *Clostridium botulinum* spores and have a measurable *D* value in the operational range of food sterilisation processes.

Chapter 3

Cultivation and Purification *Pyrococcus furiosus* α-amylase

3.1 Introduction

For use within TTIs, enzymes have to have properties that match or are similar to the micro-organism the thermal process is targeting to reduce. This makes enzymatic TTIs very specific to the process, temperature and targeted organism in which the TTI is required to work. Figure 3-1 shows the specificity of the enzymes in TTIs depending on the process temperature.

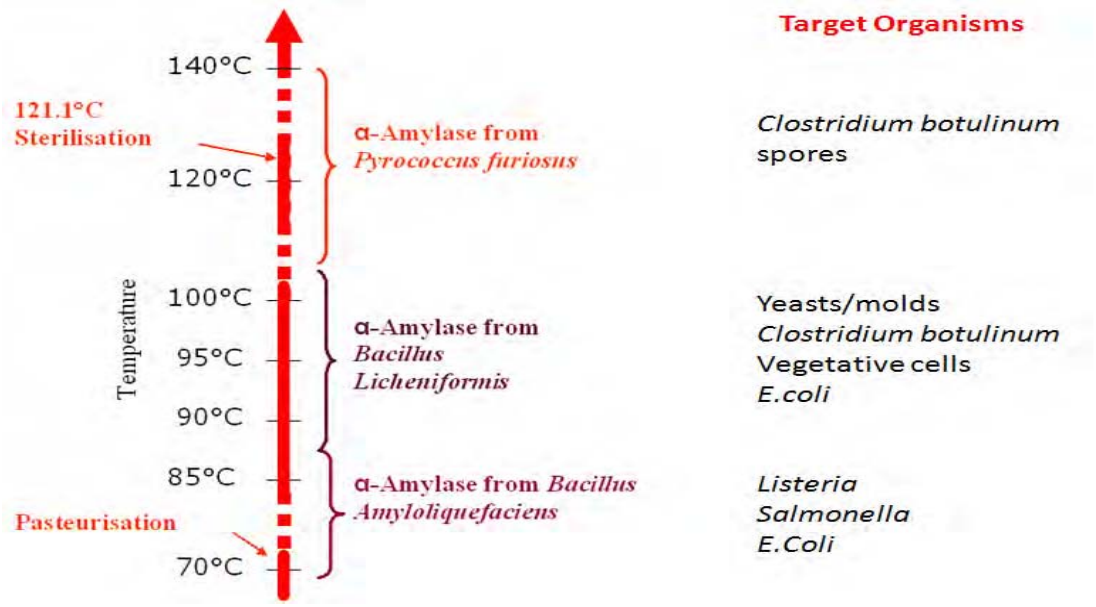

Figure 3-8 Temperature specificity and applications of enzymes for TTIs – showing relative ranges of temperatures and target organisms

As noted in chapter 2, the organism *Pyrococcus furiosus* is of great interest in the development of sterilisation TTIs (Tucker, *et al*., 2007) due to the reported heat stability of its amylases (Koch

et al., 1990). Activity of *Pyrococcus furiosus* α-amylase has been measured over broad temperatures (40-140°C), with an optimal activity, variously reported, of 100°C (Brown *et al*., 1990; Koch *et al*., 1990). This persistent activity is maintained over 121°C and so makes *Pyrococcus furiosus* α-amylase a promising candidate for use in a sterilisation TTI (Tucker, *et al*., 2007). *P.furiosus* α-amylase has a thermal resistance (z-value) close to those of *Clostridium botulinum* spores (10°C) which are one of the low-acid micro-organisms targeted by sterilisation in the canning industry.

There are many ways in which to produce *Pyrococcus furiosus* α-amylase for use within sterilisation time-temperature integrators. These would include producing extracellular α-amylase:

- From the native, genetically unmodified *Pyrococcus furiosus*.
- By genetically modifying/mutating the *Pyrococcus furiosus* to produce more α-amylase. This is not a preferred option in the conservative food industry.
- Using a recombinant α-amylase within the sterilisation TTIs, which again may fall foul of conservative parts of the food industry.

Genes for several enzymes from extremophiles have been cloned in various mesophilic hosts, including *E.coli, B.subtilis* and in yeasts (Ito, 1997; Niehaus *et al.*, 1999; Lim *et al.*, 2001). To obtain a sufficient amount of recombinant enzyme *E.coli* is recommended (Schiraldi *et al.*, 2001; Schiraldi *et al.*, 2000) because this host is easily grown and the vectors are well characterised.

Yeast though is better for industrial applications as a host and is for food industry applications classified as "safe" over *E.coli*. In these systems recombinant growth media could then be pasteurised to remove the *E.coli* or yeast cells without affecting the recombinant thermostable α-amylase. Still recombinant enzymes have a stigma involved with safety for the consumer especially when involved within the food process and so are not truly viable options. This means the first option of growing the native form of *Pyrococcus furiosus* to produce α-amylase is the most viable for use within an enzymatic sterilisation TTI.

Pyrococcus furiosus was shown by Brown *et al,* (1990) to grow in the presence of starch and other carbohydrates; suggesting that a variety of amylotic enzymes (α-amylase) may be important in metabolism with *P.furiosus* utilizing maltose, cellabiose or pyruvate as simple substrates for carbon and energy (Huber and Stetter, 1998). Monomeric sugars were shown not to be able to be utilised for growth but maltose and cellabiose are split intercellularly to form glucose.

The optimal conditions for an organism are in general the exact environment in which they would grow and replicate in. In a laboratory environment, artificial seawater is used to replicate the marine environment which *P.furiosus* comes from, with the addition of a complex media optimised by Brown *et al,* (1990) with elemental sulphur addition to stimulate the environment of sulphurous fields of Volcano Islands, Italy.

As previously stated in §2.2, *P.furiosus* is an anaerobe and as such, oxygen free conditions within the media need to be applied. This is achieved by either sparging with an inert gas, or by

the addition of reducing agents, although headspace gases must be still be purged with pressurised inert gas to drive out any oxygen.

Some of the general problems associated with the cultivation of extremophiles are that they are notoriously difficult to pre-culture and grow (Scott, 2003) and that liquid media is the only way to grow hyperthermophile organisms due to high temperatures melting any solid media used. High temperatures may cause the nutrients in the media to react (in Maillard reactions), with amino acids and sugars which can inhibit growth (Krahe *et al.*, 1996) both by reducing feed for growth as well by the formation of toxic products from reactions.

Particular interest, noted in chapter 2, has focused on the cultivation of anaerobic hyperthermophiles but because of their sensitivity to oxygen and need for extreme temperatures this provides a major obstacle to cultivation techniques.

For *Pyrococcus furiosus* it is generally very difficult to get any biological reproducibility and plating out colonies to have a cell-bank is difficult as at the temperatures required for growth the media is still liquid. In practice some of the archaea grown in the fermenter are generally used as inoculums for the next time. In this case a constant volume fed batch operation for growth of cells was used to produce a new cell bank for future fermentations to minimise mutations so no batch to batch variation of cells occured.

To use *Pyrococcus furiosus* α-amylase in sterilisation TTIs it must be possible to produce native α-amylase routinely. To produce high yields of this native hyperthermostable α-amylase, cultivation and purification must be explored.

This chapter records work done towards successful cultivation and purification of *Pyrococcus furiosus* α-amylase. It was necessary to develop reliable experimental methods for the culturing of *Pyrococcus furiosus*. This was done in a lengthy series of experiments in the following sequence; firstly *Pyrococcus furiosus* was cultured from sample in Balch tubes and Wheaton bottles (5-40ml). Through this the effects of the addition of elemental sulphur was explored (§3.3.2). The cultivation of *Pyrococcus furiosus* was then scaled up to 1 litre batch fermentation with an agitator running at 1200 rpm to remove the inhibitory hydrogen instead of elemental sulphur. This method was used to investigate the effects of carbon source on growth rate and α-amylase production (§3.3.3). Under constant volume fed batch fermentation, the effects of growth rate on the amylase production is explored in §3.3.4 and the purification techniques are reviewed in §3.3.5.

3.2. Materials and Method

3.2.1 Cultivation of *Pyrococcus furiosus*

P.furiosus was grown on a rich medium containing tryptone, yeast extract and casamino acids (1% wt/vol) as a carbon source (Adams *et al*., 2001; Robb *et al*., 1995). Artificial seawater (ASW) as modified by Robb (1995), containing a basic salt solution, a trace element solution and vitamin solution was prepared as separate stock solutions and stored at 4°C. Due to the area where the *Pyrococcus furiosus* organism is found, the complexity of the ASW replicating the *P.furiosus* natural environment is because of the minerals found in the shallow waters from the volcanoes and thermal springs.

Basic salts solution- ASW (salt g/l)		**Trace elements solution (trace element g/l)**		**Vitamin Solution (vitamin mg/l)**	
NaCl	15.0	Nitrilotriacetic acid	1.5	Biotin	2.0
$MgCl_2.6H_2O$	1.0	$MnSO_4.H_2O$	0.5	Folic acid	2.0
Na_2SO_4	1.0	$FeSO_4.7H_2O$	1.4	Pyridoxine-HCl	10.0
$CaCl_2.2H_2O$	0.15	$NiCl_2.6H_2O$	0.2	Thiamine-HCl	5.0
KCl	0.35	$CoSO_4$	0.1	Riboflavin	5.0
K_2HPO_4	0.14	$ZnSO_4.7H_2O$	0.1	Nicotinic acid	5.0
NaBr	0.05	$CuSO_4.5H_2O$	0.01	DL-Ca-pantothenate	5.0
H_3BO_3	0.02	$NaMoO_4.2H_2O$	0.01	Vitamin B12	0.1
KI	0.02	$Na_2WO_4.2H_2O$	0.3	p-Aminobenzoic acid	5.0
$SrCl_2.6H_2O$	0.01			Lipoic acid	5.0

The trace elements and vitamin solutions were added at 10ml/litre basic stock solution when used and filter sterilised.

Once the ASW, trace element and vitamin solutions were produced they were added as follows:

Per litre of artificial seawater

Trace Elements solution	10ml
Vitamins solution	10ml
Yeast Extract (Difco 0127-01-7)	1g
Tryptone	1g

0.1% Resazurin solution (0.001g final concentration)	1ml
(as an oxygen indicator and reducing agent)	

ASW was supplemented with a carbon source – casamino acids/maltose/starch (1% wt/vol.). Anaerobic conditions were maintained throughout. Anaerobicity was obtained by sparging with N_2 and any traces of oxygen were removed by adding 2.5g/litre cystine-HCl as a reducing agent. Sparging was through butyl septum-type stoppers allowing nitrogen in while a needle allowed oxygen out, degassing for 20 minutes. Resazurin was used as an oxygen indicator. When the oxygen concentration is reduced the rezazurin turns from a purple through pink and when no oxygen is present then the media becomes clear. This stage is especially important as *Pyrococcus furiosus* is extremely sensitive to oxygen. Oxygen will attach to almost any surface so the oxygen must be purged with nitrogen if entering the anaerobic environment. All equipment (syringes, bottles, tubes) used were purged with nitrogen for at least 2 minutes to remove the oxygen.

The media was transferred to Balch tubes (18 x 150mm; Bellco Glass 2047) with 5ml volume or Wheaton “400” clear serum bottles (VWR Scientific 16171-341) with 50ml volume. 5g/litre sterile elemental sulphur (S°) was added to half the tubes and bottles. The bottles or tubes were capped with gas-impermeable black butyl septum-type stoppers (Bellco Glass 2048-11800) secured with aluminium crimp seals (Markson Science 026 series or Bellco Glass 2048-11020) using a crimper (Bellco Glass 2048-10020). Vials were preheated to 98°C, sparged with N_2 and cystine-HCl added to 0.25% to remove any oxygen. Bottles were then sealed with butyl rubber stoppers and secured with aluminium crimp seals. Once clear (anaerobic) the medium was inoculated from a storage culture with 1% vol/vol inoculate (0.15mg/ml DCW) (DSMZ,

Germany). To inoculate the syringe was gassed with nitrogen for 2 minutes to remove any oxygen attached. Once the syringe was anaerobic the needle was added and the syringe was pushed shut so the nitrogen goes through the needle and the inoculum was taken up and into the media as quickly as possible.

The culture was grown in batch cultivation as stated above until late log phase, to inoculate a 1000ml working volume constant volume fed batch culture fermentation. The medium in the flask was likewise pre-heated to 98°C, sparged with N_2, and made anaerobic. The agitation was 1000<1500rpm (Raven and Sharp., 1996). Constant volume fed batch operation was started during late log phase determined by dry cell weight and optical density measurements over time.

3.2.2 Purification of extracellular *Pyrococcus furiosus* α-amylase

Cells were removed from the extracellular fraction by centrifugation at 10000 x *g* for 10 minutes at 4°C. To the supernatant, a total of 561g ammonium sulphate (80%) was added slowly over a period of 2 hours with gentle agitation. The ammonium sulphate precipitates out the extracellular protein from the crude fermentation broth. The solution was centrifuged at 10000x*g* for 10 minutes at 4°C and the precipitate was collected. Purification was carried out at 4°C so there would be no effects of protein thermal denaturation or contamination with other enzymes.The precipitated ammonium sulphate pellets were resuspended in an equivalent volume of 50mM ammonium bicarbonate buffer. This was dialysed against the same 50mM ammonium bicarbonate buffer to remove the residual ammonium sulphate. The dialysate was freeze-dried to give a freeze-dried powder (FDP) for storage.

Preparative polyacrylamide gel electrophoresis was performed in 1.5mm thick polyacrylamide gels (homogeneous, 12%w/v) at a constant voltage of 400V for 8 hours at 4°C. The protein bands were visualised by silver staining and 0.1% SDS was used and carried out under constant current of 40mA/gel. Commercially available molecular weight markers were used to calibrate the gel.

3.3 Results

3.3.1 Characterisation of *Pyrococcus furiosus*

Confirmatory scanning electron microscopy (SEM) of a cellular pellet harvested (Figure 3-2) shows organisms with a slight irregular coccoid shape found predominantly in pairs with an approximate diameter of 1.5-2.5μm; this is similar to that characterised by Fiala and Stetter (1986) for the morphology of *Pyrococcus furiosus*. The figure in the top right shows the splitting of some cells after replication. The organisms do have flagelle, but during processing for SEM, these appear to have separated from the main cocci body, which may explain the fibrous strands seen in the SEM pictures of Figure 3-2.

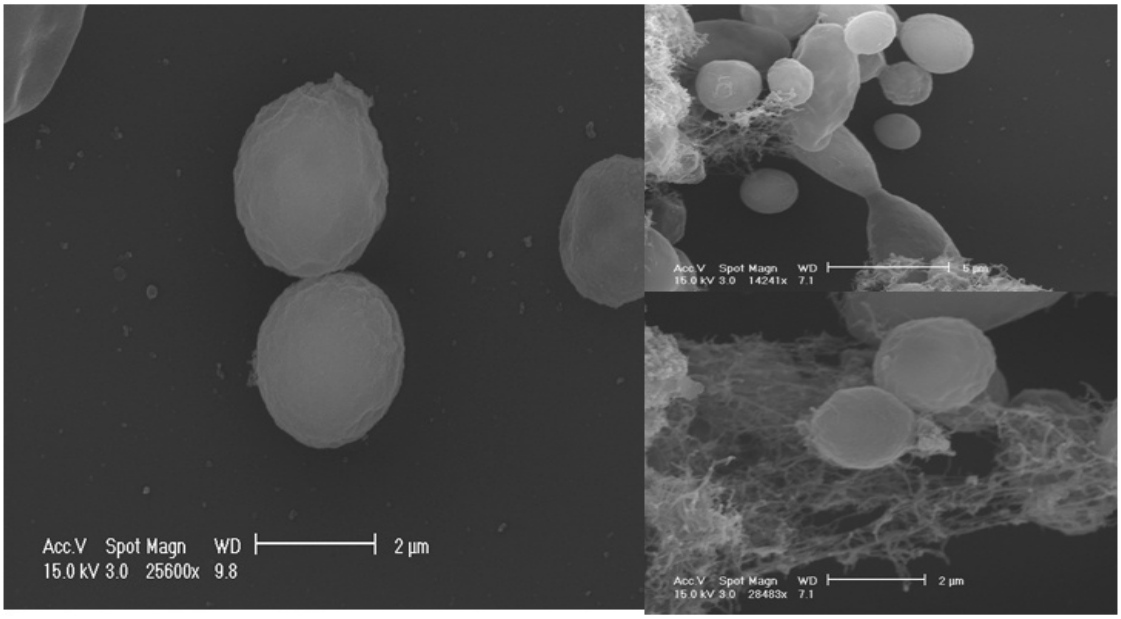

Figure 3-2 SEM scans of *Pyrococcus furiosus*

Transmission electron microscopy (TEM) of the cellular pellet (Figure 3-3) revealed the cocci surrounded by an envelope about 50nm thick, the same as found by Fiala and Stetter (1986). Figure 3-3 also shows dense circular regions shown in all the TEM scans inside the archaeal cell; these could be starch granules, inclusion bodies (because the cells were harvested in the stationary phase of growth), or the granum-like body up to 1 m width noted by Fiala and Stetter (1986).

Due to the extreme growth conditions of *Pyrococcus furiosus* (anaerobic, 98°C), the probability of micro-organism contamination and competitive inhibition is extremely low and so it remains highly likely that the scans are showing *Pyrococcus furiosus* cells.

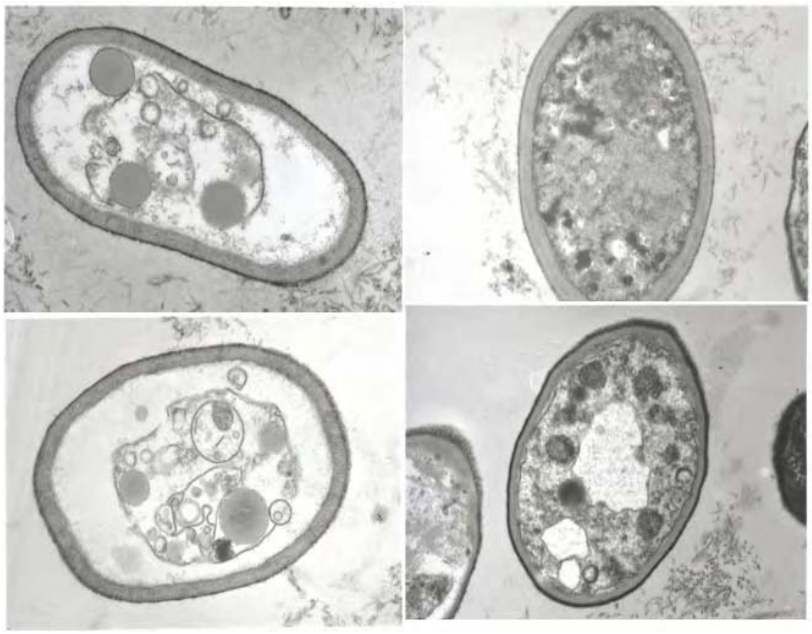

Figure 3-3 TEM scans of *Pyrococcus furiosus* (cells are 2μm diameter)

3.3.2 Sulphur effects on batch cultivation

Pyrococcus furiosus was initially cultured in 40ml of media in Wheaton bottles, as described in §3.2, using elemental sulphur. The elemental sulphur reacted with the inhibitory growth by-product, hydrogen, to produce hydrogen sulphide.

$$S^\circ + H_2 \rightarrow H_2S$$

As previously discussed in chapter 2, elemental sulphur is needed in small batch fermentation because there is no agitation to remove the hydrogen. The sulphur is needed to produce hydrogen sulphide. Typical growth curves for the batch fermentation are shown in Figure 3-4. The growth of *Pyrococcus furiosus* after the lag phase can be seen to increase considerably when elemental sulphur is added to the Wheaton bottles in the media. Results in Figure 3-4 demonstrate the

behaviour seen by Fiala and Stetter (1986), Rudiger *et al*., (1992) and Krahe *et al*., (1996). Holst *et al*, (1997) state that the hydrogen sulphide produced, which is reasonably soluble in water (especially at the high temperatures involved), will react with any transition metals present forming insoluble sulphides. These sulphides will precipitate (which can be seen as a black precipitate) and this is believed to inhibit growth of *Pyrococcus furiosus*. The metal sulphide precipitate produced can be used as an indication of growth as the sulphur reacts with the hydrogen by-product of growth. Fiala and Stetter, (1986) expected this precipitation not to affect cell growth significantly and so moderate cell densities should still be expected. Inhibition is thought to be due to the toxicity of the metal sulphides and / or the reduced metal ion concentration in the media for cell growth. This produces a complex environment in which it can be difficult for the *Pyrococcus furiosus* cells to grow.

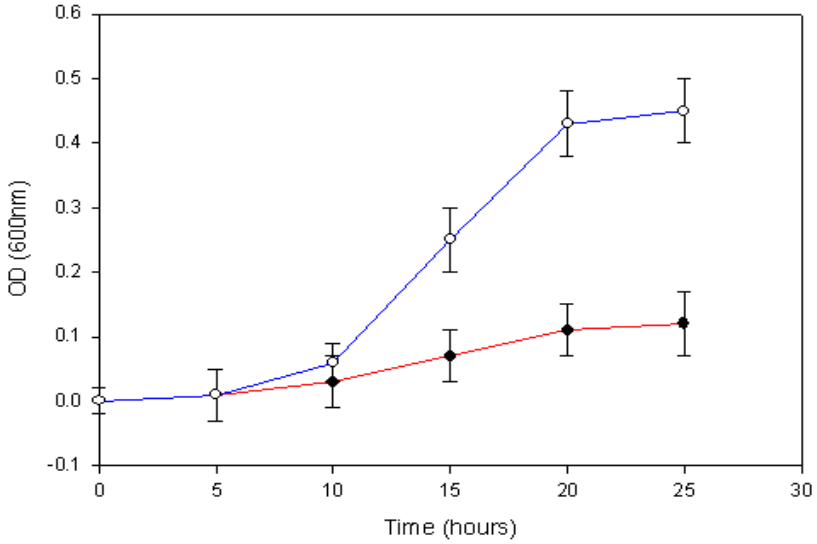

Figure 3-4 Batch cultivation in Wheaton bottles, with sulphur added at t=0 [—]; and without sulphur added [—]; the data was normalised against (i) pure media with added sulphur plot; (ii) pure media plot. The data shown is the mean of 3 replicates.

It is difficult, in the experiment shown in Figure 3-4, to estimate the amount of cellular growth to be measured accurately because DCW will include sulphur particles and metal sulphide particulates as well as cells. In the larger fermentations of 1 and 2 litres in this study, elemental sulphur was not added, as the high agitation removes the inhibitory hydrogen product and sulphur particulates will not affect the measurements of cellular growth.

3.3.3 Effects of carbon source on cultivation

Prior to investigating constant volume fed batch operation, 1 litre batch fermentations as discussed in section 3.2 with agitation were carried out with 2 different carbon sources (peptides and starch). Due to the low amount of organic matter in submarine environments, energy and a carbon source are obtained from a complex mixture of peptides from decomposition of primary producers, while a few hyperthermophiles can also use polysaccharides (starch, pectin, glycogen etc.) (Vieille and Zeikus, 2001).

Figure 3-5 shows typical data of growth curves (from 4 fermentations) of *Pyrococcus furiosus* using both starch and peptides as a carbon source. The length of time from the end of the lag phase to the start of the stationary phase (the exponential growth phase), was seen to be 14-20 hours, which is typical for *Pyrococcus furiosus* (Schicho *et al*.,1993). Using starch as a carbon source, it can be seen there is a shorter lag time (although this can be shortened by increasing the concentration of cells in the inocula), but it has a lower maximal cellular growth (0.23 mg/ml DCW) than using a peptide carbon source (0.3 mg/ml DCW). One of the disadvantages of archaebacterial fermentations is the extremely low biomass yields associated with them (0.1-1

mg/ml wet weight) compared to eubacterial fermentations (>30 mg/ml wet weight) (Cowan, 1992).

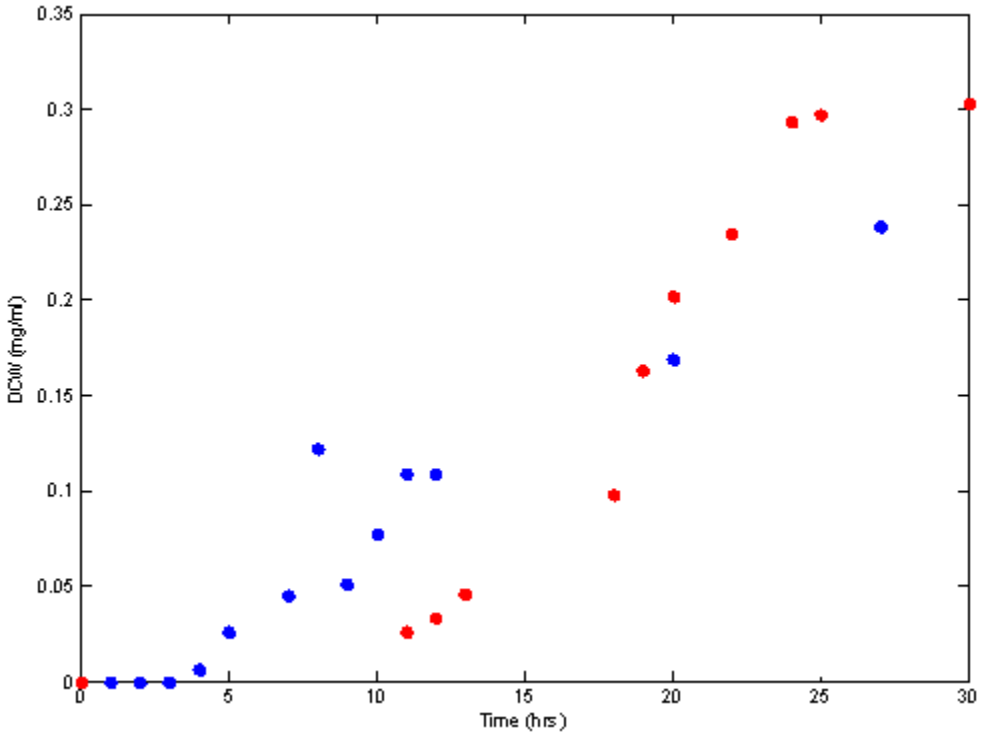

Figure 3-5 Batch growth curves of *Pyrococcus furiosus* growth under starch [●] and peptide [●] carbon sources

Using peptides as a carbon source can be seen in Figure 3-5 to give a steeper exponential phase giving a higher maximal growth rate, μ_m (0.33 h^{-1}). This is an important finding for constant volume fed batch cultivation to produce the maximal amount of biomass per unit time, and at this point ($_m$) batch operation changes to constant volume fed batch fermentation.

Lee *et al*. (2006) used DNA microarray analysis to show that *Pyrococcus furiosus* α-amylase (PF0478) is not expressed to any significant extent when starch or maltose are used as a carbon source, suggesting that the amylase is not involved in starch metabolism. In fact α-amylase is

dramatically up-regulated when the organism is grown on peptides. Peptides were thus used in this study as the carbon source.

3.3.4 Growth rate effects on amylase cultivation

The dilution rate during constant volume fed batch cultivation needs to be calculated from the growth rate at which cells are being harvested. Cultivation of cells should ideally be carried out at the maximal growth rate ($0.33h^{-1}$) when the dilution rate (D) of fresh media needs to be equal to that of the maximal growth rate. By changing the dilution rates (the amount of media pumped in and out of the fermenter) then different growth rates can be seen (Figure 3-6a). At a flow rate in and out of the fermenter of 0.5 l/h the growth rate is maximal. When this is changed to 0.11 l/h the growth rate is ~25% the maximal growth rate, and if the flow rate is increased then to 0.25 l/h there is steady growth of the cells and the growth rate is 0.5 $_m$.

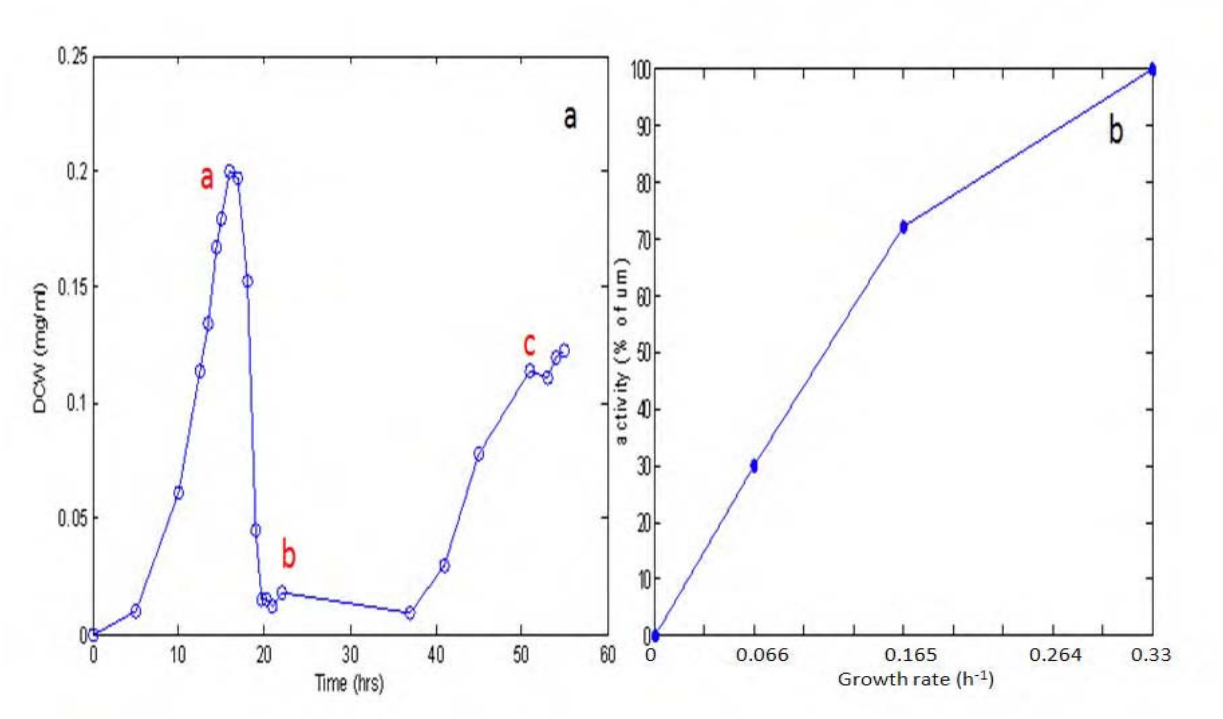

Figure 3-6 Growth rate effects on amylase production (a) growth curve with the growth rate at [a] 0.33h^{-1} [b] 0.066h^{-1} [c] 0.165h^{-1}; (b) amylase activity as a factor of growth rate (activity measured by DNS assay, defined in chapter 4)

Figure 3-6b shows that the amount of extracellular α-amylase activity is proportional to the amount of *Pyrococcus furiosus* cellular growth, and so the amount of cellular growth needs to be maximised in fermentation to produce the greatest amount of extracellular thermostable α-amylase from *Pyrococcus furiosus* for use within sterilisation TTIs.

Once the optimal parameters for constant volume fed batch fermentation were found (peptides as a carbon source, 15 hours before switching to constant volume fed batch fermentation, D = μ_m = 0.33 h^{-1}), continuous volume fed batch fermentation was set up as in §3.2. A growth curve measuring DCW for constant volume fed batch fermentation was compared to batch fermentation (Figure 3-7). For the 10 hours of constant volume fed batch fermentation found an increase in DCW (0.8g), and would increase further if the operation was rum for longer periods.

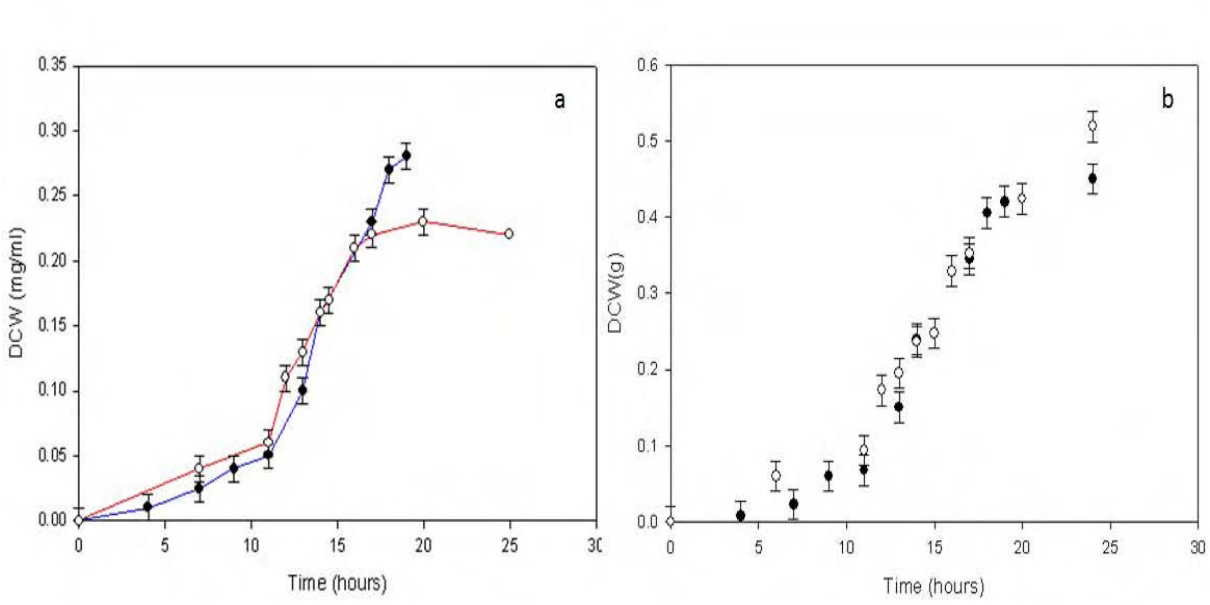

Figure 3-7 Growth curves for batch [●—] and constant volume fed batch fermentation [○—] under anaerobic 98°C conditions and agitation at 1200rpm for (a) DCW and (b) cumulative DCW for the 1.5litre fermentation. Constant volume fed batch fermentation operation applied at 15 hours. The plots are the mean of 3 replicates.

Constant volume fed batch operation was started at 15 hours and run for 10 hours and produced 1.7g/l of freeze-dried amylase powder compared to 0.9g/l freeze dried amylase powder from batch operation for the same overall operational time of 25 hours. This produces amylase for use in a large amount of TTIs and so constant volume fed batch operation was stopped after this time. Also purification caused a bottleneck effect on the production of purified freeze-dried -amylase; so long periods of continuous operation were not efficient or required.

A constant volume fed batch approach is applicable for the uses in this study. Batch fermentation is also applicable for the amount of FDP required, although if α-amylase sterilisation TTIs become common use in the canning industry and a greater quantity of FDP is required, constant volume fed batch fermentations can be easily run as a continuous fermentation. As stated in chapter 2, Heinz produces 300 million cans of soup in the UK every year, if 0.05% of cans are

measured with 10 TTIs, then using the TTI preparation method in chapter 5 approximately 500mg FDP needs to be produced every year.

3.3.5 Purification of α-amylase

The molecular mass and subunit composition of the purified enzyme was determined by size exclusion chromatography and SDS-PAGE analysis. A example of the SDS-PAGE analysis can be seen in Figure 3-8.

In Figure 3-8 the first columns (a) and (b) run a *Pyrococcus furiosus* amylopullanase sample (supplied by NCSU). The amylopullanase (PF1935) is a recombinant enzyme over-expressed in *E.coli*. The cells were then lysed with Bugbuster®. The broth was then thermally treated at 80°C for 10 minutes to deactive *E.coli* enzymes and products. The concentration of amylopullanase was 18.62 mg/ml and the activity measured at 5.9 nmol reducing sugar/min. This sample was supplied by I. Odezmir and R. Kelly at North Carolina State University (NCSU).

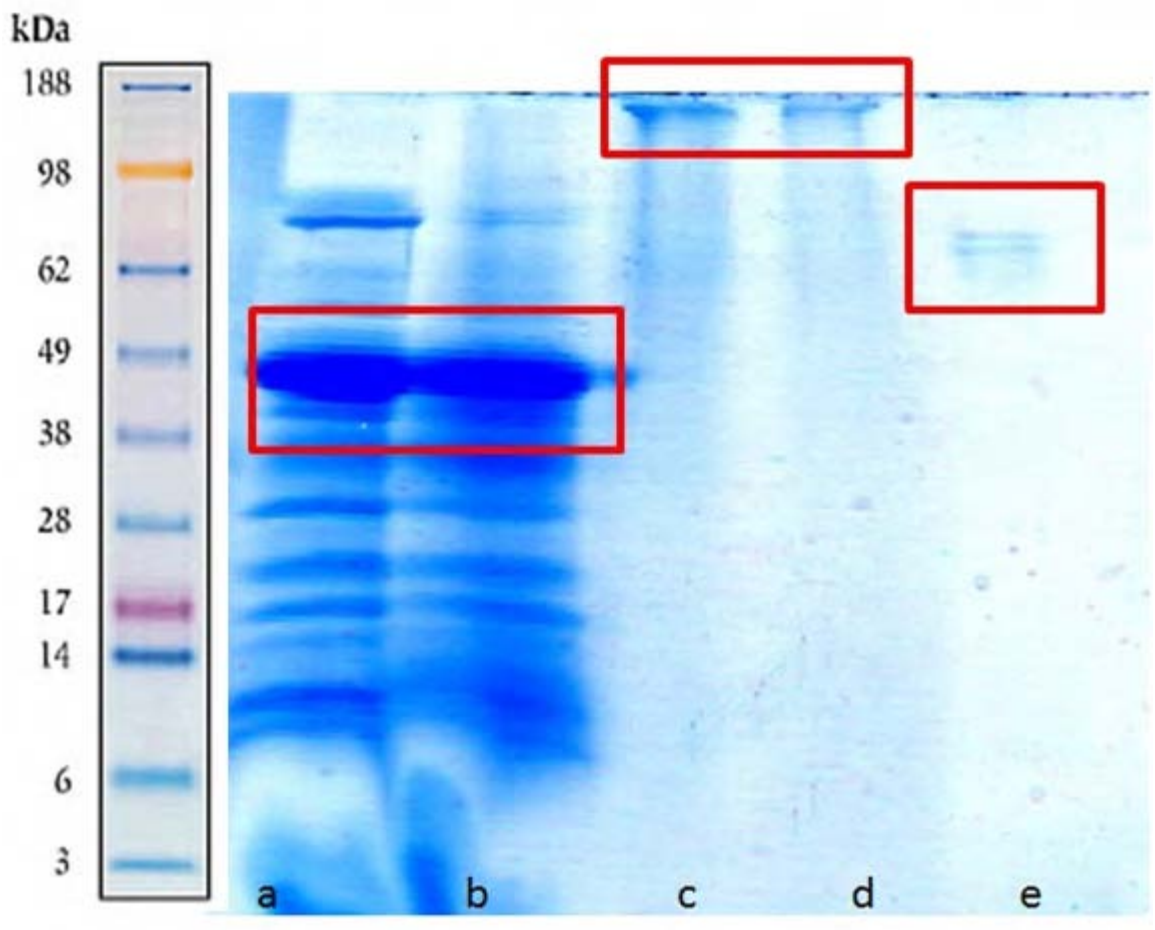

Figure 3-8 SDS-PAGE gel of *Pf* amylopullanase (a,b) unprocessed *Pf* amylase (c,d) thermally processed *Pf* amylase (e)

Amylopullanase from *Pyrococcus furiosus* was also reviewed as it also cleaves α-1, 4 glycosidic bonds in starch (Dong et al., 1997) producing malto-oligosaccharides. Both *Pyrococcus furiosus* α-amylase and amylopullanase (PF0478 and PF1935) are extracellular and have putative signal peptides (Lee *et al*., 2006). PF1935 has been cloned and characterised (Dong *et al*., 1997) with the catalytic residues indentified (Kang *et al*., 2005). The amylopullanase supplied is from a recombinant source and as such could not be used in food sterilisation TTIs.

One -amylase (PF0478) which is extracellular has been cloned and over-expressed in *E.coli* and *B.subtilis* (Jorgensen *et al*., 1997) and Laderman *et al*. (1993) stated that this *Pyrococcus furiosus* α-amylase enzyme is a homodimer with a sub-unit molecular mass of 66 kDa. This can be seen in Figure 3-8 column (e). This is after high thermal processing (140°C, 5 minutes) of the α-amylase. Without thermal denaturation (columns (c) and (d)), SDS-PAGE shows an apparent molecular weight of 130 kDa of α-amylase. This suggests that the α-amylase is a homogeneous dimer which is disassociated due to high thermal processing. That α-amylase is disassociated due to high thermal processing is important to consider for TTIs as thermal denaturation is an important factor and described in chapter 6. Figure 3-8 column (e) shows *P.furiosus* α-amylase can be a candidate sterilisation TTI.

3.3.6 Extracellular and intracellular α-amylase

As previously stated, different amylases are produced by the *Pyrococcus furiosus* cells; an intracellular α-amylase (PF0477) and an extracellular (PF0478) α-amylase used for metabolism. It has been described by Fiala and Stetter (1986) that the extracellular α-amylase constitutes approximately 80% of the total α-amylase. This was investigated in Figure 3-9 using the assay described in detail in chapter 4. Cells were removed from the broth for one set of data leaving only the extracellular amylase, and ultrasonicated cells in the other leaving both the intra- and extracellular amylase in the broth. This sees the contribution of the intracellular α-amylase on activity. Figure 3-9 shows that with the intracellular contribution, there is a 21.5% increase in α-amylase compared to the cell free broth α-amylase activity. This coincides with the results described by Fiala and Stetter (1986).

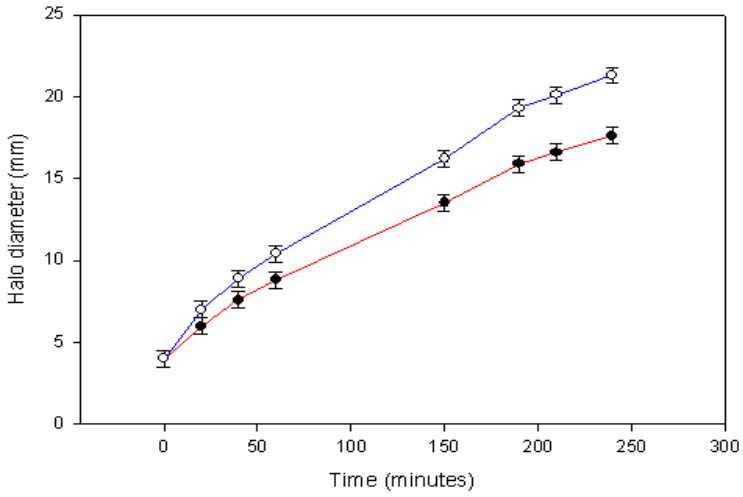

Figure 3-9 RED assay (chapter 4) on ultrasonicated broth (inc. cells) [—] and cell free broth [—]. Error bars show measurement error

For industrial use it would be more efficient to purify the supernatant as a cell free broth rather than ultrasonicate the cellular broth and then purify and extract the α-amylase for just an extra 20% α-amylase. Ultrasonicating the cellular broth may also release proteases and other unwanted proteins and enzymes which may affect the amylase activity.

3.4 Conclusion

Bacterial and fungal α-amylases, and in particular the enzymes from the *Bacillus* species, are of special interest for large-scale biotechnology processes due to their remarkable thermostability and because efficient expression systems are available for these enzymes (Fitter, 2005). *Bacillus sp.* α-amylases though are not applicable for a liable enzyme for sterilisation TTIs.

α-amylases, according to the very different habitats in which the organisms thrive, the temperature range where the native structure is present can vary significantly. In particular, thermophilic and hyperthermophilic organisms are important sources of proteins which can be used as prototypes in comparative investigations to study the determinants of structural stability under extreme conditions. This means hyperthermophiles are not usually cultured continuously as most hyperthermophilic enzymes explored and used on any scale are recombinant and so small Wheaton bottle size batches of the native strain satisfy most academic and industrial needs.

It might expected obligate aerophily not to be a predominant metabolic mode of hyperthermophiles, considering that oxygen solubility is extremely low at high temperatures, and, so far, this has been found to be true. Hence, the majority of known organisms that thrives near or above 100°C seems to be obligate anaerobes of which *Pyrococcus furiosus* is one. There are, however, many potential difficulties in expressing proteins derived from hyperthermophilic organisms, and so it is also important to consider more traditional routes to enzyme discovery (Adams and Kelly., 1998). Those who have experience in the difficult task of producing significant quantities of hyperthermophilic biomass appreciate the value of recombinant techniques in the pursuit of particular enzymes, although this is not the case in this study and as such the difficulties with the culture conditions of high temperatures and keeping anaerobic conditions were explored in sections 3.2 and 3.3.

Culture conditions for the growth of *Pyrococcus furiosus* were optimised to obtain high biomass yields. The constant volume fed batch fermentation of *Pyrococcus furiosus* cells did not need elemental sulphur adding to the media due to the high agitator speeds (1200 rpm) removing the

hydrogen quickly from the fermentation broth. It must be noted that although increased stirrer speeds increase the hydrogen removal, the shear rate may damage cells at very high (>2000rpm) agitation speeds (Raven and Sharp, 1996). Cells were cultured continuously in a 1.5 litre vessel with a dilution rate of 0.33 h^{-1} and therefore a feed rate of 0.5 l fresh media/hour. *Pyrococcus furiosus* cells were cultivated using peptides as a carbon source producing the greatest amount of biomass, although starch could also be used. Monomeric sugars could not be used (Kengen and Stams, 1994). Keeping the cells at a maximal growth rate produced the greatest amount of extracellular α-amylase, indicating that extracellular α-amylase is produced continuously or in the exponential growth phase and not at some certain point in growth such as the stationary phase or death phase.

Peptides as a carbon source producing the greater amount of biomass over starch. Accordingly, Lee *et al*., (2006) showed that *Pyrococcus furiosus* extracellular α-amylase is not expressed to any significant extent when starch, maltose, or any other of the six sugars is used as a carbon source. The function of the α-amylase is therefore not clear at present, although it does not appear to be involved in starch metabolism. In fact, its expression is dramatically up-regulated when cells are grown on peptides, a result that presumably correlates with the amylase activity measured in peptide-grown cells. Although the significance of these remains to be elucidated, one possibility is that when polysaccharides become available during peptide-dependent growth, the -amylase generates oligosaccharides, which then induce the corresponding pathways to convert the oligosaccharides to glucose. This is the major reason Peptides were used as a carbon source for growth of *Pyrococcus furiosus*.

Evaluation of apparent molecular mass, utilising size exclusion SDS-PAGE, yielded results of approximately 130kDa and upon thermal denaturation a molecular mass of 66kDa indicating a diametric quaternary structure. The rigorous means necessary to disrupt the quaternary structure of the protein shows an inherent stability of the molecule.

All α-amylase 3D structures appear rather homologous; various proposals on the stabilizing role of structural features have been reported for the individual α-amylases. In several studies specific locations in the protein structures have been identified which are relevant for thermostability. Comparative studies on various mutants of *Bacillus licheniformis* α-amylase, of *Bacillus amyloliquefaciens* α-amylase and of *Pyrococcus furiosus* α-amylase have demonstrated that mutation of individual residues either increases or decreases overall thermostability. A detailed overview about these features was also given by Nielsen *et al.* (2000). More general stabilisation features, such as oligomeric state, number of disulphide bridges, number of bound divalent ions, or the number and volume of cavities (compactness), do not show a correlation with thermostability throughout the set of homologous α-amylases. Most α-amylases need calcium ions for thermal stability which is why all defined media has excess calcium ions.

This chapter demonstrates that α-amylase could be purified and freeze-dried to a powder to be used in future studies.

Chapter 4

Assaying and modelling *Pyrococcus furiosus* α-amylase kinetics

4.1 Introduction

Thermal treatment is the most common method used by industry to ensure food is safe for consumption and to increase its storage life. To ensure safety, food is often over processed, which can significantly affect its nutritional value as well as taste and flavour attributes.

As discussed in chapter 2, enzymatic Time Temperature Integrators (TTIs) have been used to determine the heat treatment efficiency. TTIs are small free measurement devices which contain a thermally labile enzyme: determination of the degree of degradation of the enzyme at the end of the thermal process enables the integrated temperature history to be obtained. TTIs can be used for process validation, particularly when the processing environment is inaccessible for fixed devices such as thermocouples (Guiavarc'h *et al*., 2004; Mehauden *et al*., 2007; Tucker *et al*., 2007)

A number of applications for TTIs have been proposed. Most of these have been designed to work at pasteurisation temperatures (50°C-85°C) (Mehauden *et al*., 2007), using enzymes or reactive species that thermally labile over the time-temperature combinations that define the relevant processes. For example Mehauden *et al*, (2007) used -amylase from *Bacillus licheniformis* and *Bacillus amyloliquefaciens* for pasteurisation TTIs.

TTIs for high temperature sterilisation processes are difficult to obtain. However, one set of candidates are from hyperthermophilic archaea which grow and replicate at above 70°C, and these contain enzymes which can be used as the basis of sterilisation TTIs.

As discussed in previous chapters, the organism *Pyrococcus furiosus* is of great interest in the development of sterilisation TTIs (Tucker, *et al*., 2007) due to the reported heat stability of its amylases (Koch *et al*., 1990). The activity of *Pyrococcus furiosus* α-amylase has been measured over broad temperatures (40-140°C), with an optimal activity, variously reported of 100°C (Koch *et al*., 1990). This persistent activity is maintained at temperatures above 121°C and so makes *Pyrococcus furiosus* α-amylase a promising candidate for use in a sterilisation TTI (Tucker, *et al*., 2007). *P.furiosus* α-amylase has a thermal resistance (*z* value) close to those of *Clostridium botulinum* spores (10°C) which is the critical low-acid micro-organisms targeted by sterilisation in the canning industry.

However, one problem is measuring the activity of the enzyme to quantify sterilisation behaviour. Due to the high thermostability of *Pyrococcus furiosus* the usual methods for measurements of amylase activity, which take place below 40°C, will only give limited activity with *P.furiosus* α-amylase.

A number of chemical methods are routinely used to determine activity of amylase in mesophilic animal and plant extracts. Some of the more usual are those of Bernfeld (1955) and Somogy-Nelson, described by Robyt and Whelan (1968) where the assay would show a

- Decrease in viscosity

- Increase in reducing power
- Change in iodine colour reaction
- Change in optical rotary power
- Decrease in turbidity of glycogen solution

The most common methods for detecting -amylase activities on starch

- Release of reducing sugars from a starch substrate is measured
- Decrease in a specific reaction between iodine and residual starch is measured (Bird and Hopkins, 1954)
- A chromogenic group is attached to the substrate and release of this substrate into the soluble fraction is monitored by a change in optical density (Babson *et al*., 1970; Leisola *et al*., 1980)

The novel method developed in this section is based on the reaction between iodine and residual starch. This method is the most widely used for α-amylase measurement and is the most industrially relevant for ease of use, preparation and measurement. When α-amylase is added to starch, the starch polymer has the internal α-1,4-glucosidic bonds broken to smaller oligosaccharides and a blue/black colour of the complex becomes clear.

Methods of radial diffusion in agar gels are commonly used in immunological applications for the rapid determination of specific protein levels in large number of samples (Jongsma *et al*., 1993). In this method the targeted enzyme is initially placed into a well of an agar gel: as it diffuses out into the agar gel, a substrate such as starch reacts with the enzyme causing a colour change in the agar. This allows a visual representation of the activity of the enzyme to be shown by the 'halo' region it has created in the agar gel (Figure 4-1). If there is any inhibition of the enzyme, for example, the halo will be smaller than that for a non-inhibited enzyme under the same conditions.

Figure 4-9 Residual amylase activity revealed using the RED assay. The smaller the halo the more thermal processing the amylase has received (100mm plate diameter)

Control of enzymatic assay conditions poses problems at high temperatures (>75°C) (Daniel and Danson, 2001), especially control of temperature and pH, since at temperatures of greater than 100°C most biological substrates have undergone a phase change. Daniel and Danson (2001)

suggested that assaying could be carried out at slightly lower temperatures (60-70°C) especially if assays could be compared to those run at higher temperatures.

Koch *et al*, (1991) used the method devised by Bergmeyer *et al*, (1983) for the measurement of α-amylase activity. 100µl enzyme solution is added to 250µl of sodium acetate buffer (1% starch) so there is an acid hydrolysis of starch producing amylose, pullulan and maltose. These substrates are then identified by HPLC using a HP x 42A column at 85°C. For extracellular enzymes Savchenko *et al*, (2001) devised a technique for purification and testing, for which α-amylase could be permitted, although the route for purification seems overly complicated.

In previous work Randox tests of *P.furiosus* α-amylase were undertaken at 40-50°C with limited success due to the low temperatures and at 90°C the substrate precipitated from solution making it impossible to use (Tucker *et al*., 2006). Other tests proposed by Laderman *et al*. (1993) use a discontinuous assay. Laderman *et al*, (1993) and Tucker *et al*. (2006) used the method of Manning and Campbell (1961) of taking a 20µl sample of α-amylase solution with 1% sodium starch solution added, and 100mM sodium phosphate. This is then incubated at pH7 and 92°C for 10 minutes and 15µl iodine solution is added for colour (4% KI, 1.25% iodine) to a measurable range of 600nm wavelength for optical density measurements. This method however is not applicable for industrial trials due to the complexity of the process, and the time for the assay to be completed. The assay also uses a relatively large volume of amylase due to the amount of data points and hence a large number of individual samples would be needed for each trial. In addition most processing plants would not own the equipment needed for the Laderman *et al*. (1993) assay.

The aim of the this chapter is to propose and demonstrate a low effort, industrially applicable and quick method for both qualitative and quantitative assessment of activity of hyperthermostable amylases, in this case from the archaea *Pyrococcus furiosus*. It is based on the hydrolysis of a starch as a substrate for the enzyme. The gel is solid to above 70°C, and hence works within the temperature range over which *Pyrococcus furiosus* α-amylase will have significant activity. This method is proposed for the rapid evaluation of the amount of thermal processing a target has received, specifically to study thermal distributions in mixing equipment, and sterilisation treatments for the use of Time-Temperature Indicators (TTIs) (Tucker *et al*., 2006; De Cordt *et al*., 1994; Guiavarc'h *et al*., 2003; Van Loey *et al*., 1997).

This Radial Enzymatic Diffusion (RED) assay is then compared and calibrated against more established methods of hyperthermostable α-amylase detection and quantification. Chapter 5 will describe industrial uses of these methods.

4.2 Materials and Method

4.2.1 Production of *P.furiosus* α–amylase

Pyrococcus furiosus was cultivated and α-amylase purified as defined in Chapter 3.

4.2.2 Preparation of the starch-gel plates

An 8g/l Gelrite® (Sigma Aldrich, Poole, UK) solution was heated to >70°C to melt, and mixed with 10g soluble starch (Sigma Aldrich, Poole, UK)/l distilled water. Iodine was added to a level of 5ml/litre Gelrite®–starch solution to form a starch-iodine complex to produce the familiar blue/black staining. After mixing, 20ml was poured into sterile 10cm diameter Petri dishes and

allowed to cool creating a plate ca.1mm depth. Once solidified the plates were stored at 4-8°C. Wells of 4mm diameter were punched in the centre of the plates with a cork borer, and for all experiments fresh plates were used.

4.2.3 The radial enzymatic diffusion (RED) assay

The freeze-dried *P.furiosus* -amylase powder (FDP) was prepared in distilled water (100g FDP/l 0.1M Sodium phosphate buffer pH7) and diluted as required for the preliminary assays. The wells were filled with 20µl of amylase solution of various concentrations and incubated at for various times 70°C (above 70°C the iodine does not stain uniformly and the plates are not solidified). The system was thermally stable at 70°C: incubation for long periods (< 2hrs) at 70°C showed negligible impact of thermal processing on the amylase with no measurable change in activity, due to its high thermo-stability. This is unlike the Laderman *et al*., (1993) discontinuous method shown by Tucker *et al*., (2006), which were assayed at higher temperatures (92°C) where the higher assaying temperatures could increase the amount of thermal processing the amylase has already received thus giving a higher processing value than it actually received.

Any colourless zone (halo) created by the α-amylase hydrolysing the starch 1-4 glycosidic linkages was measured using callipers and digital imaging. The halo may not be exactly circular but is assumed to be circular, so the diameter is taken as an average of 3 measurements around the halo. The influence of substrate concentration on gel plates was evaluated using

(i) different concentrations of starch in the gel (1-8g/l),

(ii) different amounts of enzyme in the test solution, and

(iii)The influence of time and temperature in the development of the halo created.

This was to establish both the type of correlation and more suitable conditions to develop the assay further for industrial use.

4.2.4 Dinitrosalicylic acid (DNS) assay for detection of reducing sugars due to amylase activity

The DNS assay (Miller, 1959) was used as an alternative assay to measure the amount of activity of the *Pyrococcus furiosus* α-amylase so that the RED plate assay could be calibrated and validated.

The DNS assay uses 0.5ml of 1% starch which is added to 0.5ml 0.1M sodium acetate buffer (pH 5.5), and 50µl of enzymatic solution (100 g/l buffer). The mixture was then incubated at 90°C for 60 minutes and the reaction stopped by cooling on ice. The amount of reducing sugar was then determined by dinitrosalicylic acid (DNS), an aromatic compound that reacts with reducing sugars to form 3, 5-nitrosalicylic acid which absorbs light strongly at 540nm. This shows the amount of reducing sugars that have been created due to the hydrolysis of starch by the *Pyrococcus furiosus* α-amylase. 1ml DNS reagent, 1% (10g DNS, 0.5g Sodium sulphate, 10g Sodium hydroxide / l water) added to the sample solution and incubated at 90°C for 10 minutes to develop the red-brown colour. 0.3ml potassium sodium tartrate, 40%, solution is added to stabilise the colour and absorbance read at 540nm. The greater the absorbance the more reducing

sugars are present and therefore a greater amylase activity. A calibration curve was produced (Figure 4-2) and the residual activity was calculated by Eq. 4-6.

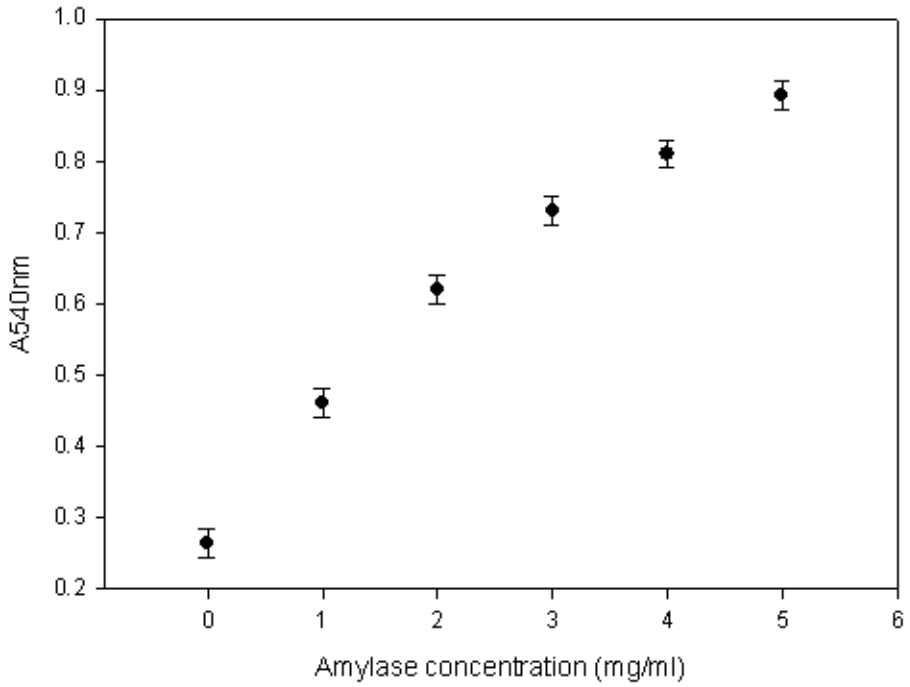

Figure 4-10 Absorbance as a function of amylase concentration for DNS assay. The data is the mean of 3 replicates.

4.2.5 Modeling the behavior of the radial assay

A model was built in MATLAB® to attempt to reproduce features of the experimental measurements of halo formation. A one-dimensional radial model was used. At the start of the experiment, amylase is placed in a small circle with radius R (mm) and then slowly amylase diffuses and reacts with starch in the gel resulting in a change of colour. The assumptions used in developing the model were as follows

(i) amylase diffuses only in the radial direction;

(ii) the starch gel is stationary and semi-infinite;

(iii) plates are homogeneous;

(iv) hydrolysis is much faster than diffusion (El-Saied *et al*., 1978), so the reaction can be considered as instantaneous and hence no reaction term is required in the diffusion equation.

The equation solved is then:

$$\frac{\partial c}{\partial t} = -D\frac{1}{r}\frac{\partial}{\partial r}\left[r\frac{\partial c}{\partial r}\right] \qquad (4\text{-}1)$$

Where c is the amylase concentration and D the effective diffusivity. The concentration is a function of time and radial position. The initial amount of amylase is added in a small well of diameter R =4 mm. Initial conditions are:

When t=0; $c=c_{(t=0)}$ at r=R and c=0 at r>R (4-2)

Throughout: c=0 at r=∞ (4-3)

As time progresses, the concentration in the central well (c_0) will decrease. The variation of c_o is given by mass balance as:

$$\pi R^2 d\frac{dc_o}{dt} = -2\pi R.d.D\left(\frac{\partial c}{\partial r}\right)_{r=R} \qquad (4\text{-}4)$$

Where d is the depth of the plate and R the well radius; simplifying gives

$$\frac{R}{2}\frac{dc_o}{dt} = -D\left(\frac{\partial c}{\partial r}\right)_{r=R} \qquad \text{for } r > R \qquad \text{and } c = c_0 \qquad r \leq R \qquad (4\text{-}5)$$

Equations (4-1) and (4-5) were solved using a MATLAB® function to give the amylase concentration as a function of time and radial position. It is assumed that there is some critical concentration of α-amylase needed to decolourise the iodine and thus for the halo to appear. The critical concentration was set at 1% of the original concentration of the well, ~0.05 mg/ml within the model. The model was then fitted to the experimental results using a MATLAB® optimization function to obtain effective diffusivity, D (m^2s^{-1}).

4.3 Identification of Optimal Assay Conditions

Radial enzymatic diffusion plates give a visual representation as the -amylase cleaves randomly the α-1, 4-glucosidic linkages to change the blue/black starch-iodine complex to a clear colour when the starch is hydrolyzed to oligosaccharides. This can be seen in Figure 4-1 where the plates and α-amylase are shown for different amounts of residual activity. For the assay to be used industrially the optimal assay conditions have to be selected.

4.3.1 Selection of assay conditions

4.3.1.1 Variation of starch substrate concentration

Experiments were carried out to investigate the effect of starch concentration on the halo produced for a given amount of enzyme activity. Results are shown in Figure 4-3 for

experiments using a constant incubation temperature of 70°C, incubation time of 4 hours, and enzyme concentration of 5mg enzyme/ml buffer. The relationship between halo diameter and starch concentration show a linear correlation over the experimental range tested. The variation of the halo diameter between experiments, using homogeneous plates from the same batch, at the same temperature, is much smaller than the variation between diameters for different process conditions.

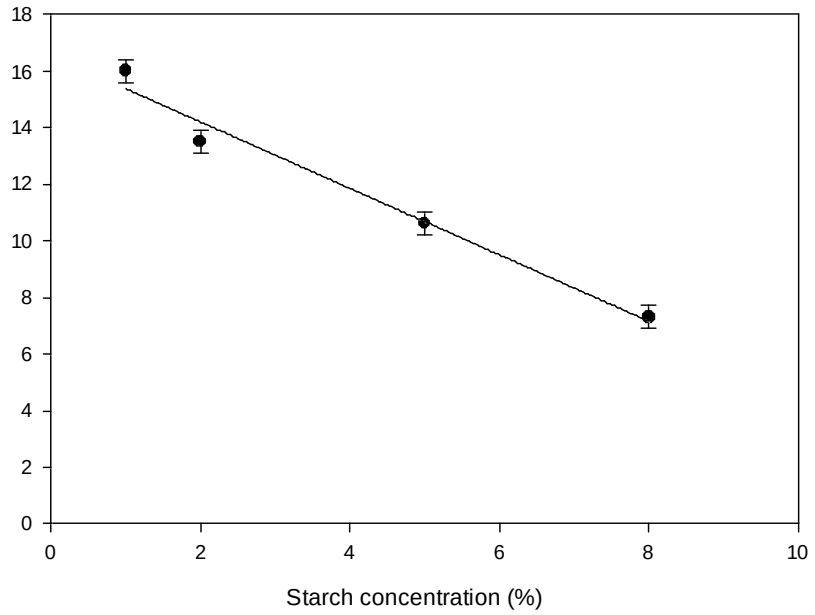

Figure 4-11 Halo diameters as a function of starch concentration in the gel for experiments at constant concentration of 5 mg/ml α-amylase and 4 hours incubation time at 70°C. Error bars show average of 3 halos.

The results shown in Figure 4-3 are for an average of 3 replicates. The lower the starch concentration, the larger the halo diameter for the same conditions and thus the more accurate the measurement. However gels containing a low amount of starch (~0.5%) did not always solidify

uniformly, so a concentration of 1% starch was selected for all other work, as this was the lowest concentration which gave a homogeneous gel plate while ensuring the largest size halo.

4.3.1.2 Variation of incubation time

A set of experiments were carried out for various incubation times and starch concentrations plates, a 5mg/ml enzyme concentration, and 70°C incubation temperature to investigate the effect of the incubation time of the plates on the assay. Data is shown in Figure 4-4 for the change in halo diameter with time for a single experiment. In the first 30 minutes there is a comparatively sharp increase in halo diameter from the 4mm of the starting conditions. Beyond this time the diameter of the halo increases to a lesser extent. Assays were performed using different starch concentrations of 1%, 2%, 5% and 8%, as shown in Figure 4-4. As the halo diameter increases, the actual absolute error stays constant (1 mm) and the percentage error of measurement decreases.

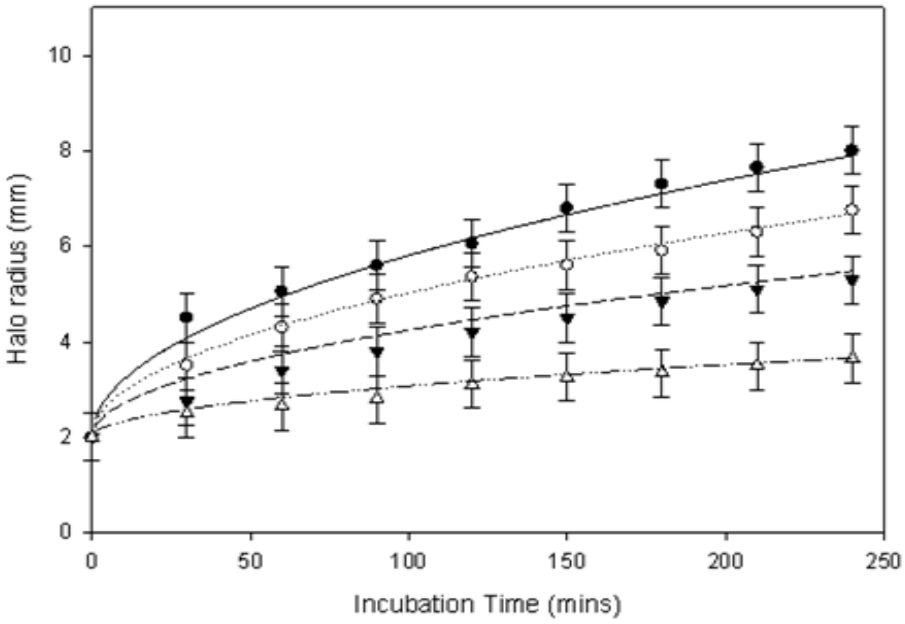

Figure 4-12 Halo radius as a function of RED plate incubation time at 70°C with a 5 mg/ml α-amylase concentration for 1% (□), 2% (□), 5% (▼), and 8% (Δ) starch plates. Lines are the theoretical model associated with each starch concentration plate.

Figure 4-4 shows that the change in halo radius is easiest to measure at the lowest starch concentration, confirming the results of 4.3.1.1. Four hour incubation times were chosen as the halo diameter is the largest shown.

4.3.1.3 Variation of enzyme concentration

The next experiments were carried out using the 1% starch gel, a constant incubation temperature of 70°C and 4 hours incubation time, to measure the influence of the initial concentration of enzyme on the diffusion area. Results are shown in Figure 4-5. The halo diameter measured on the plate increases as the concentration of α-amylase initially in the well increases.

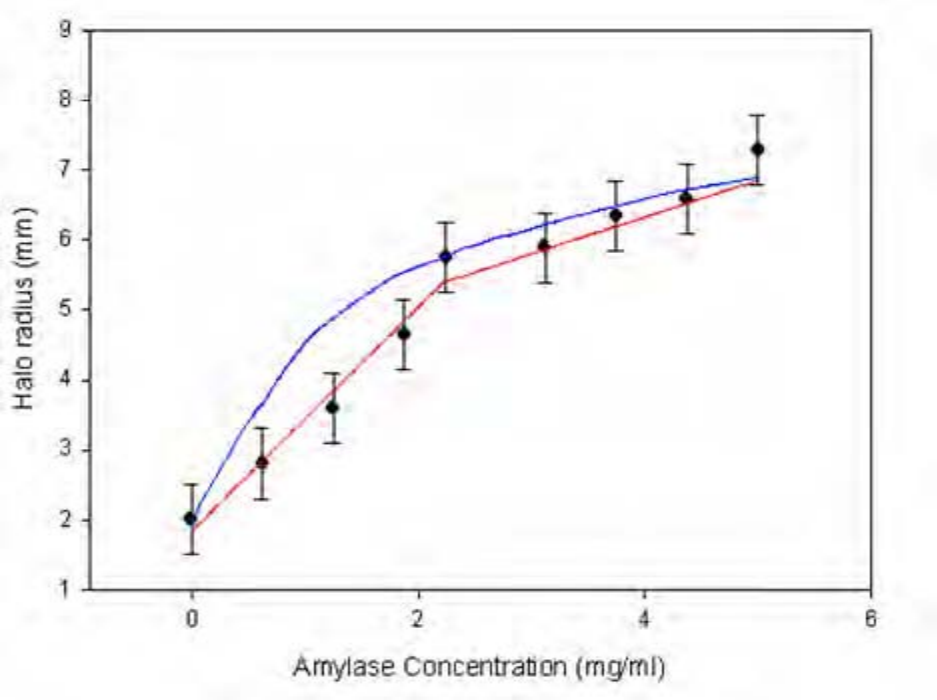

Figure 4-13 Halo diameters as a function of amylase concentration (1% starch gel plate, 4 hours incubation at 70°C). Experimental data (▯) was shown against the assay model fit (—), and double linear fit (—).

Figure 4-5 shows that the data can be fitted to two straight lines which intersect at 2.5 mg/ml. At about this amount of amylase the rate of expansion of the halo area with increasing concentration decreases. Similar behaviour was found by Fernandez *et al*., (2001) for aquaculture and fish amylases.

4.3.1.4 Variation of incubation temperature

The influence of temperature of incubation of the plates can be seen in Figure 4-6, over different incubation times. Not surprisingly for a hyperthermophilic enzyme, as the temperature increases the activity increases (the mechanism will be explored in §6). For a set incubation time of 4 hours, Figure 4-6(a) shows the effects of temperature on the activity of the amylase which can visually be shown as Figure 4-6(b). Up until the optimal temperature (T_{opt}) of *Pyrococcus*

furiosus α-amylase this plot (Figure 4-6(b)) will increase, then after this point (if the assay was viable and the plates stayed solid) it would be expected that there would then be a conflict between an increase in diffusion and rate kinetics due to the temperature, and the denaturing of the enzyme reducing the residual activity. Figure 4-6(c) shows the RED assay plates at two different temperatures for the same incubation time.

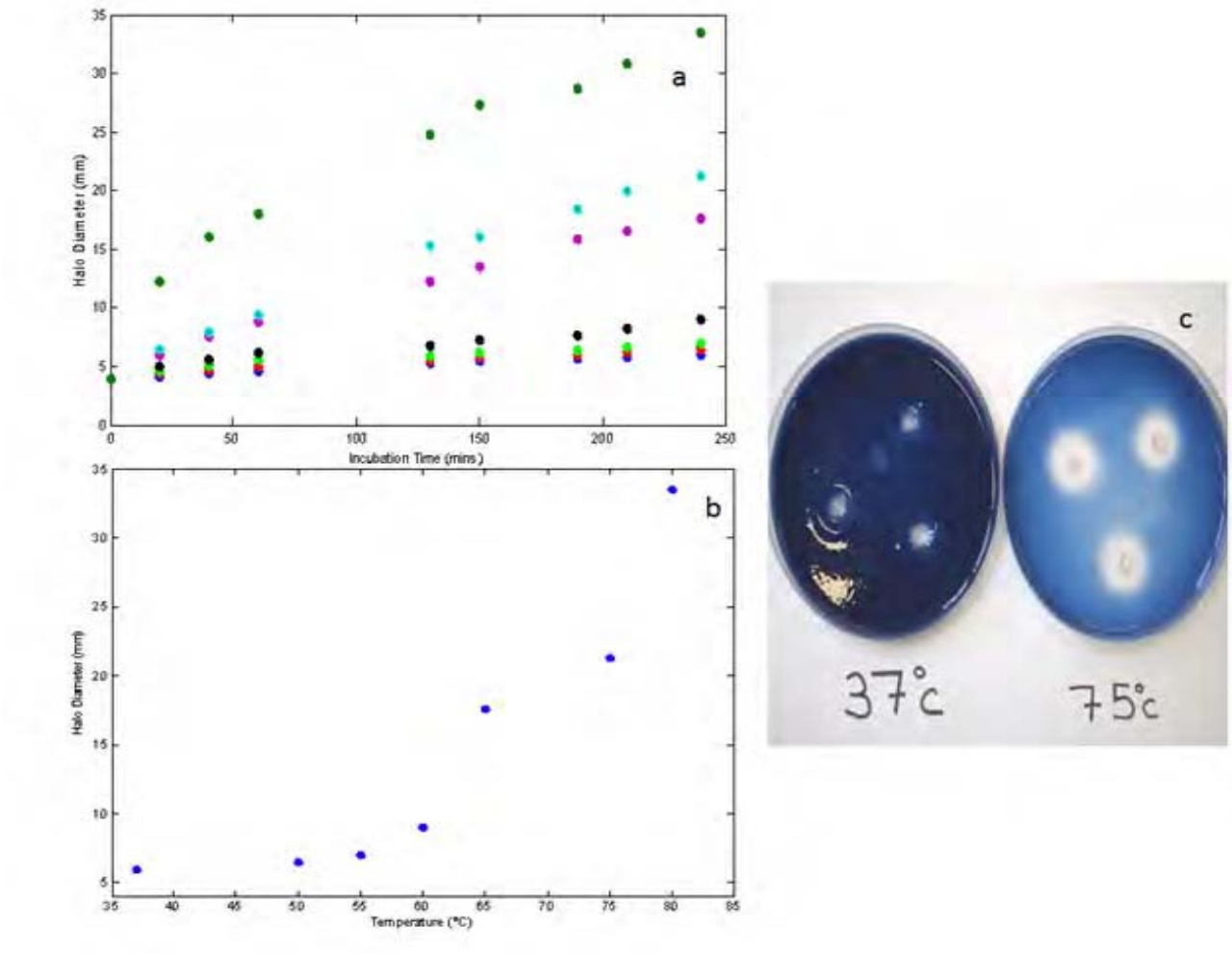

Figure 4-6 Halo diameter as a function of incubation temperature of the RED plates (a) at 37°C(?) 50°C(?) 55°C(?) 60°C(?) 65°C(?) 70°C(?) 80°C(?) (b) over an incubation time of 4 hours (c) RED assay plates at 37°C and 75°C (plate 100mm diameter)

4.3.1.5 Optimal Assay Conditions

The optimal conditions found for developing the assays were 1% starch, 4 hours plate incubation at 70°C, and 5 mg/ml amylase concentration. RED plates were then used to evaluate the residual amylase activity after various isothermal processing profiles.

The detection limits of the assay using optimal conditions above were assessed for using calipers with an absolute error of measurement of ± 0.5 mm.

4.3.2 Modeling of Radial Enzymatic Diffusion (RED) assay behavior

The program was first run to generate concentration profiles for the assay. Representative data is shown in Figures 4-7a and 4-7b; Figure 4-7a shows diffusion for the case where c_0 stays essentially constant, whilst Figure 4-7b shows the case where c_0 is depleted, leading to lower diffusion rates.

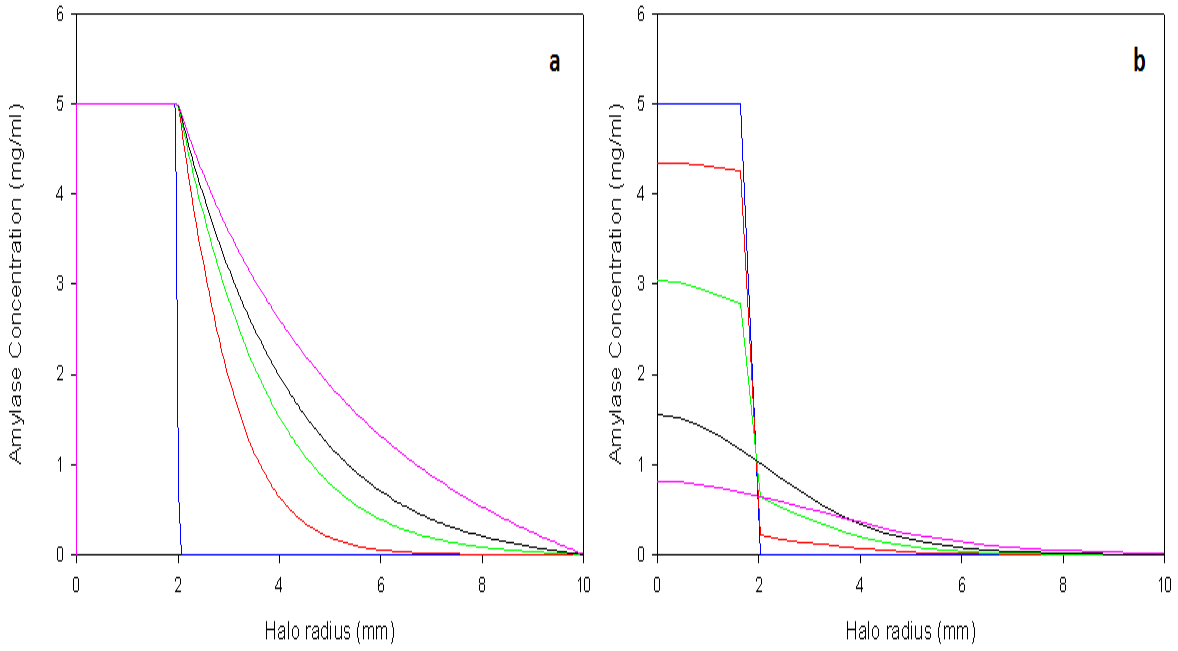

Figure 4-7 Theoretical model describing (a) diffusion of amylase from the well where c0 remains constant (b) diffusion of amylase from the well where c0 is depleted at time 0 min (—), 20 min (—), 60 min (—), 120 min (—) and 240 min (—).

Figure 4-4 shows data for the halo radius and the model, assuming that the threshold for decolourisation occurs at c = 0.05mg/ml and assuming constant diffusivity. The diffusivities of the different concentrations of starch in the assay plates used in the model can be seen in Table 4-1.

Table 4-2 Diffusion Co-efficient of the RED starch plates calculated from the model

Plate Starch Concentration (%)	Diffusion Co-efficient (m^2s^{-1})
1	$2.42x10^{-8}$
2	$1.14x10^{-8}$
5	$0.50x10^{-8}$
8	$0.10x10^{-8}$

Finally Figure 4-5 shows the data for the halo radius as a function of amylase concentration for the conditions of 1% starch gel plate and 4 hours incubation time at 70°C together with the corresponding model curve. Curve fitting analysis was undertaken for the best way to describe the experimental data for a standard curve (Table 4-2).

Table 4-3 Curve fitting analysis for halo radius as a function of amylase concentration

Curve Fit	Equation	R^2	SSE
Linear Fit	y = 1.04x + 2.4	0.94	1.615
Double Linear Fit	y = 1.605x + 1.834 y = 0.528x + 4.218	0.95	0.340
Assay Model		0.875	3.385

As seen in Figure 4-5 the model overestimated the halo radius at low concentrations of amylase in the well, while at higher concentration of amylase, the model tended to underestimate the halo diameter and keep doing so as the concentration is increased past the experimental boundaries set in this study. This suggests that the phenomenon is not accurately described by Fickian diffusion; the process is one of diffusion-reaction rather than diffusion alone. A linear relationship could be used for a standard calibration curve for calculation of residual activities as it showed a reasonable fit (R^2=0.94) to the data, a double linear fit was found to be best with the point of inflection, where the two straight plots meet, at c = 2.25mg/ml (R^2=0.95).

4.4 Determination of α–amylase kinetic parameters

The previous sections have demonstrated the accuracy of the assay. To validate the assay as a tool for possible industrial use, z values of *Pyrococcus furiosus* α-amylase were calculated using both the RED and DNS assays and the data compared to the results of Tucker *et al*., (2007). If the data of all three assays compare favourably then it is reasonable to assume the assay is validated.

Samples of amylase were taken and divided; some were processed through defined time-temperature profiles and some were left unprocessed. Using the RED assay, samples were then assayed at the optimal conditions and the halo diameters measured. Data from the plates was converted into residual activities from the following equation, first by using the double linear fit calibration in Figure 4-5 to calculate the concentrations of amylase, and then calculating residual activity as

$$Activity = \left(\frac{c_{processed}}{c_{initial}} \right) x100\% \qquad (4\text{-}6)$$

A series of experiments were carried out in which -amylase was exposed to temperatures of 115°C, 117°C, 121°C and 125°C, for 0, 3, 6, 9, 15, 20 and 25 minutes respectively. The experiments used FDP at 5 mg/ml enzyme concentration in solution. The enzyme was enclosed in 15 mm lengths of 3 mm diameter silicone tubing that was immersed in a well mixed glycerol bath and cooled by quenching in ice (the method described by Mehauden *et al*., 2007). Combination of processing temperature and time decreased the residual activity which is

reflected in a decrease in halo diameter in the RED plates (Figure 4-1). The log of residual activity is plotted as a function of the incubation time in Figure 4-8a.

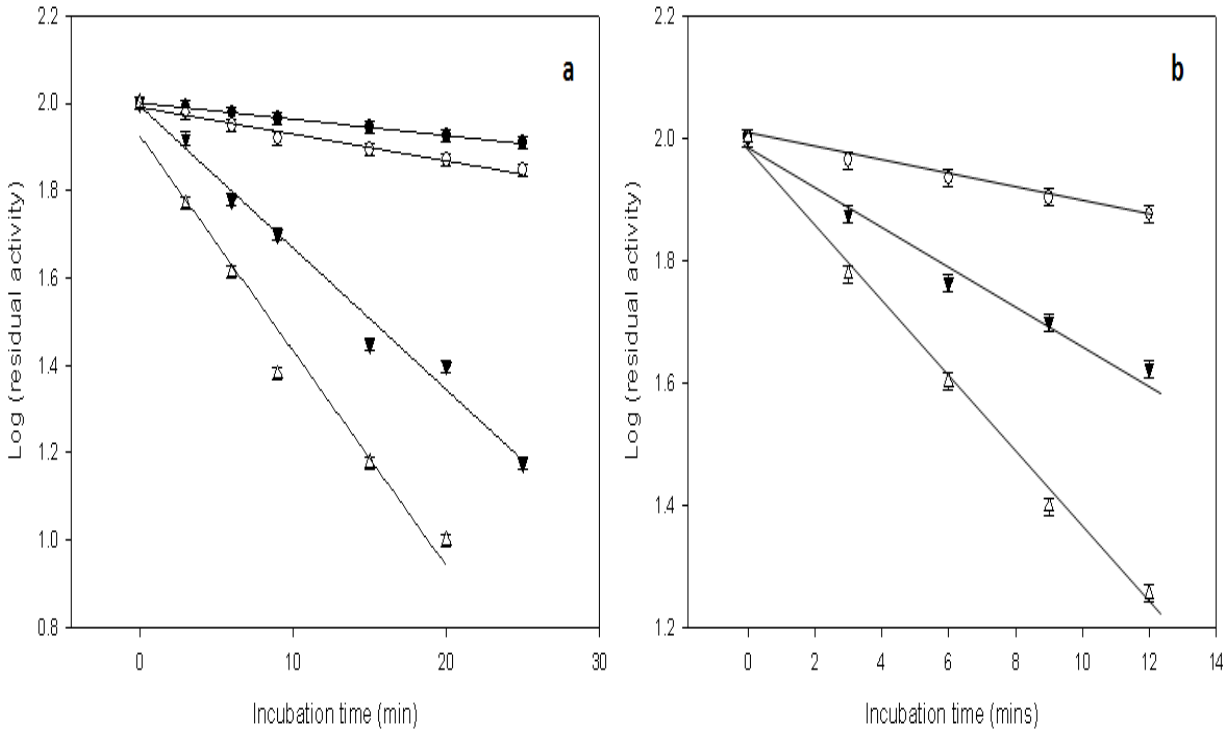

Figure 4-8 Effects of isothermal processing on residual activity of *Pyrococcus furiosus* α-amylase using the (a) RED assay and (b) the DNS assay; expressed as the logarithm of residual activity for 115°C (□), 117°C (□), 121°C (▼) and 125°C (Δ). For the RED assay the curve co-efficient (k) for 115°C is -0.003x, 117°C is -0.006x, 121°C is -0.040x and 125°C is -0.067x. For the DNS assay the curve equation for 117°C is -0.01x+1.997, 121°C is -0.031x+1.978 and 125°C is -0.062x+1.98.

Similarly, experiments were carried out in which samples of the α-amylase were exposed to isothermal time-temperature profiles of 117°C, 121°C and 125°C for 0, 3, 6, 9 and 12 minutes. These were then processed by the DNS assay: data could then be compared with the RED plates. The residual activity curve can be seen in Figure 4-8b, and the α-amylase shows a log-linear loss of activity.

For both assays, the decimal reduction time, *D*, for each temperature was calculated from the curve co-efficient (slope), k, of the lines in Figure 4-8 where;

$$D = \frac{1}{k} \qquad (4\text{-}7)$$

D values for the two assays are given in Table 4-3.

Table 4-4 z values for the thermal inactivation of *Pyrococcus furiosus* α-amylase based on different assay methods.

Assay	$D_{121°C}$ value (min)	*z* value (°C)
RED plate assay	25±2	11.3±1
DNS assay	32.3±2	10.1±0.5
Discontinuous spectrophotometer assay shown by Tucker *et al*. (2007)	24±2	9.95±0.5

Figure 4-9 plots the logarithm of the *D* value against temperature for the different methods. In both cases, there is a linear relationship between log *D* values and temperature which allows the *z* value to be calculated (Tucker *et al*., 2007). The *z* value describes the temperature sensitivity of the rate of inactivation of *P. furiosus* α-amylase. For the different assays that are presented in this study to be comparable the z value determined should be independent of the assay applied to determine the residual activity.

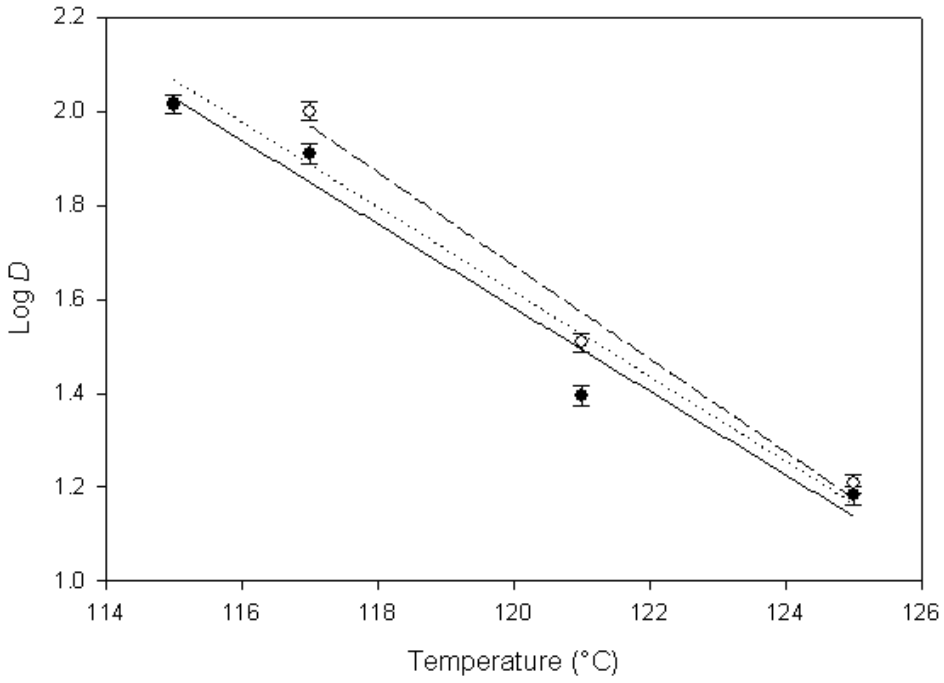

Figure 4-9 The z value curve using the RED assay (⍰). Fitting curve equation y=-0.0909x+12.49 (—) and the DNS assay (⍰). Fitting curve equation y=-0.099x +13.55 (----). Fitting curve equation for RED and DNS assays y=-0.09015+12.43 (•••••).

z values for both the RED plates and the DNS assay along with those reported by Tucker *et al*. (2007) are shown in Table 4-3. Tucker *et al*. (2007) and Laderman *et al*. (1993) used a discontinuous spectrophotometer assay at 92°C which took longer and was more difficult to assay than the RED assay shown in this paper.

4.5 Conclusion

The use of high-temperature-stable amylases has been shown in Chapter 2 and section 3.1 as an attractive route for the development of a sterilisation TTI. The problem is finding an efficient assay that is simple and efficient to use so that the TTI can be used in an industrial environment.

The Radial Enzymatic Diffusion (RED) assay has been developed and tested here as a possible assay.

The RED assay works by placing amylase in the centre of a plate made from starch-containing agar stained with iodine. The amylase diffuses out into the gel and reacts with the starch, resulting in decolourisation of the iodine, forming a round halo. The best conditions for the assay were identified as: 1% starch, incubation temperature of 70°C for a time of 4hours. The accuracy of the assay is such that radii can be measured to ±0.5 mm.

A low concentration of starch in the plates decreases the assay time by increasing the diffusion co-efficient of the gel, and hence 1% starch concentration was chosen. The effect of temperature was also reviewed. The effect of temperature showed that using the maximum temperature for processing decreases the assay time substantially because the activity of the -amylase is increased as well as decreasing the diffusion co-efficient of the gel plate. The temperature could be increased past 70°C with more than 8g/l Gelrite® added to the plate, although this would have a detrimental effect on the diffusion co-efficient and hence there is a comparative study between increasing the activity of the -amylase and increasing the diffusion co-efficient of the RED plate gel. 4 hours incubation time was chosen for this study as it gives a high halo diameter for the α-amylase concentration used, and this lowering the potential percentage error in reading the gel plates.

To validate the RED assay as a tool for possible industrial use, *z* values of *Pyrococcus furiosus* α-amylase were calculated using both the RED and DNS assays and the data compared to the results of Tucker *et al*., (2007). If the data of all three assays compare favourably then it could be

reasonable to assume the assay is validated against these more used assay techniques. Thermal kinetic parameters measured from the RED plate assay compare favorably both with those reported by Tucker *et al.* (2007) and with the DNS assay. The *D* value matches the value stated by Tucker *et al.* (2007) of 24-25 minutes. The *z* values for all assays are similar; with the RED plate assay z value the least temperature sensitive at 13.1°C. This though is still comparable to the other assays.

The RED plate assay was modeled against Fickian diffusion to view how the concentration of α-amylase diffuses across the gel plate and how the experimental results compared to the theoretical model of Fickian diffusion. The assumptions applied in the model in section 3.2.5 hold up as the model is a good fit for halo radius as a function of RED plate incubation time, for different starch concentrations.

The model fits the data well using diffusivity as an adjustable parameter; fitted diffusivities for the different concentrations of starch in the assay plates used in the model. A simple diffusion model is not correct as the process involves diffusion and reaction; this can be seen as the 'diffusivity' is a function of concentration. However the fit to the data suggests that the assumption of constant c_0 is appropriate. The computational model follows the shape of the halo diameter as a function of enzyme concentration curve but is only a reasonable fit to the data, showing that a more detailed model is needed. A linear relationship could be used for a standard calibration curve for calculation of residual activities as it showed good fit (R^2=0.94) to the data, but a double linear fir was found to be best with the point of inflection, where the two straight plots meet, at c=2.25mg/ml (R^2=0.95).

The advantage of the RED plate assay may be in an industrial setting because of the ease of the experiment, and the limited equipment needed. Spectrophotometer or titrimetric assays (such as the DNS and assay used by Tucker et al, 2007) are suitable for highly accurate determination, although these methods are time consuming. RED plates offer a cheap, rapid and sensitive method for the assessment of highly thermostable α-amylase. The method would require a series of preprepared plates and reagents. The plate assay would make it very clear if materials had been underprocessed; full sterilization would give a low halo radius whilst an unprocessed sample would have a high radius. The method could thus be used rapidly to identify safe production.

Chapter 5

TTI Validation Study and Industrial Trial

5.1 Introduction

TTIs have the potential to be used in place of thermocouples and data loggers as a monitoring technique for food safety in industry. As discussed in previous chapters, the use of TTIs for process validation is a relatively new technique for pasteurisation and has not been successfully developed for sterilisation processes. Enzymatic TTIs have been shown to be successful within a variety of pasteurisation processes (Hendrickx *et al*., 1995; Maesmans *et al*., 1994; De Cordt *et al*., 1994; Van Loey *et al*., 1996; Mehauden *et al*., 2007; 2008). The reliability of TTIs under non-isothermal conditions for pasteurisation has shown a direct correlation between TTI response and food quality (Taoukis *et al*., 1989). The *z* value (temperature sensitivity) of the enzyme should ideally be the same or very close to that of the target micro-organism (Hendrickx *et al*., 1995; Richardson, 2001). Work by Tucker *et al*. (2007) and Van Loey *et al*. (1997) have shown that *z* values of different α-amylases are suitable for the target of *C.botulinum* as α-amylases can be manipulated to have a *z* value of around 10°C.

Pasteurisation TTIs have mostly concentrated on α-amylase from *B.subtillis, B.licheniformis* and *B.amyloliquefaciens* (Mehauden *et al*., 2007), while De Cordt *et al*. (1994), Guiavarc'h *et al*. (2004) and Van Loey *et al*, (1994) have demonstrated the use of these enzymes within a sterilisation TTI. The amylase was entrapped on glass beads, and although this lowered the

aggregation of amylase and so worked well at very low *F* values, the denaturation occurred quickly as the *F* value increased slowly, so it was not ideal for sterilisation TTIs.

Previous chapters have described the preparation of α-amylase which is highly thermostable at sterilisation temperatures and can partially survive processing at 121°C for an industrially applicable period ($F_{121°C}$ = 3-30 minutes). *Pyrococcus furiosus* has previously been studied briefly for use in sterilisation TTIs (Tucker *et al*., 2007) because of the reported heat sensitivity that it possesses (Koch *et al*., 1990), and Tucker *et al*. (2007) found an initial *z* value of 9.9°C, which is very close to the ideal target pathogen *C.botulinum* spore *z* value of 10°C. This makes *Pyrococcus furiosus* α-amylase a strong candidate for sterilisation TTIs and to be investigated properly.

An extensive validation process for the sterilisation TTIs is required before they can be used in industry for monitoring heat treatment efficiency of foods. It is essential to know the accuracy and reliability of any sterilisation TTI.

This chapter will describe the TTI validation tests performed. First the kinetic parameters were determined, and then the TTI accuracy and reliability over process duration was studied. A set of time-temperature profiles, in which free flowing TTIs were placed in various fluids was studied to analyse heating rate effects on amylase activity. In addition, once the physical parameters of the TTI were established then an industrially relevant trial was undertaken using real foods sterilised in cans within model sterilisation retorts.

5.2 TTI validation study

This section describes the methods used to determine the efficiency of TTIs for food sterilisation conditions. Most of the work described was performed on *Pyrococcus furiosus* α-amylase from a native strain of the micro-organism but some work was also performed on amylopullanase from *Pyrococcus furiosus*. The use of amylopullanase as a test system for sterilisation TTIs has been described in chapter 3.

5.2.1 Production of *Pyrococcus furiosus* α-amylase

Pyrococcus furiosus was cultivated and purified as described in §3.2. The freeze-dried powder was resuspended at 5mg/ml 100mM sodium acetate buffer pH6. The solution was prepared freshly for each batch of TTIs.

5.2.2 Preparation of TTIs

TTI tubes were made from silicone tubing of 2.5 mm bore and 0.5 mm wall (Altec; Alton, Hampshire) cut into 10-15 mm lengths. One end was sealed by dipping it into uncured Sylgard 170 elastomer (VWR International Ltd) and allowing capillary action to draw 2–3 mm of liquid up the tube and left to solidify. A minimum of 25 µl of the FDP solution was injected into each plugged tube and uncured Sylgard 170 was drawn into the other end of the tube to form another 2–3 mm plug. Care was required to prevent drying of the solution or thermal damage to the amylase. Once the FDP solution was encapsulated the TTI tubes were ready for use. Filled TTI tubes were stored in frozen distilled water at -18°C until ready for use.

5.2.3 The radial enzymatic diffusion assay (RED)

Measurements of the residual activity of the processed *Pyrococcus furiosus* α-amylase used the radial enzymatic diffusion assay developed and validated in chapter 4. The radial enzymatic diffusion assay was carried out under optimal conditions using 1% starch gel plates and 4hrs incubation time at 70°C incubation temperature.

5.2.4 Determination of the sterilisation value

Sterilisation values (*F* values) numerically describe the impact of heat processing from an applied time-temperature profile. *F* is defined as the equivalent amount of time at a reference temperature of 121°C; a target would have to have to receive the same amount of thermal processing. The time-temperature profile may change but the *F* value could stay the same.

Measurements of the thermal processing using thermocouples and data-loggers can be calculated using the equation:

$$F = \int_0^t 10^{\frac{T(t)-T_{ref}}{z}} .dt \qquad (5\text{-}1)$$

This equation needs prior knowledge either of the target micro-organisms or of the enzyme's thermal resistance in terms of the *z* value.

When the inactivation is a first order reaction, the *F* value measured by the TTIs can be calculated using the equation:

$$F = D \cdot log\left(\frac{A_{initial}}{A_{final}}\right) \quad (5\text{-}2)$$

Where $A_{initial}$ / A_{final} , is the ratio of the enzyme activities before and after heat treatment measured by the RED assay. This equation needs prior knowledge of the enzyme *D* value to be able to calculate the thermal processing imposed on it. Combining equations (1) and (2) gives:

$$F = \int_0^t 10^{\frac{T(t)-T_{ref}}{z}}.dt = D \cdot log\left(\frac{A_{initial}}{A_{final}}\right) \quad (5\text{-}3)$$

where,

F is the sterilisation value calculated at the reference temperature (T_{ref}), minutes

A_{final} is the final activity

$A_{initial}$ is the initial activity

D is the decimal reduction time at the reference temperature (T_{ref}), minutes

T_{ref} is the reference temperature (for sterilization 121°C)

t is the process time, minutes

z is the temperature change required to effect a ten-fold change in the D_T value (°C)

5.3 Isothermal experiments

Determination of the enzyme kinetic parameters is important as it determines the D value used in subsequent *F* value calculations. A first set of experiments was carried out to study the behaviour of the enzyme under conditions where it was held at constant raised temperature for a series of times. The experimental design and time-temperature profiles used for the determination of the *z* and *D* value were chosen around the sterilisation reference temperature of 121°C.

5.3.1 Evaluations of D and z-values under isothermal conditions

Kinetic data was determined from a series of isothermal experiments. The evaluation of *D* and *z* values under isothermal conditions has been described in chapter 4 and shown in Table 4-3. The *D* and *z* values were calculated as 25 minutes and 11.3°C respectively at 121°C, and these were used for all future experimental calculations. These are within the range applicable to the *botulinum* cook. To monitor safety of sterilisation processes, spores of proteolytic strains of *Clostridium botulinum*, characterized by a *z* value of 10°C, are generally accepted as target microorganisms (Van Loey *et al*., 1997). *Pyrococcus furiosus* α-amylase is therefore ideal for measurement of bacterial spore destruction.

5.3.2 Thermocouple error effects on F value

Thermocouples used are accurate to $\pm$0.5°C. The effect of this error is transferred into an associated error in the *F* value. This effect of the absolute error of the thermocouple reading on the error in *F* value calculations using the mathematical model can be seen in Figure 5-1. The error in *F* value resulting in the error in temperature can be seen as Eq 5-4.

$$\frac{\pm\Delta F}{F} = 10^{\frac{\pm\Delta T}{z}} \quad (5\text{-}4)$$

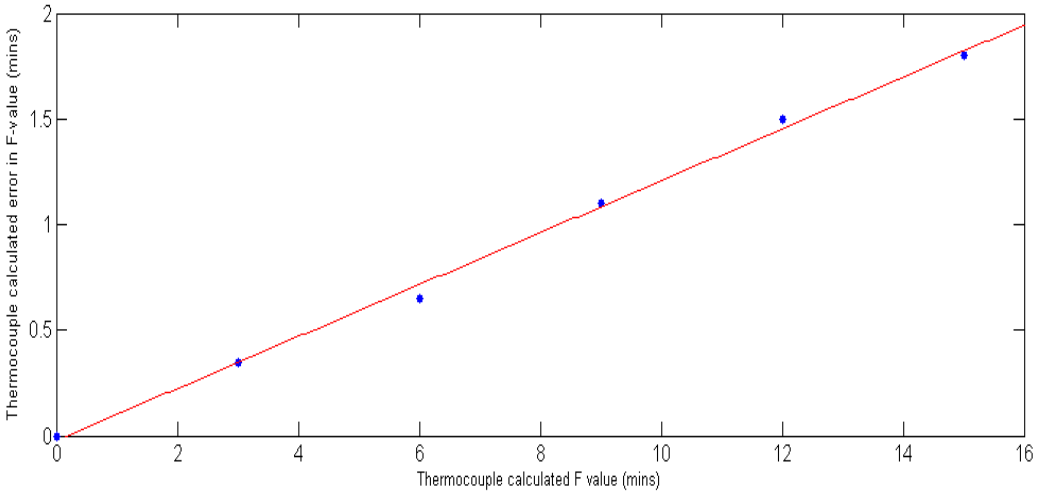

Figure 5-14 *F* value error from thermocouple accuracy

The error in *F* value increased linearly as the amount of thermal processing is increased. So at small *F* values there is a small corresponding error. The error resulting from the thermocouples accuracy corresponds to an approximate 10% error in calculated *F* value. This inbuilt error in the thermocouple is much smaller than that of the error involved in TTIs and the assays described in chapter 4.

5.3.3 Effects of heat treatment

One of the drawbacks of TTIs compared with thermocouples and data-loggers is that TTIs are measuring the thermal denaturation of an enzyme. When the enzyme is denatured further measurement of the thermal process is not possible. Therefore TTIs have a maximum effective life within the process: after some point the enzyme will have denatured to the point where it is

no longer possible to use it. According to the type of α-amylase chosen and hence its kinetic parameters of *D* and *z*, the length of time in which the enzyme can work will vary. The following experiment checked the maximum time that the TTIs made *Pyrococcus furiosus* α-amylase could be used.

Tucker *et al*., (2002) and Mehauden (2008, PhD thesis) showed that amylase activity could be measured accurately for 2 log reductions of activity for pasteurisation TTIs of *Bacillus licheniformis* and *Bacillus amyloliquefaciens* using the Randox method and therefore, TTIs could be used for durations equal to 2 × *D* values at 85˚C. This assumption was then tested for sterilisation temperatures at 121°C using *Pyrococcus furiosus* α-amylase. Isothermal treatments were applied using a glycerol bath and the heat treatment duration at 121°C for the enzyme was converted into *F* values for the various thermal processes.

Pyrococcus furiosus α-amylase was subjected at hold times up to 40 minutes at 121°C (~2 × $D_{121°C}$). As the industrial safety standard is $F_{121°C}$ = 3 minutes this was thought to be in the right range. Figure 5-2 shows the *F* values measured from the TTIs for the isothermal experiments plotted against the process time (time that the TTIs stayed in the glycerol bath at 121°C). The y = x curve plotted on Figure 5-2 represents the ideal relationship between TTIs and process time at 121°C. Fitting the data gives R^2 values of 0.82 over 40 minutes, but if the process time is shortened the R^2 increases to 0.89 at 30 minutes and 0.94 at 15 minutes hence showing better agreement. At 15 minutes the residual activity is 30% and at 30 minutes it is 10% (see Figure 5-5), so the assay becomes less sensitive. The data suggests that if the α-amylase is processed more than 15 minutes it loses accuracy and this occurs increasingly rapidly after 30 minutes. In this instance the maximal heat treatment duration is possibly 2 × *D* values at 121°C.

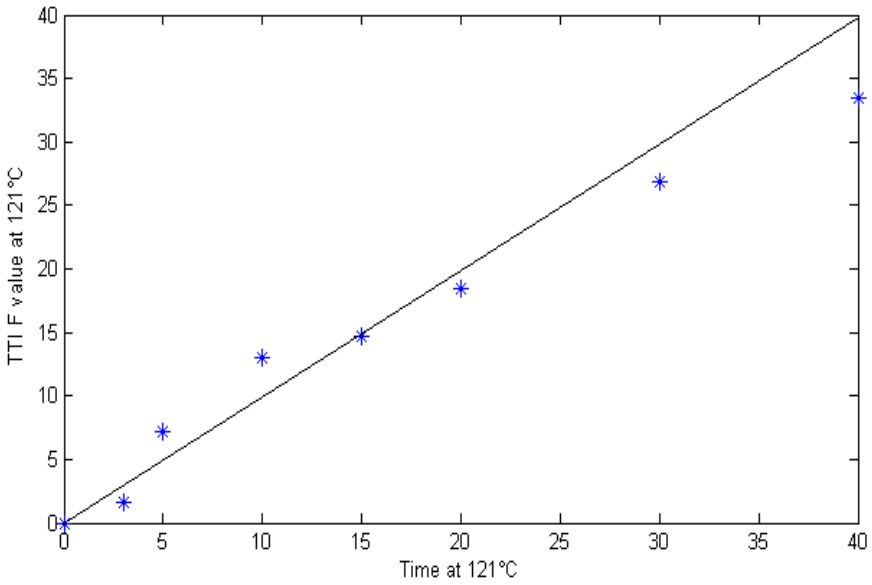

Figure 5-15 Process time at 121°C verses TTIs $F_{121°C}$ value Ideal relationship Y=X [—]

5.3.4 Temperature effects on sterilisation TTIs

The effect of hold temperature on a *Pyrococcus furiosus* α-amylase TTI was examined using isothermal processing. Keeping the *F* value constant and varying the temperatures also means a difference in the process hold time. Here α-amylase TTIs were held at a variety of temperatures and times to establish the range over which they could be accurately used. A common F_0 of 6 minutes was used. This corresponds to;

- 4536 seconds at 110°C
- 1434 seconds at 115°C
- 360 seconds at 121°C

- 144 seconds at 125°C

The temperature dependence of the process time is very large as illustrated in Figure 5-3.

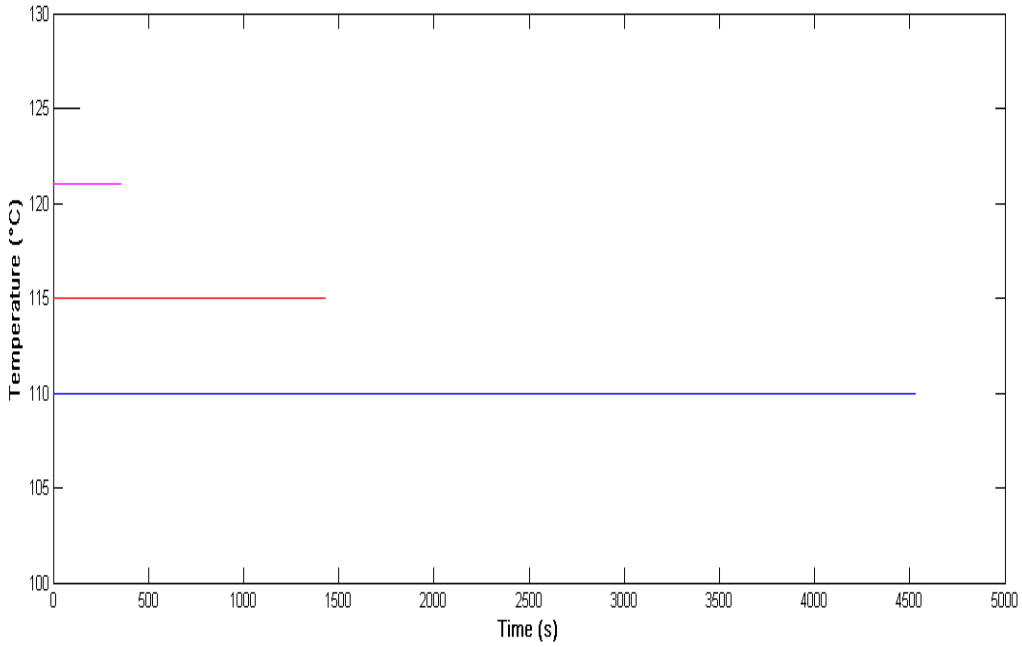

Figure 5-16 Hold time length at different temperatures to give F_0=6 minutes for z=11.3°C

The TTIs were immersed in a glycerol bath at constant temperature and at the end of the experiment cooled rapidly in ice as referred to in chapter 4.

The results, shown in Figure 5-4, show the effects of hold time and temperature on the thermal processing on the *Pyrococcus furiosus* α-amylase in the sterilisation TTIs. Figure 5-4 shows that using a lower temperature (110°C) and a high processing time (4536 seconds) appears to have less effect on the α-amylase denaturation than using a high temperature (125°C) for a short amount of time (144 seconds). These isothermal profiles can be seen in Figure 5-3. This can be

seen in Figure 5-4 as a best fit straight line that shows ~0.5 minutes change in *F* value over the change in processing hold time and temperature. However, the scatter in the data is ± 0.5 minutes in each case. It is clear that the TTI is able to measure an *F* value of 6 ± 0.5 minutes over the temperature range 110-125°C. The next stage, described below, is to study how changes in temperature during the process affect the measured *F* value. Both time and temperature can not be individually explored because both contribute to the *F* value and as such have to be taken as 1 variable.

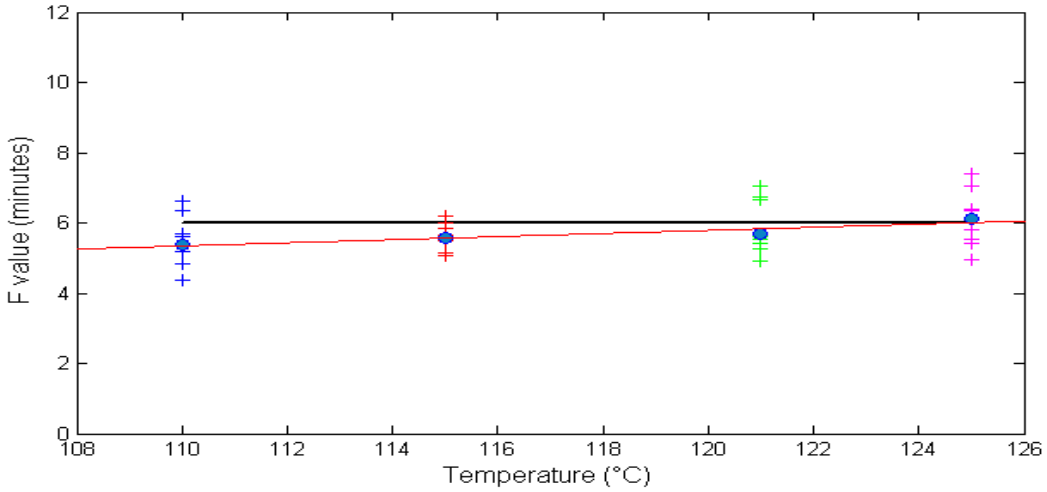

Figure 5-17 Effects of hold temperature and time on F value; mean average of TTIs [•]; data fitting of mean average [—]; thermocouple F value [—]

5.3.5 Calibration of *F* value and residual amylase activity

TTIs were exposed to time-temperature profiles that correspond to $F_{121°C}$ values of 0-37 minutes and the residual activity compared to that of the amylase which had been exposed to no thermal processing was analysed (Figure 5-5). The function of the plot is $y = 100e^{-0.0812x}$. The exponential thermal decay of *P.furiosus* α-amylase at 121°C shows measurable activity past $F_{121°C}$ = 37 minutes which is 2 x *D* value decay. At constant temperature, first order behaviour is known to

give rise to an exponential decay of activity and as such very good correlation to the data is shown. Having exponential decay in a measurable range up to $F_{121°C}$ = 25 min shows *P.furiosus* α-amylase is a strong candidate for a sterilisation TTI, as most sterilisation processes occur only up to $F_{121°C}$ = 30 minutes.

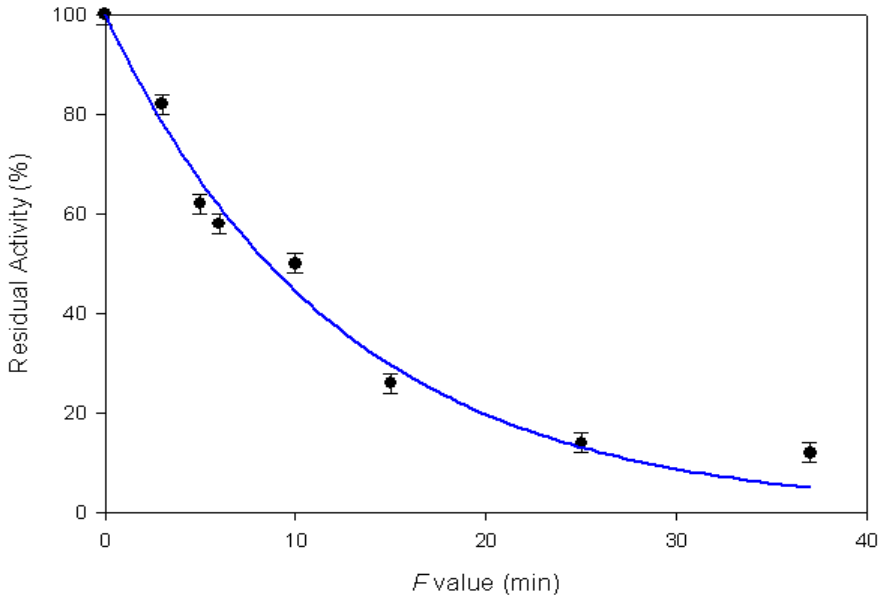

Figure 5-18 Residual activity of α-amylase after thermal processing

Isothermal processing of foodstuffs does not occur. The data of Figure 5-5 relates the level of thermal processing the TTIs receive to the measured activity. If the process is not isothermal, then Figure 5-5 can be used to find the equivalent processing the material had received, which can then be correlated to the *F* values calculated from the thermocouple data. This is calculated using the residual activity (%) of the amylase after the process described in chapter 4.

5.4 Non-isothermal heat treatment experiments

A series of experiments were carried out in an autoclave using different carrier fluids; TTIs were immersed in different fluids:

- Water
- Ethylene glycol
- Tomato soup (5% starch concentration)

Different fluids were chosen because they had different heat capacities and viscosities so heating rates would differ.

These experiments were to investigate non-isothermal processing of TTIs. Mehauden *et al*. (2006) used a Peltier stage to investigate various temperature profiles. The Peltier stage for pasteurisation TTIs worked effectively to change the heating and cooling rates from 1°C/min to 30°C/min. For sterilisation temperatures it is impossible to use the Peltier stage because the TTIs burst as a result of a pressure gradient formed as the temperature increased, between the inside of the TTI and the atmospheric conditions outside of the TTI. This causes the TTI to break open, and is a major disadvantage of TTIs for use in open or dry sterilisation processes outside of the food industry, for example in medical apparatus sterilisation. Using an autoclave, and suspending the TTIs in liquid, minimises pressure differential and eliminates bursting.

Mehauden *et al*. (2006) also used polymerase chain reaction (PCR) technology for accurate measurements of various time temperature profiles but again this was not suitable for sterilisation TTIs as the maximal temperature to use is 100°C.

To look at non-isothermal processing of TTIs, the external thermal profile was kept consistent for each thermal process; the time-temperature profile of the autoclave measured can be seen in Figure 5-6. The time-temperature profile was measured for the autoclave using a data logger within an open can, to simulate the position the data-logger would be for the rest of the non-isothermal experiments.

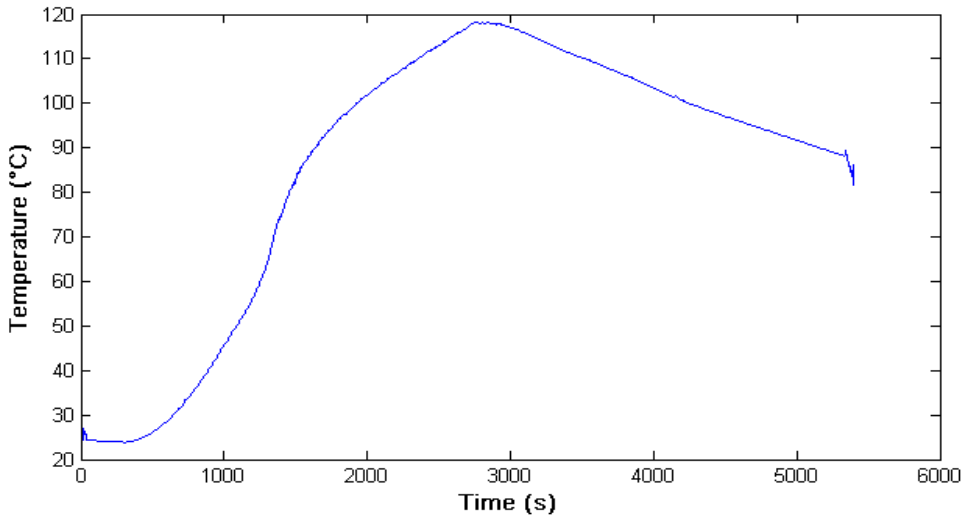

Figure 5-19 Time-temperature profile of the autoclave

The experiments were carried out by placing a sealed glass bottle containing a data logger (Ellab) and some (usually nine) free floating TTIs using one of the three liquids. The autoclave was then run through the same cycle, which, because of the different properties of the liquids, gave rise to different time-temperature profiles as shown in Figure 5-8.

The viscosities (Table 5-1) and specific heat capacities, Cp, of the fluids (Table 5-2) which the TTIs are immersed resulted in different time-temperature profiles. Data for water and ethylene glycol is known (Table 5-2) but it was necessary to measure the soup viscosity. Tomato soup is essentially a starch-based system: apparent viscosities both of starch mixtures close to the consistency of soup, and the tomato soup were determined using an AR1000 rheometer from TA instruments (Newcastle, Delaware, USA) equipped with a 0.06 m diameter 2^o cone and plate geometry. An upward shear stress sweep was performed for applied stresses, τ of $0.01 < \tau < 100$ Pa and each experiment was repeated twice. The apparent viscosity μ_{app} was calculated at each applied shear rate, $\dot{\gamma}$, as $\mu_{app} = \tau/\dot{\gamma}$. The starch mixtures and the soup exhibited shear thinning behaviour (Figure 5-7).

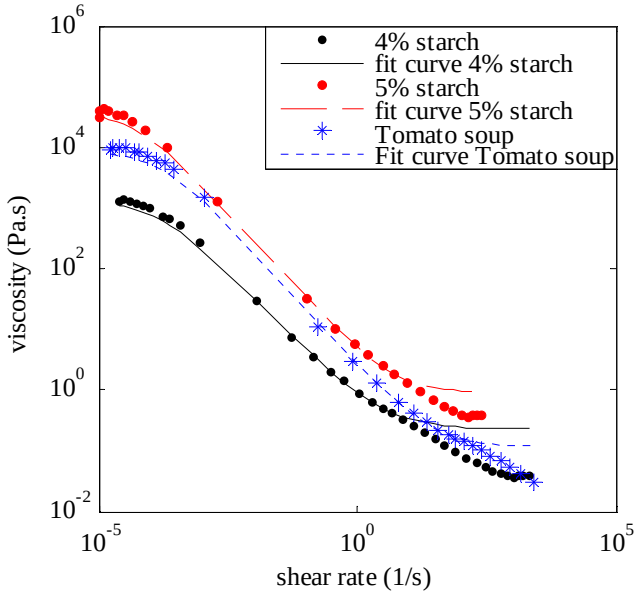

Figure 5-20 Viscosity curve of Starch 4% and 5% and Tomato Soup

The Carreau model was selected as the most appropriate model to fit all the data (Eq. 5-5), (Holdsworth, 1993).

$$\frac{\mu - \mu_\infty}{\mu_0 - \mu_\infty} = \left[1 + (K\dot{\gamma})^2\right]^{\frac{m-1}{2}} \qquad (5\text{-}5)$$

Where *K and m* are constants with dimensions of time and μ_0 and μ_∞ are the viscosities at shear rate ($\dot{\gamma}$) = 0 and $\dot{\gamma} = \infty$ respectively. Values of the model parameters for the fluids are given in Table 5-1.

Table 5-5 Values of the Carreau model parameters

	Tomato soup
μ_∞	0.119
μ_0	8360
K	6640
m	1.92
R^2	0.854
At shear rate $10s^{-1}$	430-550 mPa.s

Table 5-6 Specific heat capacities of processed fluids

Fluid	Viscosity at room temperature (Pa.s)	Specific Heat (kJ kg^{-1} K^{-1})
Ethylene Glycol	0.016	2.512
Tomato Soup	0.119	4.04
Water	0.001	4.186

The three fluids differ in thermal and flow properties. The time-temperature profiles caused by the difference in thermal and flow properties of the fluid when thermally processed within the

autoclave can be seen in Figure 5-8. Ethylene glycol had the fastest heating rate but within the shoulders of the range (when the TTI values increase more dramatically, >90°C) it still received enough thermal treatment to overcome the minimal amount due to the thermal lag and sensitivity of the TTIs. Tomato soup had the slowest cooling rate increasing the *F* value; even though the maximum temperature it reached during the autoclave cycle was not close to that which the water received.

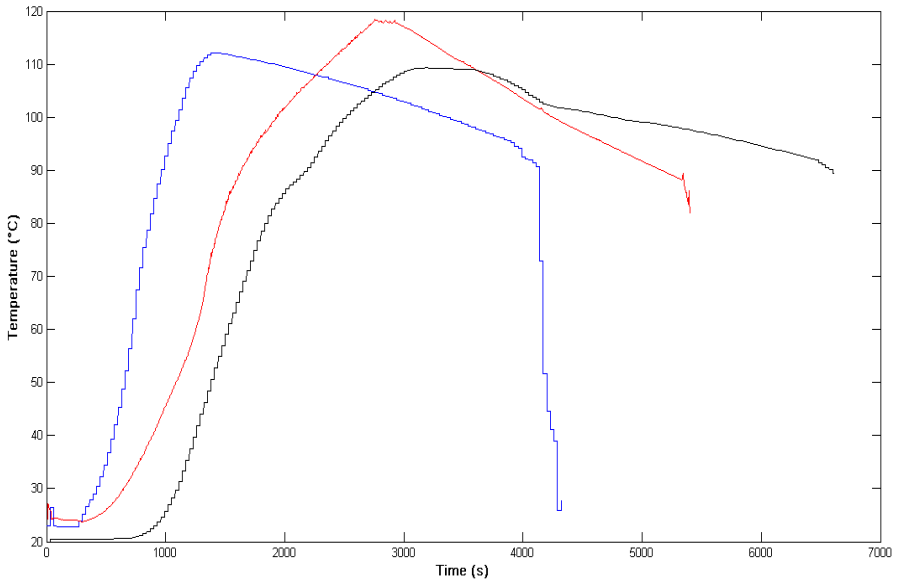

Figure 5-21 Time-temperature profiles of fluids in an autoclave. The water time-temperature profile [—]; the tomato soup time-temperature profile [—]; the ethylene glycol time-temperature profile [—]

This experiment attempted to represent industrially relevant time-temperature profiles in which heating and cooling rates are not constant. Inside the fluid the TTIs were allowed to float; ideally they should be neutrally buoyant, otherwise the TTIs would sink or float to the top of the can which might give different results to that of the bulk fluid which the data-logger was recording. The sedimentation times of the TTIs were measured for the different fluids used and

are given in Table 5-3. To calculate the sedimentation times, a TTI was dropped to the surface of the fluid and the time it took for the TTI to drop 10 cm was recorded for each fluid.

Table 5-7 Sedimentation rate of TTIs (at room temperature)

Fluids used	Water	Ethylene Glycol	Tomato soup
Sedimentation time	0.0082 ms^{-1}	0.0075 ms^{-1}	Neutrally buoyant

The time-temperature profiles inside the system were recorded by a data-logger (Ellab), and the *F* values were obtained by integration of the temperatures from the data-logger values to compare with TTIs. TTIs were also attached to the tip of the data-logger to receive in effect the exact same time-temperature profile that the data-logger encountered. The *F* values for the TTIs were inferred from the curve fit in Figure 5-5.

F values from calibrated thermocouple data were estimated using Eq. 5-3 where *D* and *z* were equal to 25 minutes and 11.3°C respectively for *Pyrococcus furiosus* α-amylase calculated from chapter 4. In Figure 5-9, *F* values calculated from thermocouple data are plotted against *F* values measured from the TTIs for non-isothermal conditions. The mean relationship between the *F* values obtained from thermocouples and TTIs is plotted on Figure 5-9. In addition, a y = x curve which represents the ideal relationship between TTIs and thermocouples has been plotted on the same graph (Figure 5-9).

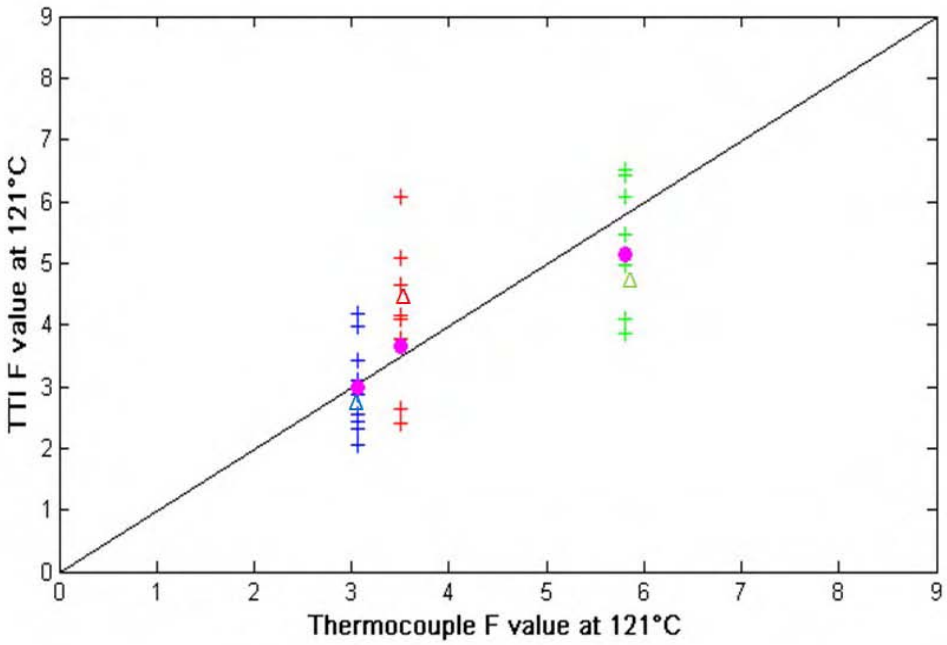

Figure 5-22 Non-isothermal comparison between TTIs and thermocouples in tomato soup [+]; ethylene glycol [+]; water [+]; mean TTI *F* value [•]; TTI attached to the data logger [Δ]; Y=X ideal relationship [—]

The average of the TTIs for each process in ethylene glycol, tomato soup and water, all fit to within F = 0.8 minutes of the ideal relationship with this average moving further away from the ideal y = x relationship as the F values increase. The data-logger was placed approximately in the centre of the processed substance and the TTIs free mixed into the processed substance. Each TTI will have seen an individual process time-temperature profile which will not resemble exactly the same time-temperature profile of the data-logger and so give a different F value. With enough TTIs in the process this can be averaged out to give an overall process F value which will be close to the data-logger if the data-logger records typical temperatures. In Figure 5-9 it shows that at lower F values, the TTI tends to overestimate the F value; and with large F values most of the TTIs underestimate the F values calculated by the thermocouples and data-loggers. This can also be seen in the industrial trial.

5.5 Industrial trial in sterilisation retort

The previous work has shown that the combination of the α-amylase TTI and the radial assay can measure *F* to ±0.5 minutes for F < 15 minutes. The next series of trials were carried out at CCFRA (now Campden BRI) on an industrial plant. The process used a pilot scale steam heated reel and spiral cooker-cooler at CCFRA with cylindrical metal cans. Two cans (75 mm diameter, 110 mm height) were used for each run. Inside each two temperature sensors were used, one near the top and one near the bottom of each metal can. In all cases, two TTIs were attached to the tip of the probe. Two calibrated thermocouple (type K) data loggers (accuracy ±0.5°C) were used for the temperature measurements (Figure 5-10).

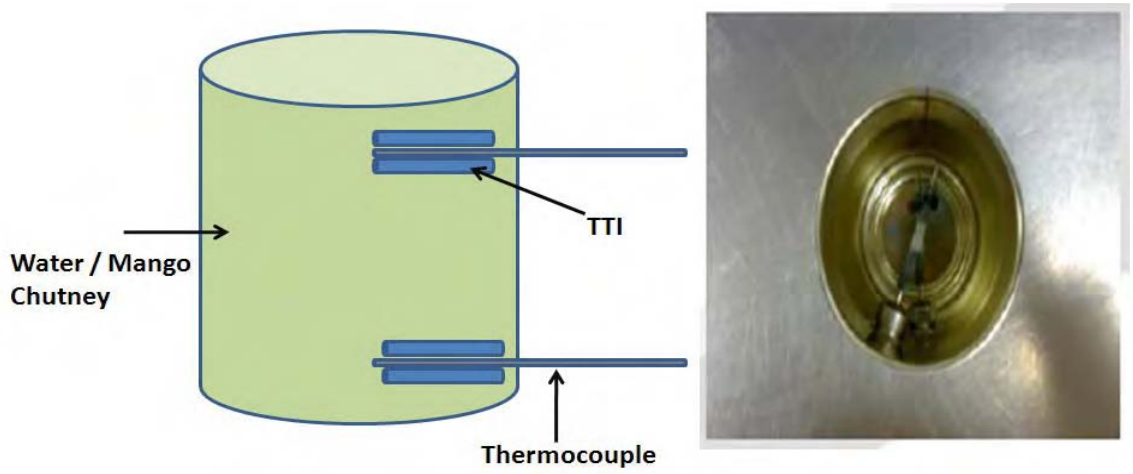

Figure 5-23 Setup of industrial trial thermocouples and TTIs

A common measuring position was assured by only having a few millimetres between each matching pair of TTIs and thermocouple. The materials would thus have the same time-temperature profile. All processes were carried out at up to 124°C maximum retort temperature; different profiles can be seen in Table 5-4.

Table 5-8 Run profiles of industrial trial

Run	Can	F-value (mins)
1	Water	Low (5-7 range)
2	Mango Chutney	Low (9-11 range)
3	Water	High (15-18 range)
4	Mango Chutney	High (13-23 range)

Figure 5-11 shows the time-temperature profiles measured for these products. The different runs/ time-temperature profiles given by the thermocouple data give a range of *F* values (5-23 minutes) over which the TTIs can be compared to the thermocouples. Water in the cans (Figure 5-11a,c) is used as a process reference. The processes time-temperature profiles show for water a very high heating rate and there is no hold time in Run 1 (Figure 5-11a), whereas in Run 2 (Figure 5-11c) there is a hold time to increase the *F* value. Mango chutney, although high in acidity and hence not susceptible to *Clostridium botulinum* growth, is also sterilised by conduction heat processes. The time-temperature profiles for mango chutney trials can be seen in Figure 5-11b and Figure 5-11d. The mango chutney having a higher specific heat capacity, Cp, has a slower heating rate than water and, and takes a longer time to get to sterilisation temperatures. This in turn gives a higher *F* value.

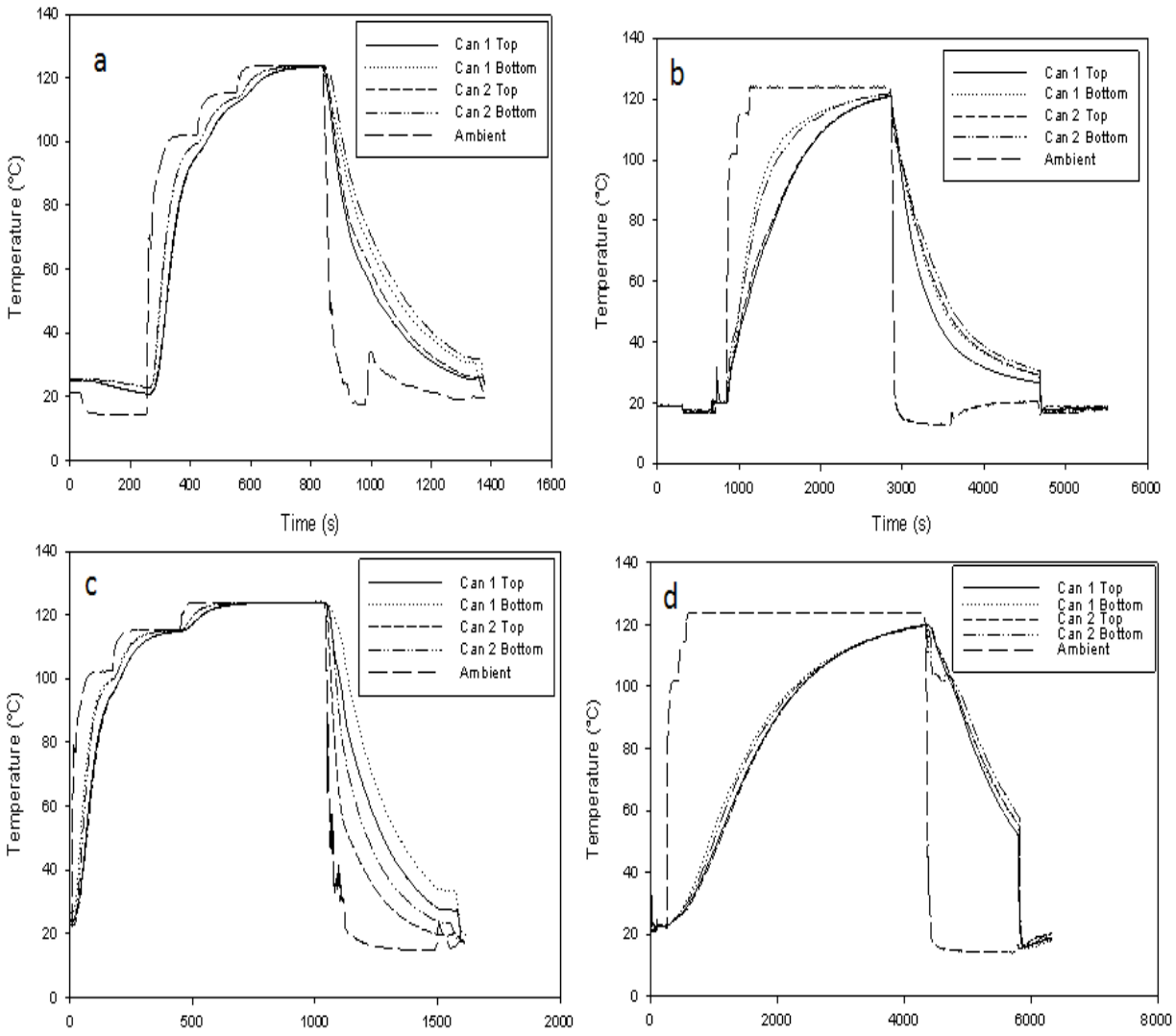

Figure 5-24 Time-temperature profiles for industrial trial (a) run 1 (b) run 2 (c) run 3 (d) run 4. Note that the horizontal scales are different.

The parameters of mango chutney were established for this industrial non-isothermal trial. Mango chutney has a specific heat capacity different to that of water and soup. Through differential scanning calorimetry (DSC) the specific heat capacity was calculated as 3.0 kJ kg^{-1} K^{-1}. The viscosity was calculated as in §5.4 and the Carreau model was chosen as the best fit also as with §5.4. This can be seen in Figure 5-12. Values of the model parameters for the fluid are given in Table 5-5.

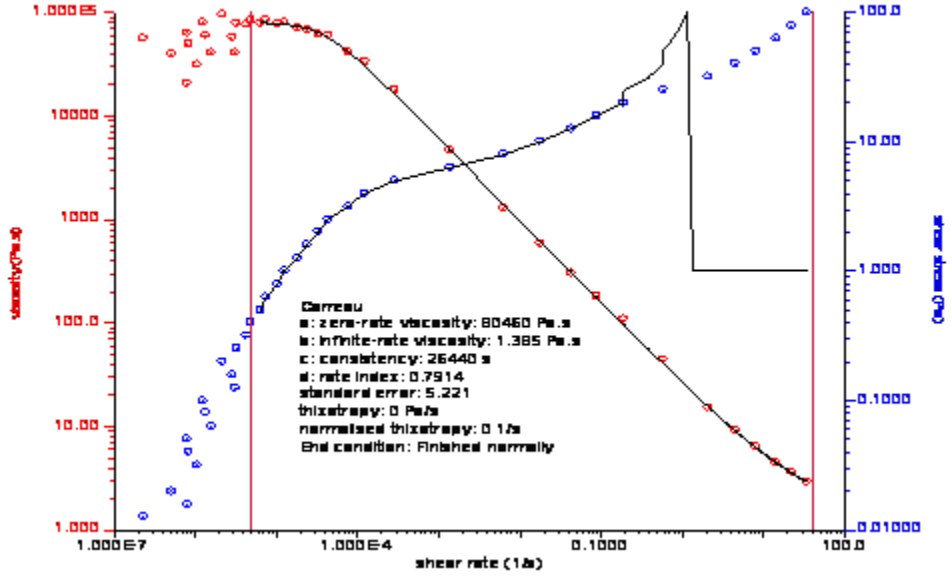

Figure 5-25 Viscosity curve of mango chutney; Carreau model fit [—]; Carreau model fit parameters [—]

Table 5-9 Model parameters of Carreau model for mango chutney

	Mango Chutney
μ_∞	1.385
μ_0	80460
K	26440
m	0.7914

TTIs were subjected to the 4 separate time-temperature profiles shown in Figure 5-11. Thermocouple data was integrated using Eq.5-3 using the experimentally derived z value of 11.3°C. Figure 5-13 plots the F-values calculated from thermocouple data against the F value measured from the TTIs for the non-isothermal experiments. The two sets of F value data were plotted against one another for the relationship between them. Figure 5-13 demonstrates the ideal relationship between TTIs and the process measured by thermocouples and hence demonstrates TTI accuracy. Regression analysis showed that the TTIs correlate well with the thermocouple

data with the R^2 for the ideal equation y = x being 0.8. Therefore the data adequately fits the equation y = x and the TTIs responses correlate with the data from thermocouples responses.

This data suggests that there is an upper limit where the accuracy compared with the thermocouple decreases rapidly and this occurs at around $F_{121°C}$ = 15 minutes. If a trend line is taken of the first six points of Figure 5-13 then it will intercept the *F* value axis at around $F_{121°C}$ = 15. Figure 5-13 suggests that this is also the case with the accuracy compared to thermocouple measurements.

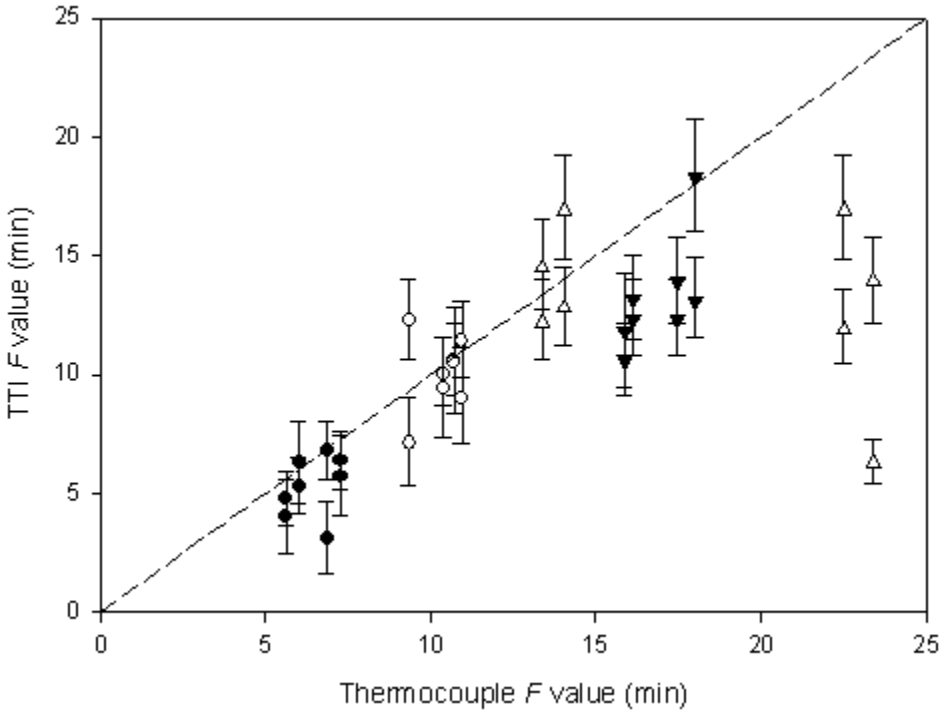

Figure 5-26 Scatter of the thermocouples F-values verses the TTIs F-values calculated for isothermal time-temperature profiles for; Run 1 (●), Run 2 (○), Run 3 (▼), Run 4 (Δ).

At low *F* values ($F_{121°C}$<15 min) the correlation of the TTI and thermocouple is high with an R^2=0.96. This is encouraging as for sterilization "*botulinum* cook" is $F_{121°C}$ = 3 min. At low *F*

values, with the isothermal results, large changes in the residual activity will only give small changes in the *F* value so accuracy is reasonably good when compared to thermocouple data, as the residual activity data can fall within a large range for a known *F* value. After $F_{121°C}$ = 15 min there is a decline in accuracy as there is a move away from the y = x ideal curve. Using water inside the can showed a marked improvement in the accuracy of the TTI compared to the viscous mango chutney, but this may be due to the higher *F* values the mango chutney was exposed to, and not mixing and thermal convection inside the can. The decrease in accuracy of the TTIs compared to the thermocouples within mango chutney could be down to the slower heating and cooling rates the TTIs are exposed to, but this is not investigated in this study. At very high thermocouple *F* values, the TTI values are considerably lower which could also be down to a fouling over the TTI by the mango chutney.

5.6 Conclusions

One major advantage of a liquid TTI compared with a TTI in powder form is the option of encapsulation within silicone TTI tubes. These provide a TTI of neutral density in water with heat transfer characteristics, e.g. thermal conductivity and diffusivity suitable for representing foods. The study shows that the TTI's responses to thermal processing within industrial applications and substrates for a range of non-isothermal processes correlate well with the integrated data from thermocouples responses.

In general, prior to this study, there was a lack of knowledge on sterilisation TTIs accuracy and efficiency and especially using hyperthermophilic enzymes as sterilisation TTIs. Errors in measurement were found to arise from a number of factors, including variability in the

manufacture of the TTIs, errors in determining the final and initial value of activity, as well as non-linearity's and variations in the kinetics of the enzyme (which will be explored in chapter 6).

At 15 minutes of iso-thermal processing at 121°C the residual activity is 30% and at 30 minutes it is 10%. This suggests that if the α-amylase is processed more than 15 minutes it loses accuracy and this occurs increasingly rapidly after 30 minutes. In this instance the maximal heat treatment duration is possibly 2 × *D* values at 121°C. This corresponds to the non-isothermal processing of the mango chutney trails. The maximal heat treatment duration compares to that described by Tucker *et al*. (2007).

The effects of hold time and temperature on the thermal processing on the *Pyrococcus furiosus* α-amylase in the sterilisation TTIs showed that using a lower temperature and a high processing time appears to have less effect on the α-amylase denaturation than using a high temperature for a short amount of time. However, the scatter in the data is $\pm$ 0.5 minutes in each case. It is clear that the TTI is able to measure an *F* value of 6 $\pm$ 0.5 minutes over the temperature range 110-125°C. Both time and temperature can not be individually explored because both contribute to the *F* value and as such have to be taken as 1 variable.

The average of the TTIs for each process in non-isothermal processing all fit to within $F = 0.8$ minutes of the ideal relationship with this average moving further away from the ideal $y = x$ relationship as the *F* values increase. With enough TTIs in the process this can be averaged out to give an overall process *F* value which will be close to the data-logger if the data-logger records typical temperatures. At lower *F* values, the TTI tends to overestimate the *F* value; and

with large *F* values most of the TTIs underestimate the *F* values calculated by the thermocouples and data-loggers. This can also be seen in the industrial trial.

Mehauden *et al*. (2007) commented on the accuracy of TTIs being constrained by the lower limit of thermal processing, where there is sufficient thermal lag between TTIs and the process, so the TTI was not correct for very low values of *F* (<2minutes). This is not the case for the industrial study as the TTIs were attached to the thermocouple. For real industrial trials use though there will be free TTIs in cans. There is also a higher limit of *F* value, where the enzymatic percentage activity is low enough that there is not as sensitive to change in *F* value. The data suggests that for a higher limit this occurs at around $F_{121°C}$ = 15 minutes. Below this is the operational window in which measurements can be taken with greater accuracy. This data suggests that the inherent accuracy of the TTI is of the order of ±20% over a wide range of *F* values and a lot less for low *F* values. With an increased number of TTIs per can then this accuracy can be increased significantly. This will be acceptable for a food process where it is not possible to obtain thermocouple data.

In practice, the accuracy of the TTIs will be constrained by

- A lower limit of *F*, where there is sufficient thermal lag between the TTIs and the process, so that the TTI value is not correct

- A higher limit of *F*, where the value of the residual enzymatic activity is so low that it is not sensitive to the change in F anymore.

In between is the operational window where measurements can be taken with sufficient accuracy which is approximately $F_{121°C}$= 2-30 minutes at 121°C and optimally working at $F_{121°C}$= 4-15 minutes.

Similar work done was by Guiavarc'h *et al*. (2005) using *Bacillus licheniformis* α-amylase encapsulated on alginate beads for the processing of ravioli in a spiral retort. The Guiavarc'h *et al*. (2005) study showed a much greater variation in TTI *F*-values calculated than that shown within this study on mango chutney. The Guiavarc'h et al. (2005) study also showed that measuring the temperature in the sauce overestimated the effect of the process by 30%. This may be the case with using a thermophilic enzyme in the study rather than the hyperthermophilic enzyme which is more optimized to the process temperatures involved in sterilisation within this thesis. No industrial trials using a hyperthermophilic enzymatic TTI has been recorded.

Chapter 6

Effects of thermal processing on the thermostability of *Pyrococcus furiosus* α-amylase

6.1 Introduction

The previous chapters have described the development of an assay for the α-amylase of *P.furiosus*, and tests on the accuracy and repeatability of the assay. This chapter describes studies of the thermostability of the amylase. The data in the previous chapters have suggested that the rate of loss of activity is first order. Here the stability of the enzyme is studied using calorimetry and spectroscopy.

Thermodynamic protein stability is of interest from an applied perspective for sterilisation TTIs and biocatalysts. Increasing the thermodynamic thermostability is the main issue when the α-amylase is used under denaturing conditions (sterilisation temperatures). If the mechanism and thermodynamic stability can be understood, then the α-amylase can be engineered to be more or less thermally stable. By controlling the thermostability the *z* value can then be increased or decreased to match the target micro-organism in the foodstuff. The implications of varying z can be seen in chapter 4. Long-term storage stability can also be improved by knowing the mechanisms of protein unfolding at lower temperatures for *Pyrococcus furiosus* α-amylase.

Native and functional protein structures are held together by a subtle balance of non-covalent forces or interactions; H-bonds, ion pairs, hydrophobic interactions, and van der Waals

interactions. At elevated temperature (or in the presence of a denaturant) these non-covalent interactions are too weak or become counterbalanced by other interactions and the protein unfolds. Protein unfolding can be observed by many different techniques, including differential scanning calorimetery (DSC), circular dichroism (CD) and Fourier transform infrared (FT-IR) all of which will be used in this chapter to explore the denaturation characteristics of *Pyrococcus furiosus* α-amylase.

Differential scanning calorimetry (DSC) is a thermoanalytical technique in which the difference in the amount of heat required to increase the temperature of a sample as compared to a reference is measured as a function of temperature. Both sample and reference are closely maintained at the same temperature throughout the experiment. Generally, the temperature program for a DSC analysis is designed so that the sample holder temperature increases linearly with time.

The main application of DSC is in studying phase transitions, such as melting, glass transitions, or exothermic decompositions. These transitions involve energy changes or heat capacity changes that can be detected by DSC with great sensitivity. As the temperature increases the sample eventually reaches its melting temperature (T_m). The melting process results in an endothermic peak in the DSC curve as the protein unfolds. This is important for looking at the thermostability of enzymes and to assay where the irreversible denaturation occurs by viewing a glass transition in the heat capacity curves.

Circular dichroism (CD) spectroscopy measures differences in the absorption of left-handed polarized light versus right-handed polarized light which arise due to structural asymmetry. The

absence of regular structure results in zero CD intensity, while an ordered structure results in a spectrum which can contain both positive and negative signals.

Circular dichroism spectroscopy is particularly good for determining whether a protein is folded, and if so characterizing its secondary structure, tertiary structure, and the structural family to which it belongs by studying the conformational stability of a protein under stress and hence, looking at thermal stability, pH stability, and stability to denaturants

Secondary structure can be determined by CD spectroscopy in the far-UV spectral region (190-250 nm). At these wavelengths the chromophore is the peptide bond, and a signal arises when it is located in a regular, folded environment.

α-helix, β-sheet, and random coil structures each give rise to a characteristic shape and magnitude of CD spectrum. This is illustrated in Figure 6-1, which shows three different conformations.

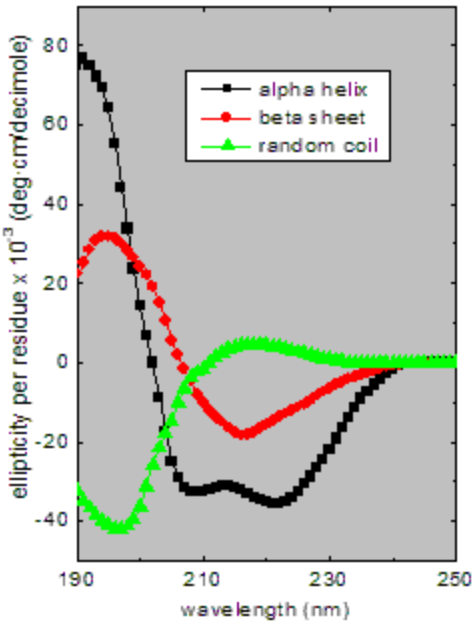

Figure 6-27 CD spectrum in the far-UV spectrum with three different conformations (http://www.ap-lab.com/circular_dichroism.htm)

Fourier transform infrared (FT-IR) spectroscopy is a measurement technique for collecting infrared spectra. Instead of recording the amount of energy absorbed when the frequency of the infra-red light is varied by a monochromator, the IR light is guided through an interferometer. After passing through the sample, the measured signal is the interferogram. Performing a mathematical Fourier transform on this signal results in a spectrum identical to that from conventional (dispersive) infrared spectroscopy. The infrared spectrum of a sample is collected by passing a beam of infrared light through the sample. Examination of the transmitted light reveals how much energy was absorbed at each wavelength. From this, a transmittance or absorbance spectrum can be produced, showing at which IR wavelengths the sample absorbs. Analysis of these absorption characteristics reveals details about the molecular structure of the sample.

Under extreme conditions of temperature, pH and pressure, amino acids can be damaged irreversibly by processes such as deamidation, β-elimination, hydrolysis, Maillard reactions, oxidation, and disulphide interchange (Daniel *et al*., 1996; Jaenicke, 1998). The hydrolysis of peptide bonds sets theoretical limits to protein stability (Jaenicke and Böhm, 1998). A number of enzymes from hyperthermophiles are stable and active at temperatures exceeding the upper growth limit of the producing organism. α-amylase from *Pyrococcus woesi* (identical to the extracellular α-amylase from *Pyrococcus furiosus* , Linden *et al*., 2003) has been reported to be resistant to thermal inactivation above the organisms maximal growth temperature (Koch *et al*., 1991). Rubredoxin from *Pyrococcus furiosus* is the most thermostable protein characterised, with an extrapolated T_m value of almost 200°C (Hiller *et al*., 1997; Cavagnero *et al*., 1998).

6.1.1 Mesophilic and hyperthermophilic differences

Hyperthermophilic enzymes are often barely active at room temperature (Figure 4-6b), but are as active as their mesophilic counterparts at their corresponding physiological temperature (Jaenicke, 1991).

It has been postulated that the low activity at low temperatures is due to the high rigidity, which is relieved at elevated temperatures at which hyperthermophilic enzymes work *in vivo* (Jaenicke, 2000). This can be seen by work on hyperthermophilic enzymes in which denaturants (Kujo and Oshima, 1998), or detergents (Rugiger *et al*., 1995) are added, and where the hyperthermophilic enzyme is often activated by these substances at sub-optimal temperatures. This activation then tends to disappear as the temperature gets closer to the enzymes optimal temperature, T_{opt}.

Danson and Hough (1998) focused on the structures and stabilities of archaeal enzymes. Comparison of the three-dimensional structure of hyperthermophilic, thermophilic and mesophilic citrate synthase revealed many similarities but differences associated with the increasing thermostability were apparent. Thermophilicity was characterised by a more compact structure arising from shorter surface loops, fewer internal cavaties, improved internal packing, and ion pairing, which were found to be more prevalent in the hyperthermophilic enzyme than in only the moderately thermophilic enzyme.

6.1.2 Stabilising Ions

Early studies on *Pyrococcus furiosus* α-amylase at room temperature demonstrated that Ca^{2+} ions are not required for stability (Jorgenson *et al*., 1997) but at elevated temperatures >75°C Ca^{2+} ions are required for thermostability (Savchenko *et al*., 2002). The role of other ions for structural stabilisation appears less important but it is assumed Zn^{2+} ions at least participate in the thermostabilisation of *Pyrococcus furiosus* α-amylase.

6.1.3 Inactivation Models

A common inactivation model for an enzyme involves the unfolding, or denaturation of the polypeptides tertiary structure and occurs as a two step process according to the proposed model by Lumry and Eyring (1954):

$$N \underset{k_1}{\leftrightarrow} U \xrightarrow[k_2]{} I \qquad (6.1)$$

Where N is the native active enzyme, U is the reversibly unfolded enzyme and I, the irreversibly inactive enzyme.

The folding stability of an enzyme describes the $N \rightleftarrows U$ equilibrium and can be denoted by the T_m value (temperature at which the protein is 50% unfolded). Cooling on ice allows the reversibly unfolded form, U, to fold into the native form, N (Tanford, 1968).

Often the inactivation of N follows a first-order exponential decay with rate constant k ;

$$\frac{A_t}{A_0} = e^{-kt} \qquad hence \qquad Ln\ (residual\ activity) = -kt$$

(6.2)

Where A_t and A_0 represents the activities at time t, and time 0 respectively and k is the first-order rate constant. If this were the case here it would help the application of *Pyrococcus furiosus* α-amylase in sterilisation TTIs.

With a first-order rate constant, one can calculate a true half-life, $t_{1/2}$ = (0.693 / k), as a measure of stability at various temperatures. Investigations into thermally unfolded states are complicated by the rapid and irreversible aggregation of the chains, leading to flocculation and precipitation (Sharma and Bigelow, 1974).

Arrhenius plots for hyperthermophilic and mesophilic enzymes have been typically linear (Bauer *et al*., 1999; Bock *et al*., 1999) suggesting that mesophilic and hyperthermophilic enzyme functional conformations remain unchanged throughout their respective temperature ranges (Vielle and Zeikus, 2001).

6.2 Materials and Methods

6.2.1 Circular Dichroism (CD)

Circular dichroism experiments were carried out using a Jasco J-810 spectropolarimeter (Jasco UK, Great Dunmow, UK). Samples of the same concentration (100µl sample / 990µl water – 100mg FDP / ml sodium acetate buffer 100mM pH5.5) were used and loaded into a 1-mm path-length quartz cuvette (Starna Optiglass Ltd.). The buffer scans were subtracted from the enzyme scans. The wavelength range recorded was 300–190 nm with a data pitch of 0.2 nm, a bandwidth of 1 nm, a scanning speed of 100 $nm.min^{-1}$ and a response time of 1 second. All measurements were carried out at various temperatures 25°C-110°C (temperature controlled by Peltier stage). Circular dichroism data were analysed by averaging the data points from 300 to 190 nm (inclusive) for each of the 4 spectra repeats scans per sample.

Fixing the wavelength at 220nm, data was taken every 0.2°C. 220nm was chosen as it is the point at which there is a change is secondary structure in a α- and β-sheet shape (Figure 6-1). Full wavelength scans were undertaken every 5°C from 50-110°C. 110°C being the upper limiting temperature of the Peltier stage in the Jasco J-810 spectropolarimeter.

6.2.2 Differential Scanning Calorimetry (DSC)

Differential scanning calorimetry experiments were carried out using a Perkin Elmer DSC 7 calorimeter (Perkin Elmer UK). Temperature control was preformed by a Perkin Elmer Intracooler 3 for cooling of samples to -50°C for exploring cold denaturation, and heating up to 130°C for exploring heat denaturation. Samples of dry FDP and also samples of the same

concentration (100mg FDP / ml sodium acetate buffer 100mM pH5.5) were used and loaded into a 40mg pans. Buffer scans were subtracted from the enzyme scans. The temperature ramp for each sample was set at 1°C / min so as to allow for equilibrium and no thermal lag for the enzyme. This has been shown on an average thermophilic α-amylase by Nielsen *et al*, (2003). When the heating rate decreases, the heat absorption peaks of denaturation shift towards lower temperatures (Grinberg *et al*., 2000). Molar excess heat capacities (*Cp*) were obtained by normalising with the *Pyrococcus furiosus* α-amylase concentration and the volume of the calorimeter cell. Apparent denaturation temperatures (T_m) values were determined as the temperature corresponding to maximum Cp.The thermodynamic parameters of unfolding were calculated using the relations shown in the following equations;

$$\Delta G = \Delta H - T\Delta S$$

$$\Delta H(T) = \Delta H_m + \Delta Cp(T - T_m)$$

$$\Delta S(T) = \frac{\Delta H_m}{T_m} + \Delta Cp \ln\left(\frac{T}{T_m}\right)$$

$$\Delta G(T) - \Delta H\left(1 - \frac{T}{T_m}\right) + \Delta Cp(T \quad T_m) - T\Delta Cp \ln\left(\frac{T}{T_m}\right) \qquad (6.3)$$

The temperature dependence that can be seen in equation 6.3 for ΔG allow deeper insights into the mechanisms of how thermostability is achieved. Enthalpic contributions are often related to the structural stability of a protein, and the entropic contributions have been shown to play a role in reaching high thermostabilities (Fitter, 2005).

6.2.3 Fourier Transform Infrared Spectroscopy (FT-IR)

A Nicolet 380 Fourier Transform Infrared instrument (Thermo Electron Company, USA) was used. The machine used a diamond crystal to measure absorbencies from 30000cm^{-1}-200cm^{-1}, although this study only studied the mid-infrared region of 4000cm^{-1}-1000cm^{-1} where the structural bonds appear. Each result was an average of 32 scans. A subtraction from a pure water standard was made for all scans.

6.3 Results

The effects of thermal denaturation on *Pyrococcus furiosus* α-amylase have been explored in chapters 4 and 5 but in the results shown in this chapter describe the irreversible thermal inactivation of *Pyrococcus furiosus* α-amylase.

6.3.1 Kinetic study of the irreversible thermal denaturation

The deactivation of the α-amylase at various temperatures (117°C to 125°C) and times (0 - 40 minutes) was preformed and the specific activity measured using the RED assay (chapter 4). The initial effects of thermal processing can be seen in Figure 6-2(a) over various temperatures.

Chapter 4 describes the loss of activity of the enzyme under various process conditions. A plot of the natural logarithm of residual activity versus incubation time is shown in Figure 6-2(b). The data in Figure 6-2(b) is linear over the short incubation times of up to 9 minutes at the three temperatures. Note that this is the same as Figure 4-8, and reproduced for clarity. This implies that under these conditions the denaturation of *Pyrococcus furiosus* α-amylase is a one step

denaturation process and can be described as a single first-order exponential decay as described previously by equation 6.2.

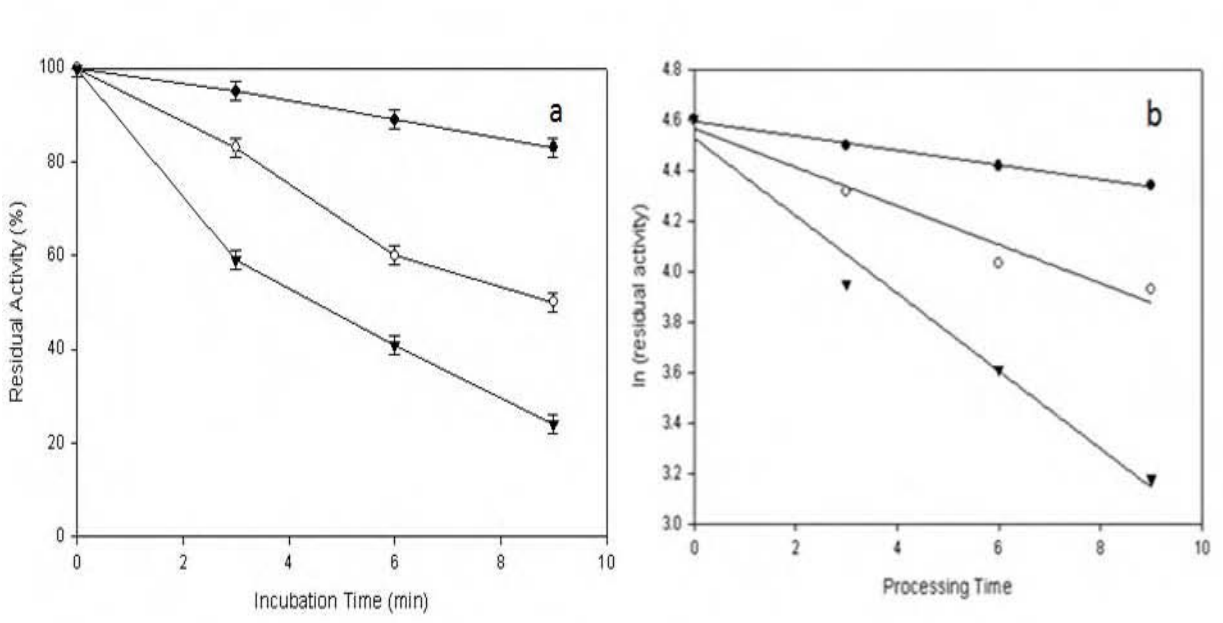

Figure 6-28 Effects of isothermal processing on residual activity of PFA (a) expressed as % and (b) expressed as the natural logarithm of residual activity for 117°C (●), 121°C (○) and 125°C (▼). Points are an average of 3 experiments

When the incubation time is increased up to 40 minutes as shown in Figure 6-3(a) (a repeat of Figure 5-5) the plot of natural logarithm of residual activity at 121°C shown in Figure 6-3(b) is slightly biphasic after an *F* value of 20 minutes. This has been previously described for potato acid phosphate (Gianfreda et al., 1984), guinea-pig liver transglutaminase (Nury and Meunier, 1989) and most relevant for *Pyrococcus furiosus* α-amylase is the data for the moderately thermophilic α-amylase from *Bacillus licheniformis* (Violet and Meunier, 1989) for use in pasteurisation TTIs described in chapter 2. Figure 6-3 (b) includes a straight line fitted to the first 6 points, i.e. for $F<15$ minutes. The data diverges from this line at $F\sim20$ minutes. This should be compared with the $F>15$ minutes for which the data of chapter 5, Figure 5-13, suggests the

enzyme can no longer differentiate different *F* values accurately. Figure 6-3(b) suggests that the plots are biphasic as the two step process according to the proposed model by Lumry and Eyring (1954) for *F* > 20 minutes. It is postulated here that the mechanism of denaturation is not biphasic but that aggregation of the protein occurs leading to flocculation and precipitation. This is a special case of the Lumry and Eyring (1954) model in equation 6.1 where $k_2 >> k_{-1}$, so that most of the reversibly unfolded molecules, U, will be converted to the irreversibly inactive, I, molecules as an alternative to refolding back into the native state. The folded state, U, is a transient form and the process might be described by equation 6.4. In this case, the denaturation process can be regarded as one-step process following the first order kinetics, so can be described as shown in equation 6.4.

$$N \xrightarrow[k_s]{} I \qquad (6.4)$$

This analysis extends that of chapter 4 to suggest first order behaviour over the full range of applications of the enzyme at 121°C

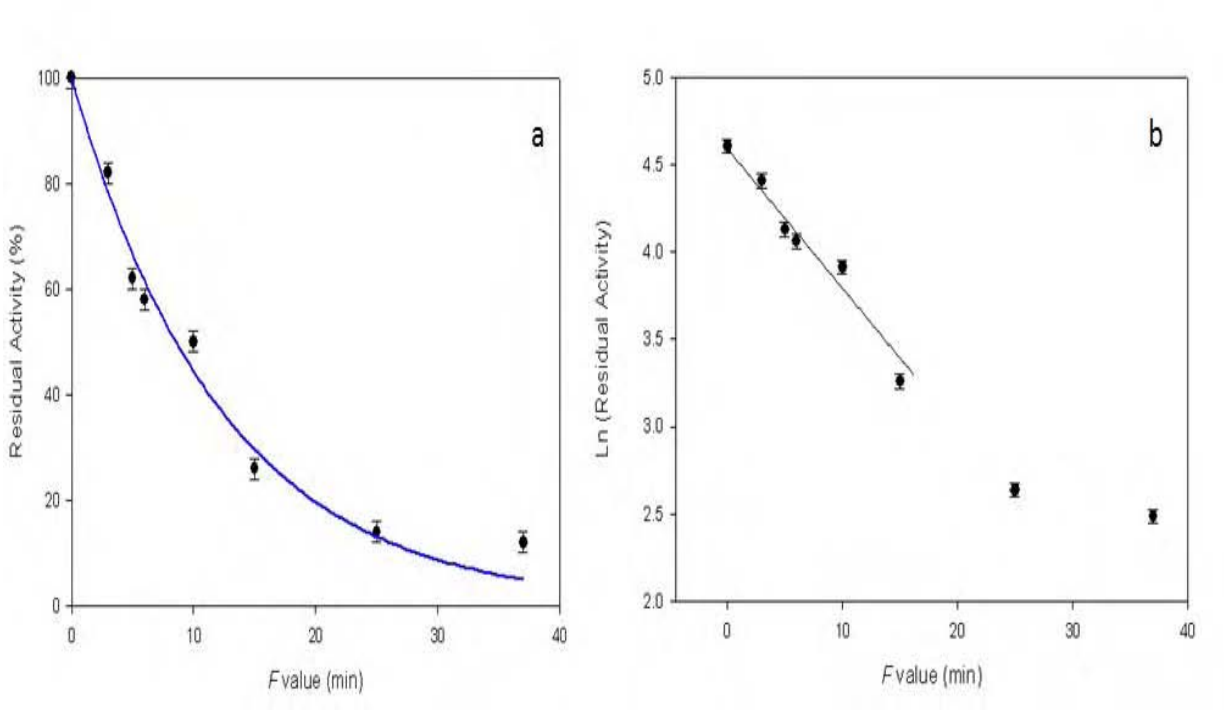

Figure 6-29 Effect of isothermal processing at 121°C on residual activity of PFA (a) expressed as % and (b) expressed as the natural logarithm of residual activity and trend lines [—].

To test the exact mechanism further DSC, FT-IR and CD experimentation was carried out on the *Pyrococcus furiosus* α-amylase.

The deactivation rate constants (k) and hence the half-life ($t_{1/2}$) were calculated for each temperature (117°C, 121°C, 125°C) and are presented in Table 6-1. The deactivation rate constant (k) followed the Arrhenius law (Figure 6-4), where the activation energy (Ea) determined through linear-regression analysis was found to be 316 kJ / mol.

Table 6-10 Effects of temperature on rate constant and half life

Temperature (°C)	k x10^{-3} (s^{-1})	$t_{1/2}$ (minutes)
117	0.606	19.1
121	1.896	6.1
125	4.299	2.7

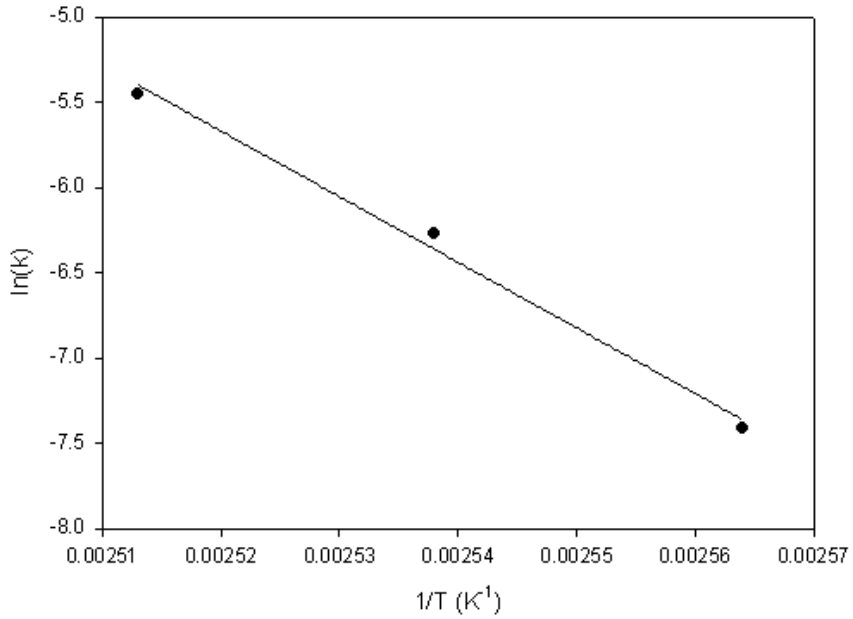

Figure 6-30 Arrhenius plot for *Pyrococcus furiosus* α-amylase.

6.3.2 Thermal processing effects on thermostability

The thermal stability of *Pyrococcus furiosus* α-amylase was investigated using differential scanning calorimetry (DSC). Cold denaturation was initially studied to look how the storage temperature of the enzyme effects the denaturation and hence the activity when at its optimal conditions. Figure 6-5 shows the effect of cooling of the freeze-dried α-amylase powder down

from 30°C to -50°C at a cooling rate of 1°C / minute. Figure 6-5 shows no cold denaturation of the α-amylase as there is no change in heat capacity over the range studied that shows a change in state or glass transition. This is contrary to Laderman *et al*. (1993) who stated the theoretical mathematical cold denaturation point being -3°C. This means that storage of *Pyrococcus furiosus* α-amylase is not affected by the minimum temperature and as such it can be stored at temperatures below its minimum activity temperature (~35°C Figure 4-6b). *Pyrococcus furiosus* α-amylase was stored at 4°C for times up to 7 days, and at -18°C for times up to a year. There was no discernable loss of activity of the amylase.

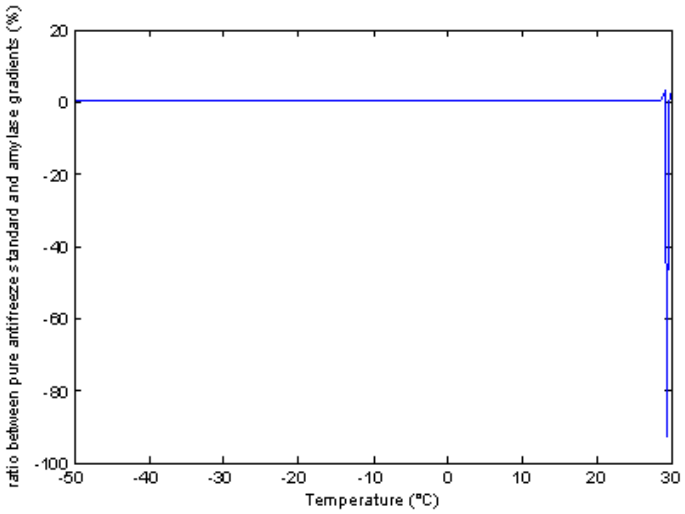

Figure 6-31 Thermal cooling of α-amylase cooled from 30 to -50°C at a rate of 1°C /min

To identify any T_m, α-amylase was heated from 90°C to 130°C. α-amylase freeze dried powder (FDP) was used without the addition of 0.1M sodium acetate buffer, as with previous experiments. FDP was used to avoid any effects of water boiling in the DSC. Figure 6-6a shows a DSC curve for a scan rate of 1°C / min; there is a denaturation linearly and at 106-107°C there

is a denaturation peak for an apparent transition, T_m where U→I. This is consistent with the T_m described in a previous study where the T_m was found to be ~110°C, but the scan rate was not given in this work (Jorgenson *et al*., 1997). For *Bacillus halmapalus* α-amylase, decreasing the scan rate from 1.5 to 0.5°C/min resulted in a 6°C lower apparent T_m value, and it was noted that scan rate dependence was a typical hallmark of kinetically controlled processes (Nielsen *et al*., 2003). The sample was then cooled back to 90°C, and then rerun from 90-130°C (Figure 6-6b) giving the curve shown with no change in *Cp*, indicating that the amylase had gone through irreversible transition induced in the first DSC scan up to 130°C.

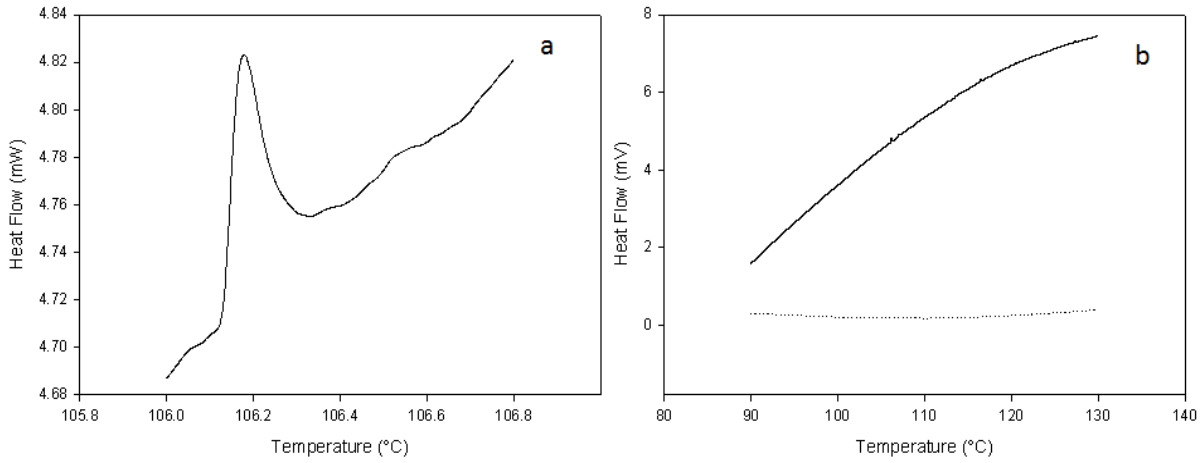

Figure 6-32 DSC thermogram of FDP showing (a) denaturation peak (b) complete thermogram for FDP (—) and re-run FDP (·····). Heating from 90°C to 130°C at 1°C/min.

In order to further examine the reversibility of the *Pyrococcus furiosus* α-amylase denaturation process, scans were preformed before the T_m value and scans after the T_m value. From the resulting thermograms (Figure 6-7) it can be seen that the process is almost completely reversibe up to a temperature beyond the T_{opt} of 98°C. It can be seen that the process does lose some enzyme to the irreversible inactive state, but most is reversible. Both Figure 6-6 and Figure

6-7 show that past a certain amount of thermal processing the denaturation is irreversible. Up to the T_m value the protein was almost completely reversible in accordance with previous studies (Tanford, 1973) so (i) at temperatures below the T_m value the model for denaturation of PFA is in accordance with Eq. 1, and (ii) above the T_m value the special case of the Lumry and Eyring model where $k_2 >> k_{-1}$ and hence k_3 applies. This is important for sterilisation TTIs because it implies there must be a minimum amount of thermal processing / temperature required for the *Pyrococcus furiosus* α-amylase to reach the irreversibly inactive state and hence work as a TTI, where there is a measurement between the native and irreversibly inactive states. Although the *F* value increases very slowly in thermal processes before 105°C, these results suggest that processing below this temperature does not result in irreversible denaturation of the α-amylase and this should be taken into account in the calculations of *F* value made by the TTI. This only highlights both the specificity of TTIs and the importance of choosing the correct enzymatic TTI for the process.

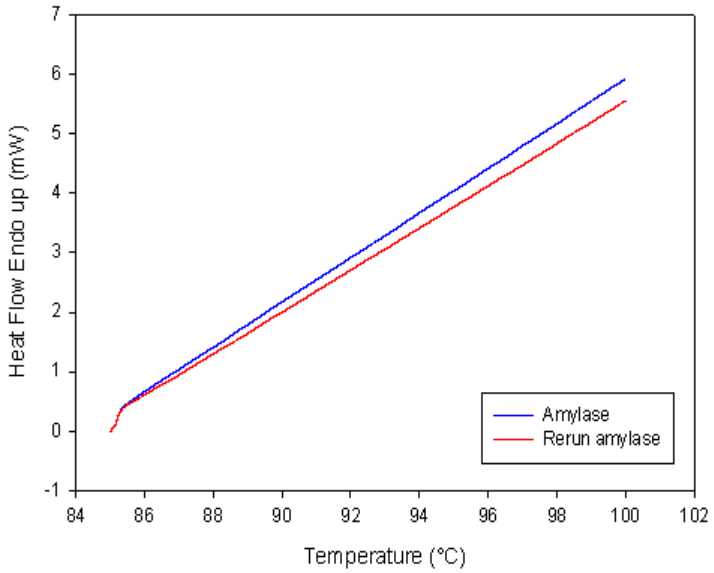

Figure 6-33 DSC thermogram rerun amylase under T_m from 85-100°C at 1°C/min

The DSC was then used to view the amount of thermal treatment incurred during processing. Dry FDP was not used as thermal processing would affect the amylase differently if the enzyme was not in solution to if it was in sodium acetate buffer. The protein was in solution at a concentration of 100mg FDP / ml buffer, and a scanning rate of 1°C / min. The thermograms were plotted for a previously isothermally processed *F* value at 121°C of 0 and 12 minutes. The thermograms are plotted in Figure 6-8. The peaks for T_m were shown at 106.5 and 103°C respectively. The ΔH values for the peaks were 99 J/g and 11 J/g. This method shows a decisive decrease in enthalpy due to the thermal processing and with enthalpic contributions often related to the structural stability of a protein, it shows that the structure of the α-amylase is denatured. This is not match with the isothermal processing seen in Figure 6-3(a), where the residual activity is 30-40% the initial activity for an $F_{121°C}$ = 12, the ΔH is only 11% the initial from $F_{121°C}$ = 0 to $F_{121°C}$ = 12.

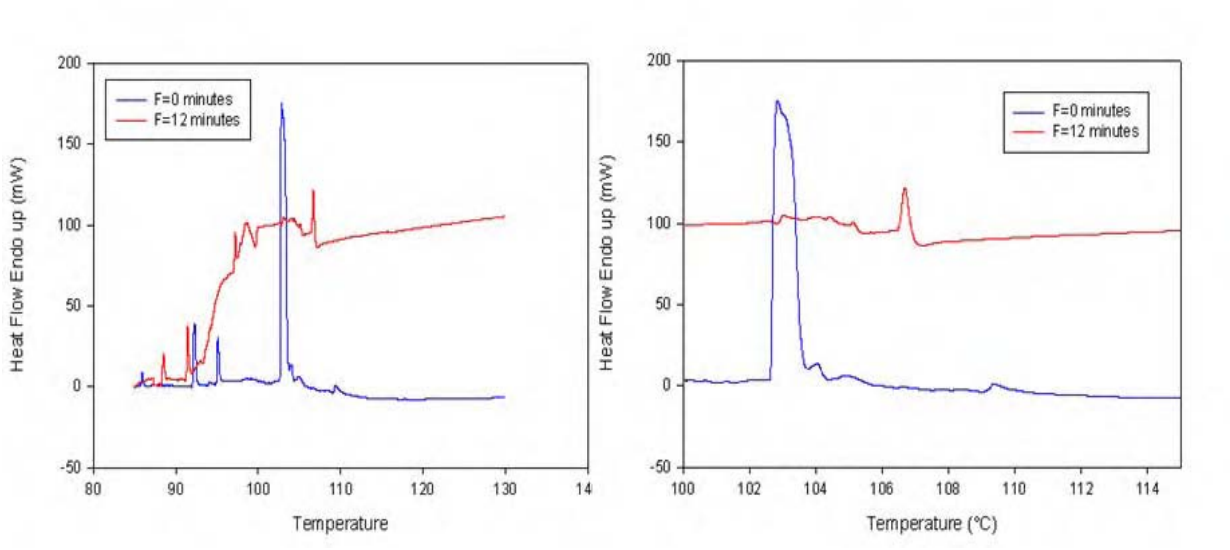

Figure 6-34 DSC thermogram of amylase in sodium acetate buffer with thermal processing from 85-130°C at 1°C/min

The stability of proteins is primarily characterised by their thermodynamic stability, which in the most general case is determined by the difference in the free energy between the folded native state, N, and the irreversibly inactive state, I. The Gibbs free energies were calculated using the Gibbs-Helmholtz equation (equation 6.3) and can be seen in Figure 6-9. The temperature dependence of ΔG allows deeper insights into the mechanisms of how thermostability is achieved. The plot in Figure 6-9 is a skewed parabola and if extrapolated, theoretically intersects the x-axis twice indicating that unfolding occurs both at high and low temperatures this is due because protein unfolding is known to be accompanied by a non-zero ΔCp, and so the plots are distinctly non-linear. By definition the melting temperatures (T_m) are given as the points where ΔG = 0. A negative ΔG and the α-amylase are thermodynamically favourable to unfold.

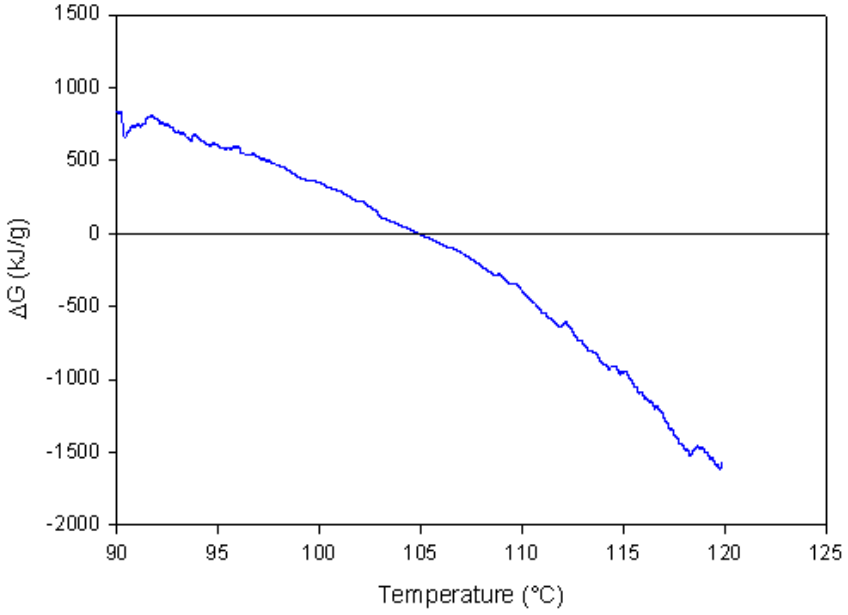

Figure 6-35 Gibbs free energy; Gibbs-Helmholtz plot

6.3.3 Thermal processing effects on structure (CD)

Circular dichroism (CD), illustrates the disruption of secondary structural elements upon increasing the thermal processing of the *Pyrococcus furiosus* α-amylase. The effects of temperature, processing time and *F* value were observed on the structural integrity of the *Pyrococcus furiosus* α-amylase.

CD was first undertaken at room temperature, 22°C (Figure 6-10), to explore if the buffer absorbed light in the 190-320nm wavelength range and hence change in the actual reading given by the scan.

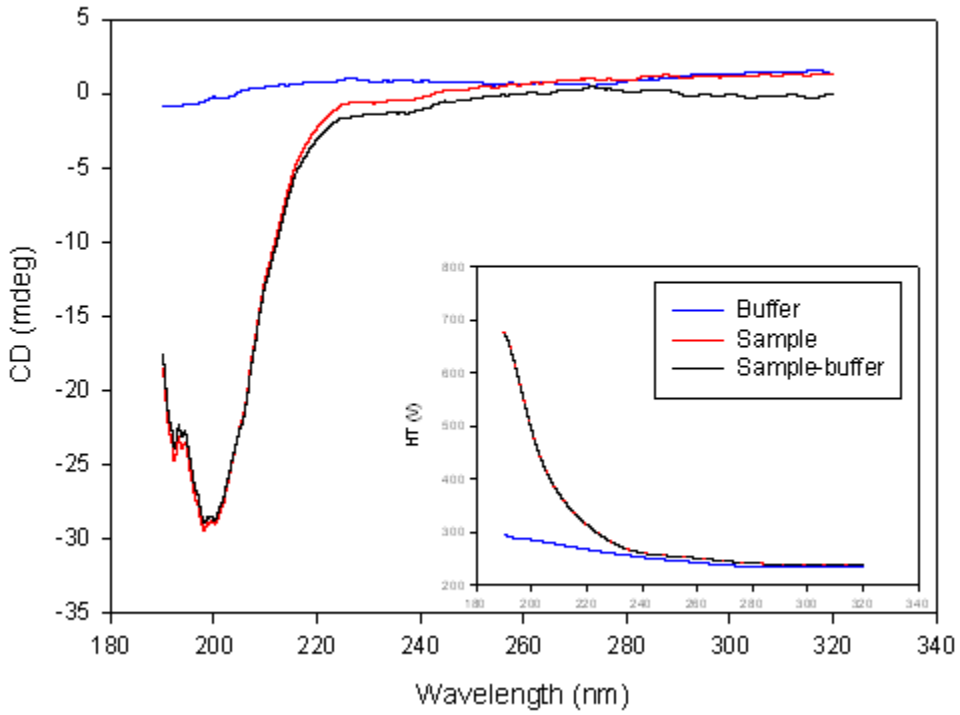

Figure 6-36 Buffer effects on CD for room temperature

From Figure 6-10 it is evident that the buffer does not affect the shape or intensity of the sample. The sample FDP showed a α-helical structure, as characterised in Figure 6-10. The inset is the plot of high tension (HT) voltage verses wavelength. If the HT is under ~700V and does not spike then the data is valid. This is because if the HT voltage is above ~700V then the detector is saturated. The amplitude of the spectrum will then oscillate wildly.

Pyrococcus furiosus amylopullanase supplied by North Carolina State University (NCSU) was also explored as a second hyperthermophilic *Pyrococcus furiosus* enzyme with a α-helical secondary or tertiary structure. The amylopullanase became less rigid and more folded as the temperature increased from 20°C to 90°C (Figure 6-11). Amylopullanase can be compared to the

α-amylase in Figure 6-10 in having the α-helical secondary structure but the rest of the wavelength scan shows decidedly different shape. The amylopullanase in Figure 6-11 could not be processed to 110°C in this case as the buffer evaporated therefore a pressure cell was used to be able to increase the temperature for further plots.

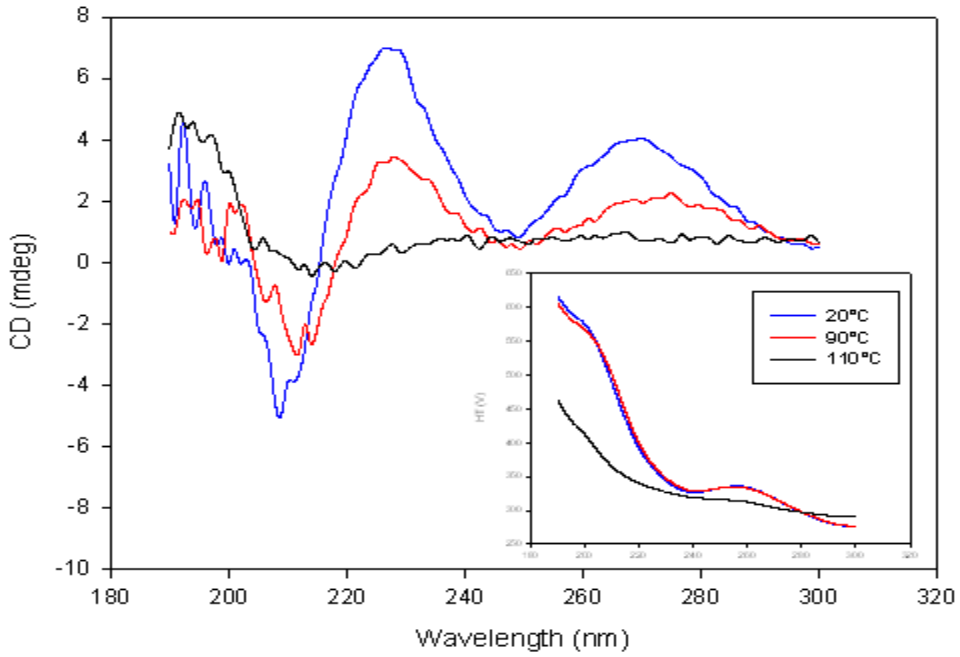

Figure 6-37 Temperature effects on amylopullanase structure

Figure 6-12(a), Figure 6-12(b), and Figure 6-13 show the effects of increasing temperature on the structure of the α-amylase and the α-helical secondary structure in particular from 50°C to 100°C at 5°C intervals.

The denature pattern becomes clearer when the temperature was increased but the wavelength is fixed at 220nm (Figure 6-12(b)). Both plots show an increase in folded structure and a decrease in rigidity as temperature increases as there is a smaller peak. In the main plot the maximum

temperature the equipment could only reach 110°C and the α-amylase still showed structure and so is believed not to be completely denatured. The plot in Figure 6-12b is non-linear and so it is thought that the α-amylase is reaching its denatuation temperature. This can also be seen in Figure 6-12(a) where the distances between the temperature peaks correspond to the temperature dependence assaying results in chapter 4 (Figure 4-6b).

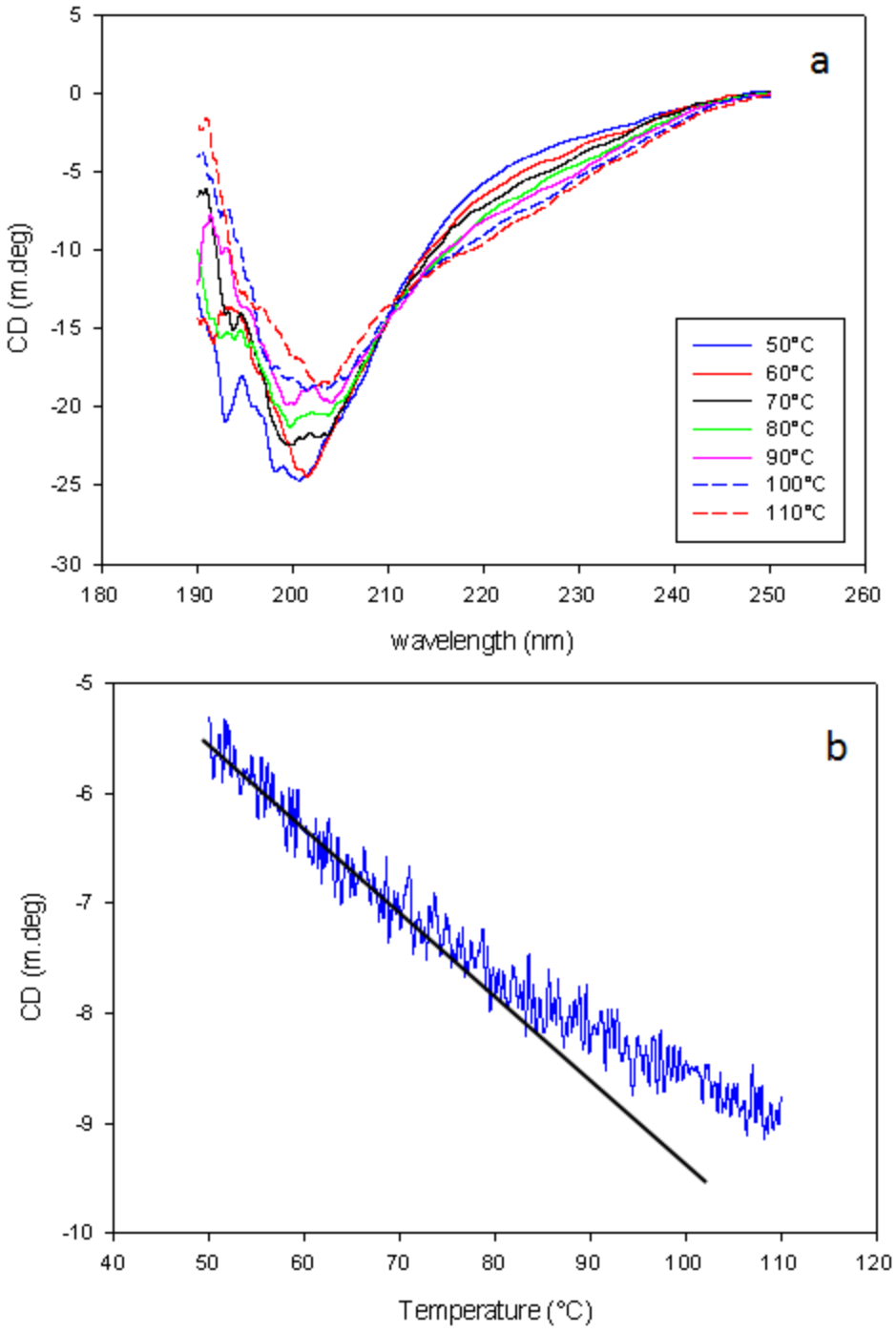

Figure 6-38 Temperature effect on α-amylase structure (a) full wavelength scans (b) at 220nm and a linear trend line for the initial temperatures [—].

Figure 6-13 gives a 3-dimensional representation of Figure 6-12 (a) and Figure 6-12(b). Further investigations either in increased temperature or using excess EDTA to increase denaturation at lower temperatures would be needed to see full denaturation of PFA using CD techniques.

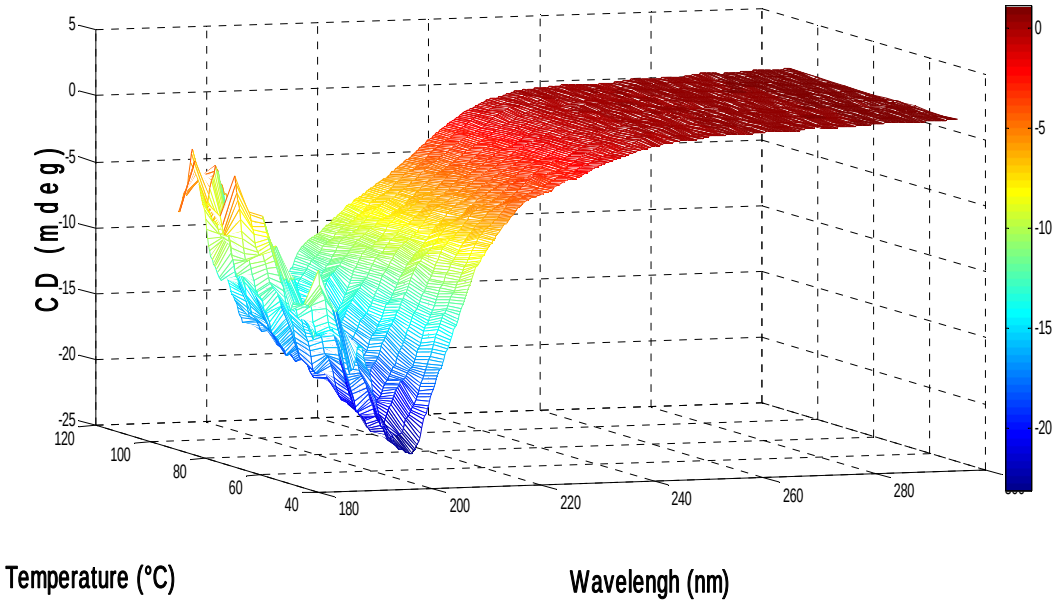

Figure 6-39 3-dimensional CD plot examining temperature effects on α-amylase structure

The effect of thermal processing was investigated by holding the α-amylase solution isothermally at 105°C for up to 25 minutes (Figure 6-14). The processing time-temperature profile only gave an *F* value of 0.6 minutes (36 seconds), giving no real change in the peak intensity which as Figure 6-14 and Figure 6-3(a) and chapter 4 shows, the thermal processing applied does not affect significantly the denaturation of the α-amylase.

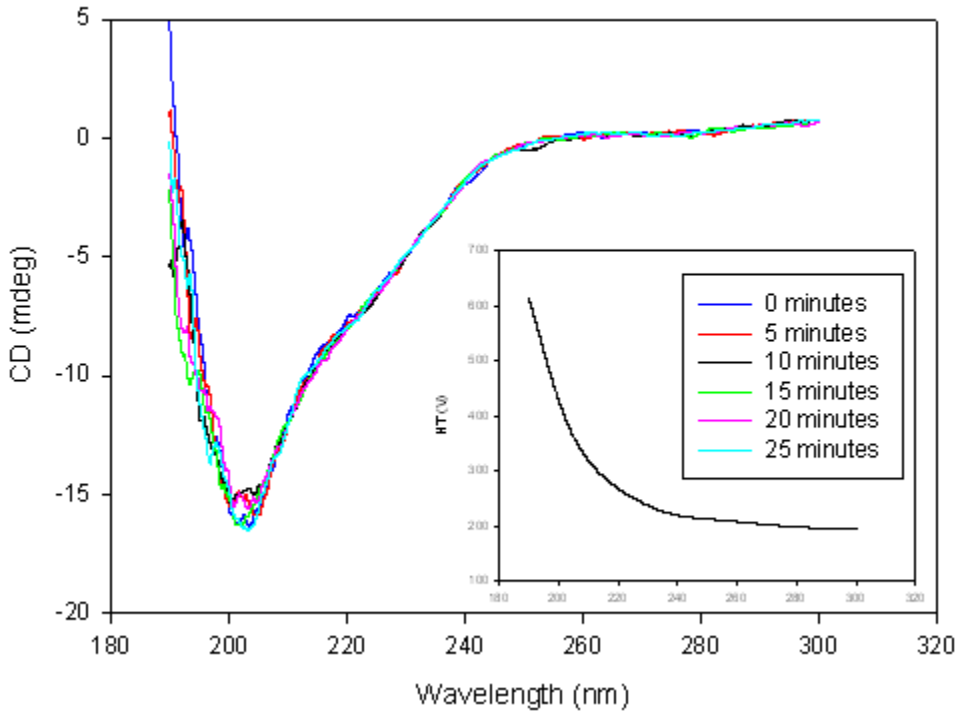

Figure 6-40 The effect of different hold times at 105°C on the CD spectrum of a-amylase, showing effects on structure

Figure 6-15 shows experiments in which the CD spectrum of α-amylase which was previously isothermally processed at 121°C and then at the temperature where the α-helix has previously been seen as structured, 90°C (Figure 6-12(a)), processed through circular dichroism. The intensity of the CD spectrum decreases implying the α-helical structure and folded state decreases considerably as the *F* value was increased to a high level (30 minutes at 121°C).

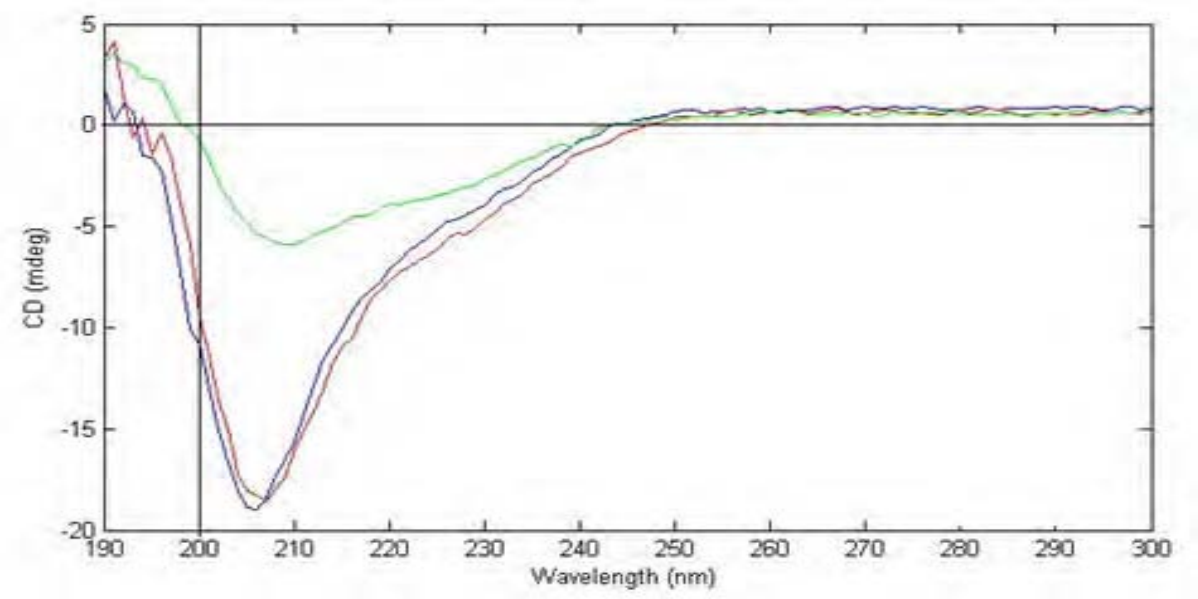

Figure 6-41 CD scan of thermal processing effects on α-amylase secondary structure for; 0 minutes [—], 3 minutes [—] and 30 minutes [—] processing isothermally at 121°C

6.3.4 Thermal processing effects on structure using FT-IR

In the mid-infrared range there are 9 absorptions associated with peptide bonds shown in Table 6-2.

Table 6-11 Absorbances associated with peptide bonds

Band	Origin	Frequency (cm^{-1})
A	NH stretch	3300
B	NH stretch	3100
1	C=O stretch, CN stretch, CCH deformation	1650
2	NH in plane bend, CN stretch	1550
3	CN stretch, NH in plane bend	1300
4	C=O deformation, CC stretch	625
5	NH out of plane bend, CN torsion	725
6	C=O out of plane bend, CN torsion	600
7	CN torsion	200

Figure 6-16 shows the regions in the mid-infrared range for *Pyrococcus furiosus* α-amylase for 3 different amounts of thermal processing. The amide 1 band (1600-1690cm^{-1}) is generally used for the structural analysis of proteins, and consists of two main contributions, a C=O stretch accounting for 80% of the absorbance, and C-C-N deformation and C-N stretch making up the other 20% absorption. The data collected was normalised against a water standard. Figure 6-16 implies that as the α-amylase was initially processed and the thermal processing increases the concentration increases as the buffer (water and sulphate) is evaporated and the peaks become shallower in the region of 3200-3400cm^{-1}.

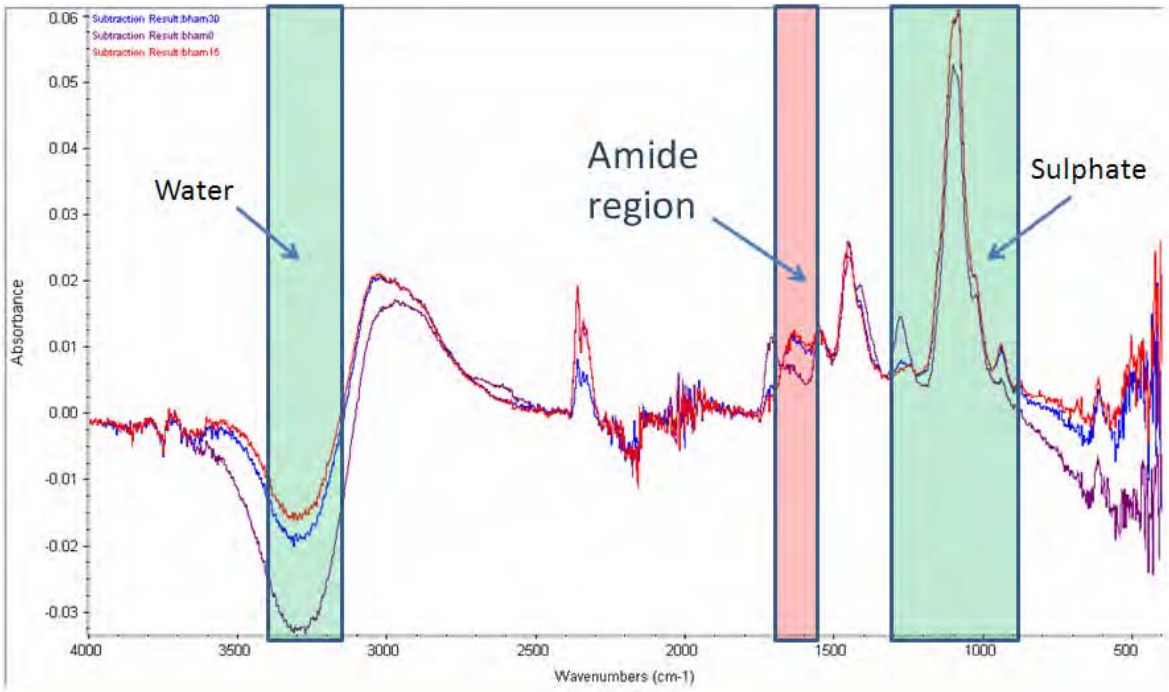

Figure 6-42 FT-IR mid-infrared range and regions of absorbance for no thermal processing [−], 15 minutes thermal processing [−], and 30 minutes thermal processing [−] at 121°C

Proteins are complex, not structurally homogeneous and contain a variety of secondary and tertiary structure types, therefore the amide 1 region appears as a single, broad, unsymmetrical

band which is a composite of all the overlapping bands (from each type of secondary structure). The secondary structure types are shown in Figure 6-17 and how they appear in the FT-IR plots. The secondary structure types described by Arrondo *et al.*, (1993) and their wavelengths are shown in Table 6-3.

Table 6-12 Secondary structure types

Secondary Structure Type	Frequency (cm^{-1})
α-helix	1648-1655
random coil	1640-1645
β-sheet	1630-1636
aggregation	1612-1620

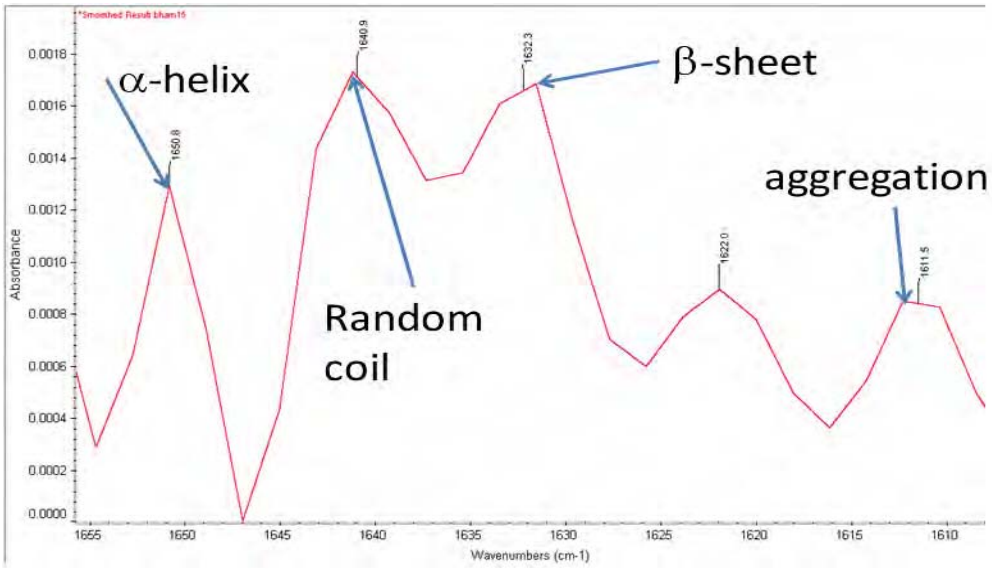

Figure 6-43 Amide 1 region and structural absorbencies of α-amylase after 15 minutes isothermal processing at 121°C and hence not completely denatured

The moderately thermophilic *Bacillus licheniformis* α-amylase was initially used as a standard because apart from being moderately thermophilic, *Bacillus licheniformis* α-amylase is also used

in pasteurisation TTIs. Figure 6-18 shows the FT-IR scan of BLA in the mid-infrared region. Figure 6-18 shows a decrease in the signal in the amide region suggesting as the amount of thermal processing is increased gradually from $P_{85°C}$ = 0 up to $P_{85°C}$ = 60 minutes then the absorbance of the FT-IR plot decreases over this processing range. This FT-IR scan of the thermophilic α-amylase from *Bacillus licheniformis* is comparable to that of the α-amylase from the hyperthermophilic *Pyrococcus furiosus* in Figure 6-16 where there is a water region and an amide region showing secondary structure. In both of these plots there is a region/ peak around the frequency of 2350cm^{-1} which is unaccounted for.

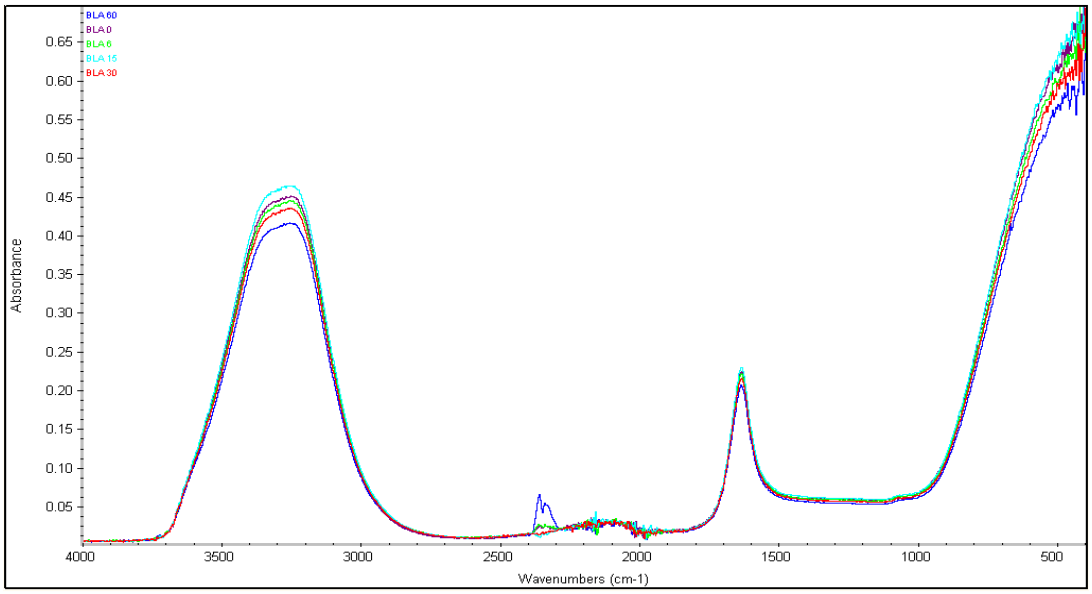

Figure 6-44 Thermal Processing on BLA standard which has been processed for 0 [−], 6 [−], 15 [−], 30 [−] and 60 [−] minutes at 85°C

Figure 6-19 shows a larger mid-infrared region (1000-1800cm^{-1}) of the spectrum showing the effects of thermal processing outside of just the amide 1 region for BLA. With no heat treatment there is a peak at ~1750cm^{-1} which is not present after 15 and 30 minutes of isothermal treatment

at 85°C respectively. This is typically the absorbance range for lipids, and is seen to disappear as the thermal treatment was increased.

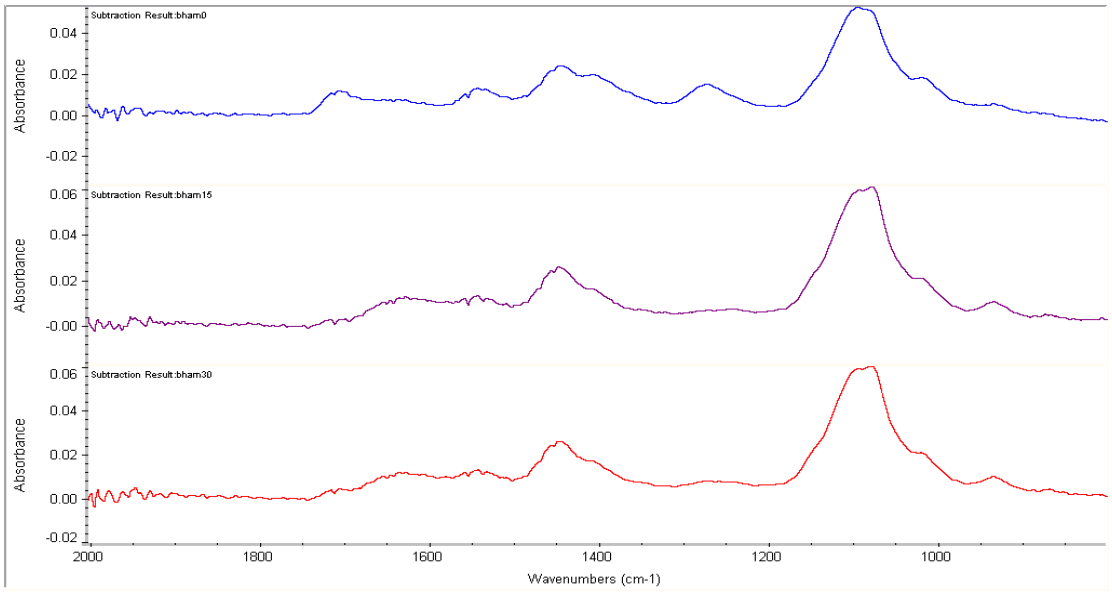

Figure 6-45 Effects of thermal processing of BLA on the mid-infrared region for 0 minutes [—], 15 minutes [—] and 30 minutes [—] thermal processing at 85°C

Figure 6-20 and Figure 6-21 compare the effect of unfolding of the *Pyrococcus furiosus* α-amylase through thermal processing isothermally at 121°C. Figure 6-20 shows the initial effect of thermal processing, between 0 and 15 minutes at 121°C. With no thermal treatment, the spectrum suggests significant α-helical shape of the *Pyrococcus furiosus* α-amylase, but as thermal denaturation occurs the spectrum, and thus the structure changes significantly. The α-helical structure decreases and the spectrum shows a significant increase in β-sheet structure and more aggregation, suggesting that thermal denaturation unfolds this secondary structure to aggregation.

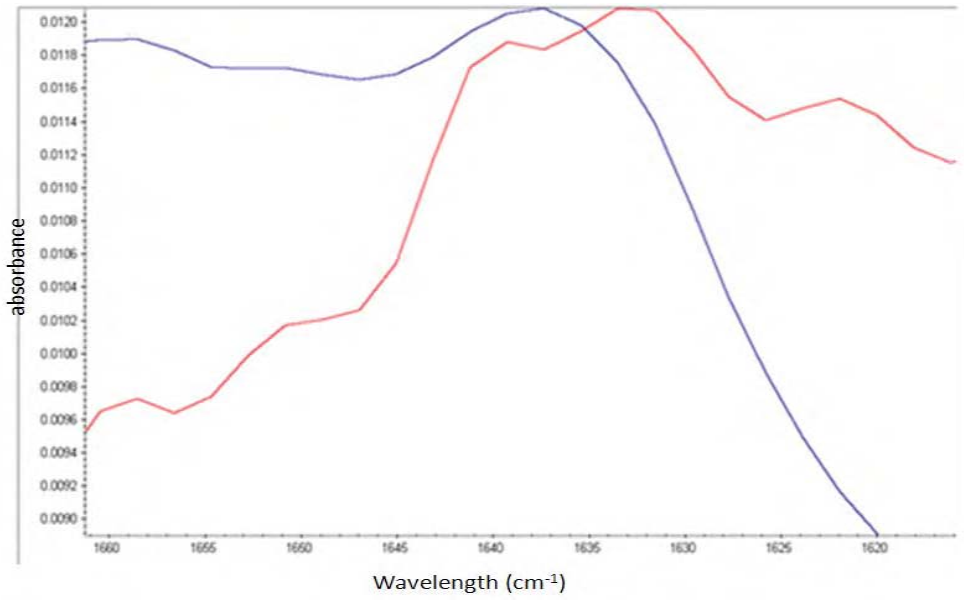

Figure 6-46 FT-IR scan with thermal processing effects on amide 1 region; no thermal processing [—]; 15minutes at 121°C [—]

Figure 6-21 suggests that this unfolding continues in this manner; with the α-helical structure unfolding through a β-sheet structure until unfolding and aggregation has occurred. In Figure 6-21, after 30minutes thermal processing there is much more β-sheet and aggregation that at 15 minutes processing at 121°C. This suggests that in Figure 6-3(b) the mechanism for unfolding and denaturation is exponential first-order decay, with aggregation making the plots seem biphasic.

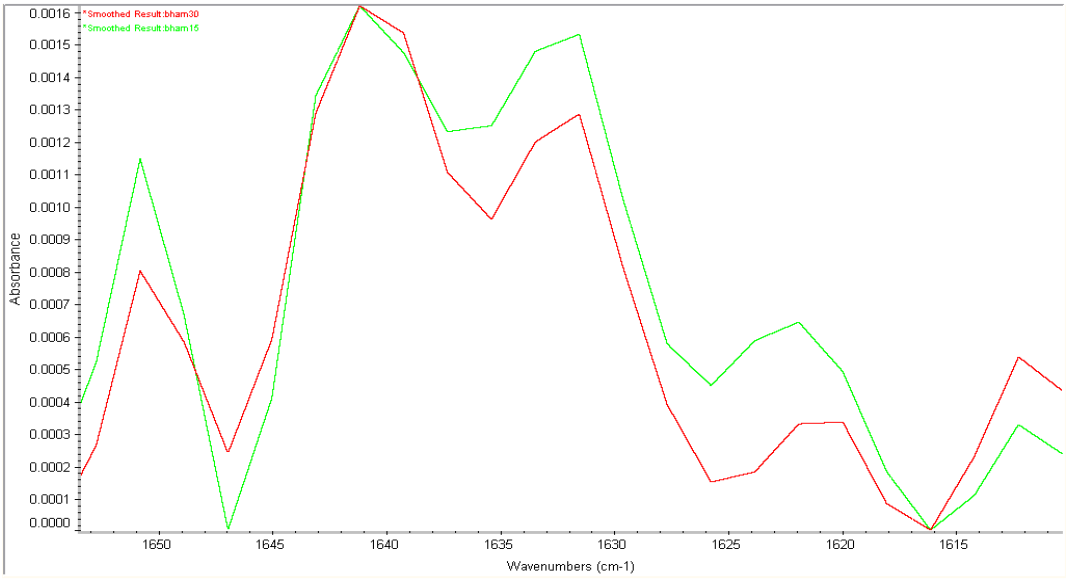

Figure 6-47 The effects of significant thermal processing on the amide 1 region of α-amylase: 15 minutes at 121°C [–], and 30 minutes processing isothermally at 121°C [–]

6.4 Conclusion

In recent years an increasing number of studies on thermophilic and hyperthermophilic proteins aiming to elucidate determinants of protein thermostability have yielded valuable insights about the relevant mechanisms. In particular, comparison of homologous enzymes with different thermostabilities (isolated from psychrophilic, mesophilic, thermophilic and hyperthermophilic organisms) offers a unique opportunity to determine the strategies of thermal adaptation. In this respect, the medium-sized amylolytic enzyme α-amylase is a well-established representative. Various studies on *a*-amylases with very different thermostabilities (melting temperature T_m = 40 –110°C) report structural and dynamical features as well as thermodynamical properties which are supposed to play key roles in thermal adaptation.

Native and functional protein structures are held together by a subtle balance of non-covalent forces or interactions, such as H bonds, ion pairs, and hydrophobic and van der Waals interactions. At elevated temperatures these non-covalent interactions are too weak or become counterbalanced by other interactions, and proteins start to unfold. Protein unfolding can be observed by many different techniques, including differential scanning calorimetry (DSC), fluorescence, circular dichroism (CD) and Fourier transform infrared spectroscopy (FTIR).

A kinetic and mechanistic study of the thermal denaturation of *Pyrococcus furiosus* α-amylase is presented. DSC, CD and FT-IR are shown, along with kinetic data. The Arrhenius plot gave a straight line correlation with activation energy of 316 kJ/mol at 121°C. The FT-IR data indicated that the mechanism of unfolding is to aggregate after 15 minutes thermal processing at 121°C and is supported by the kinetic data (Figure 6-3b) which shows a biphasic distribution after approximately 15 minutes. This suggests that the denaturation is first-order decay at the high temperatures encountered in sterilisation. The biphasic nature of the denaturation of α-amylase might also be described by the processes of aggregation as the protein denatures. This shows that the mechanism of denaturation is a special case of the Lumry-Eyring model (equation 6-1) where $k_2 >> k_1$ and so k_3 as N→I (Eq. 6-4). The rates of inactivation are shown in Table 6-1 for sterilisation temperatures i.e. for 121°C the rate of inactivation N→I is 1.9×10^{-3} s^{-1}. The rate constants were also increased as temperature is raised.

The effect of temperature on denaturation of α-amylase was explored by examining the α-helical content changes during increasing temperature up to the experimental limits of 110°C. This showed that the amylase became less rigid with temperature as shown by the data in Figure 6-12,

and the FT-IR and CD spectroscopy data concurrently suggested a decrease in α-helical structure as the isothermal processing time at 121°C increased.

Such observations were re-enforced by the melting temperature (T_m) data of the α-amylase which was found to be in the region of 106-107°C. Above this temperature the protein becomes denatured in to an irreversible inactive state (Figure 6-6b), but below this temperature the protein is in a reversible intermediate stage. This has significant implications for industrial use of PFA in an industrial context as it suggests there is a temperature above which irreversible thermal inactivation of the α-amylase occurs. Such data strengthens the use of PFA for sterilisation data as the correlation between process time and residual enzyme activity will not include material reformed via the k_{-1} kinetic route. Knowledge of how the *Pyrococcus furiosus* α-amylase denatures may be useful to manipulating the unfolding kinetics for use in many industrial applications, such as different applications of TTIs. Conditions of incubation reinforce findings as any change to primary or secondary structures will almost certainly cause denaturation due to temperature.

Chapter 7

Conclusions and Future Work

This thesis describes an experimental study in using a native hyperthermophilic enzyme as a candidate sterilisation time-temperature integrator for use in thermal treatment of foods. The work has been focused on the following objectives.

- Produce a reliable and consistent supply of native extracellular *Pyrococcus furiosus* α-amylase (PF0478);
- Produce an industrially relevant prototype assay for rapid quantifying the activity of the highly thermostable α-amylase;
- Validation of statistical reliabilities of the candidate sterilisation TTIs and application of the TTI techniques in pilot scale trials;
- Determine the kinetics and mechanism of unfolding on *Pyrococcus furiosus* α-amylase due to thermal processing.

7.1 Production of *Pyrococcus furiosus* α-amylase

The ability to cultivate *Pyrococcus furiosus* and purify the extracellular α-amylase was reviewed in chapter 3. Growth curves and activity tests showed that α-amylase was produced consistently through the growth phase, and to maximise the yield of α-amylase the maximum growth rate

needed to be achieved. It was seen that 80% of α-amylase activity was found from the extracellular fraction, PF0478. In batch cultures, in the presence of elemental sulphur (S°) the growth of *Pyrococcus furiosus* was greatly increased. In continuous fermentation a high agitator speed removed the inhibitory hydrogen product, as growth increased with increased agitation speed. Through purification a highly purified extracellular α-amylase was produced with enough activity to be used within TTIs. Only a short fermentation time was needed to provide enough amylase to produce enough TTIs to enable a large number of experiments.

7.2 Industrially relevant hyperthermostable amylase assay

For the extracellular *Pyrococcus furiosus* α-amylase to be measured accurately a radial enzymatic diffusion assay was developed. The optimal conditions for the assay were found to be; 1% starch plate, 4 hours incubation time, and 70°C incubation temperature and 2.5mg/ml amylase concentration. It was found that the effect of concentration on the halo diameter was a double linear fit, which could then be used to determine the *D* and *z* values of the α-amylase. The assay compared very well with more established methods, but may have better industrial relevance due to its ease of use and measurements, the time it takes for measurements to be taken and the cost of the assay. To reduce the variability that TTIs produce, many TTIs would be used in industry, and with this assay many samples can be run at the same time. Also for use within the food industry the assay has to have no harmful substances which could impact the consumer if there is contamination to foods. The model associated with the assay correlates well with the experimental data.

7.3 Validation of sterilisation TTIs and trials

The ability of TTIs to evaluate the thermal efficiency of thermal treatment was investigated using a range of time-temperature profiles. The study shows that there is a good correlation between the responses of TTIs and thermocouples for a range of non-isothermal processes. It was found that the variability of the responses of the TTIs increase when the *F* value is increased.

In practice the accuracy of TTIs are constrained by

- The lower limit of *F*, where there is sufficient thermal lag between the TTIs and the process, so that the TTI value is not correct.
- The higher limit of *F*, where the value of the enzyme activity is so low that it is not sensitive enough to show a change in *F*.

In between the constraints is the operational window in which measurements can be taken with accuracy, which is approximately 3 to 25 minutes at 121°C for the *Pyrococcus furiosus* α-amylase. The TTIs were found a good substitute for measurements of sterilisation thermal efficiency when data-loggers and thermocouples are not practical for use.

7.4 Effects of thermal processing on *Pyrococcus furiosus* α-amylase denaturation

It was found that the melting temperature (T_m) of *Pyrococcus furiosus* α-amylase is in the region of 105°C to 107°C. This is important to thermal processes as it can be seen that using the Lumry-Eyring model, that up to this temperature the denaturation is reversible, so the *F* value calculations are not quite accurate. The thermal denaturation showed a shift from an α-helical

structure, through β-sheet structure to aggregation in a first-order exponential decay model. Through circular dichroism experimentation, the effects of temperature were explored on the *Pyrococcus furiosus* α-amylase structure and found that at room temperature the protein is unfolded but increasing the temperature to its optimal temperature (T_{opt}) the enzyme shows an increased structure which is characteristic to hyperthermophilic organisms.

7.5 Future work

Based on the findings from this work, some further work could be undertaken in the following areas:

- The growth of the native hyperthermophilic organism *Pyrococcus furiosus* was investigated to produce the α-amylase PF0478. For sterilisation processes other than in the food industry, recombinant forms of this enzyme, in yeasts or *E.coli*, could be explored for high production of the enzyme. Purification would have to include a pasteurisation step to denature any host cells and host enzymes associated with growth. Also different hyperthermophilic enzymes can be explored, looking at different *D* and *z* values for different target organisms in sterilisation, or for the same *z* value and target organism but changing the operational window depending on the *F* value needed.

- The variability of the TTI itself was investigated in this work under controlled conditions by the author. In industry, it is most probable that the analysis of TTIs would be performed by several people, which introduces uncertainty. It would be interesting to

understand the variability in the results obtained from the analysis performed by various individuals.

- Due to the high temperatures involved in sterilisation it was difficult to create and measure various time-temperature profiles. If it is possible using a specially built Peltier system or another temperature profiling system, such as a PCR then these profiles could be created. It would be interesting to see the effects of heating rates, cooling rates and non-isothermal profiles on the enzymatic TTIs measurements where the physical mathematical model using thermocouple data shows the *F* values as the same value.

- An investigation of using *Pyrococcus furiosus* α-amylase TTIs in a full scale industrial sterilisation trial would be needed before these sterilisation TTIs could be used with any certainty in industry. This trial could be continued straight from the work shown in this thesis. This would include using a statistically viable amount of free TTIs in a range of cans (centre and edge of the sterilisation retort) and using a variety of foods in the cans, including pure liquids and liquid/particulate systems in the cans, symbolising different varieties for instance of soups.

- The circular dichroism data was impaired by the constraints of the equipment involved. The circular dichroism equipment temperature only went up to 110°C and so nowhere near the 121°C of sterilisation temperatures. If this could be rectified it would be increasingly interesting for not just sterilisation TTIs and *Pyrococcus furiosus* α-amylase but for use on hyperthermophilic organisms and proteins in general.

References

Adams, M., Holden, J., Menon, A., Schut, G., Grunden, A., Hou, C.(2001). Key role for sulfur in peptide metabolism and in regulation of three hydrogenases in the hyperthermophilic archaeon *Pyrococcus furiosus*. *Journal of Bacteriology* , **183**, 716-724.

Adams, M. W. W. and Kelly, R. M. (1998) Finding and using hyperthermophilic enzymes. *Trends in Biotechnology* **16,** 329-332.

Adams, M.R. and Moss, M.O. (2000) *Food microbiology* 2nd Ed, The Royal Society of Chemistry: Cambridge

Adams, J. B. and Langley, F. M. (1998) Nitrophenyl glucoside hydrolysis as a potential time temperature integrator reaction. *Food Chemistry* **62**, 65-68.

Anthon, G., and Barrett, D. (2002). Kinetic parameters for the thermal inactivation of quality-related enzymes in carrots and potatoes. *Journal of Agricultural and Food Chemistry* **81**, 4119-4125.

Antranikian, G. (1990) Physiology and Enzymology of Thermophilic Anaerobic-Bacteria Degrading Starch. *Fems Microbiology Reviews* **75,** 201-218.

Arroyo, G., Sanz, P., & Préstamo, G. (1999). Response to high-pressure, low-temperature treatment in vegetables: determination of survival rates of microbial populations using flow cytometry and detection of peroxidase activity using confocal microscopy. *Journal of Applied Microbiology* **86**, 544.

Babson, A., Tenney, S., & Megraw, R. (1970). New amylase substrate and assay procedure. *American Association of Clinical Chemistry* **16**, 30-43.

Ball, C. and Olson, F. (1957) *Sterilization in food technology*. Mc Graw Hill: New York.

Baross, J. A. and Holden, J. F. (1996) *Overview of hyperthermophiles and their heat-shock proteins*.

Bauer, M., Driskill, L., Callen, W., M, S., Mathur, E., & Kelly, R. (1999). An endoglucanase, EglA, from the hyperthermophilic archaeon Pyrococcus furiosus hydrolizes b-1,4 bondsin mixed linkages. *Journal of Bacteriology* , ***181,*** 284-290.

Bergmeyer, H. U., Grassl, M., and Walter, H. E. (1983) *Methods of Enzymatic Analysis*. Verlag Chemie: Deerfield Beach, Florida.

Bernfeld, P. (1955). Amylase α and β. *Methods in Enzymology* , ***1,*** 149-154.

Bigelow, W. D. (1921). The logarithmic nature of thermal death time curves. *Journal of Infectious Diseases* **29**, 528-536.

Bird, R., & Hopkins, R. (1954). The action of some α-amylases on amylose. *Biochemical Journal* , ***56,*** 86-99.

Bock, A., Glasemacher, J., Schmidt, R., & Schonheit, P. (1999). Purification and characterisation of two extremely thermostable enzymes, phosphate acetyltransferase and acetate kinase, from the hyperthermophilic eubacterium Thermtoga maritima. *Journal of Bacteriology* , **181**, 1861-1867.

Bonchosmolovskaya, E. A. and Stetter, K. O. (1991) Interspecies Hydrogen Transfer in Cocultures of Thermophilic Archaea. *Systematic and Applied Microbiology* **14,** 205-208.

Brock, T. (1978) *Thermophilic Micro-organisms and Life at High Temperatures*. Springer-Verlag: New York.

Brown, S. H., Costantino, H. R., and Kelly, R. M. (1990) Characterization of Amylolytic Enzyme-Activities Associated with the Hyperthermophilic Archaebacterium Pyrococcus-Furiosus. *Applied and Environmental Microbiology* **56,** 1985-1991.

Brown, S. H. and Kelly, R. M. (1989) Cultivation Techniques for Hyperthermophilic Archaebacteria - Continuous Culture of Pyrococcus-Furiosus at Temperatures Near 100-Degrees-C. *Applied and Environmental Microbiology* **55,** 2086-2088.

Bull, M., Szabo, E., Cole, M., & Stewart, C. (2005). Toward Validation of Process Criteria for High-Pressure Processing of Orange Juice with Predictive Models. *Journal of Food Protection* , **68**, 949-954.

Cavagnero, S., Debe, D., Zhou, Z., Adams, M., & Chan, S. (1998). Kinetic role of electrostatic interations in the unfolding of hyperthermophilic and mesophilic rubredoxins. *Biochemistry* , **37**, 3369-3376.

Claeys, W. L., Van Loey, A. M., and Hendrickx, M. E. (2002). Intrinsic time temperature integrators for heat treatment of milk. *Trends in Food Science & Technology* **13**, 293-311.

Cowan, D. A. (1992) Enzymes from Thermophilic Archaebacteria - Current and Future Applications in Biotechnology. *Biochemical Society Symposium* 149-169.

Daniel, R. (1996). The upper limits of enzyme thermal stability. *Enzyme and Microbial Technology* , **19,** 74-79.

Daniel, R., & Danson, M. (2001). Assaying activity and assessing thermostability of hyperthermophilic enzymes. *Methods in Enzymology* , **334**, 283-293.

Danson, M., & Hough, D. (1998). Structure, function and stability of enzymes from the Archaea. *Trends in Microbiology* , **6,** 307-314.

Decordt, S., Avila, I., Hendrickx, M., and Tobback, P. (1994) DSC and Protein-Based Time-Temperature Integrators - Case-Study of Alpha-Amylase Stabilized by Polyols And/Or Sugar. *Biotechnology and Bioengineering* **44,** 859-865.

Decordt, S., Hendrickx, M., Maesmans, G., and Tobback, P. (1992) Immobilized Alpha-Amylase from Bacillus-Licheniformis - A Potential Enzymatic Time Temperature Integrator for Thermal-Processing. *International Journal of Food Science and Technology* **27,** 661-673.

De Haan, S. W. H., Roodenburg, B., Morren, J., and Prins, H. Technology for preservation of food with pulsed electric fields (PEF). IEEE AFRICON Conference 2, 791-796. (2002).

Devlieghere, F., Vermeiren, L., and Debevere, J. New preservation technologies: Possibilities and limitations (2004) *International Dairy Journal* **14**, 273-285

Dong, G., Vieille, C., Sachenko, A., & Zeikus, J. (1997). Cloning, sequencing, and expression of the gene encoding extracellular a-amylase from Pyrococcus furiosus and biochemical characterisation of the recombinant enzyme. *Applied Environmental Microbiology* , **63**, 3569-3576.

Esty, J. R. and Meyer, K. F. (1922). The heat resistance of the spores of B. botulinus and allied anaerobes. Journal of Infectious Diseases **34**, 650

Fernandez, I., Diaz, M., Martinez, T., & Moyano, F. (2001). A quick method for the assessment of activity and inhibition of fish amylases. *Aquaculture Nutrition* , **7**, 19-23.

FDA. (2005). *Food and Drugs. Chapter 1 - Food and drug administration.* Department of Health and Human Services.

Fiala, G. and Stetter, K. O. (1986) Pyrococcus-Furiosus Sp-Nov Represents A Novel Genus of Marine Heterotrophic Archaebacteria Growing Optimally at 100-Degrees C. *Archives of Microbiology* **145,** 56-61.

Fischer, F., Zillig, W., Stetter, K. O., and Schreiber, G. (1983) Chemolithoautotrophic Metabolism of Anaerobic Extremely Thermophilic Archaebacteria. *Nature* **301,** 511-513.

Fitter, J. (2005). Structual and dynamical features contributing to thermostability in a-amylases. *CMLS* , **62,** 1925-1937.

Frazier, W. C. and Westhoff, D. C. (1978) *Food microbiology*. McGraw-Hill: New York.

Fryer, P. J., Pyle, D. L., and Rielly, C. D. (1997) *Chemical engineering for the food industry*. Blackie Academic & Professional: London.

Fu, B., & Labuza, T. (1993). *Shelf-life prediction: theory and application.* New York: Butterworth-Heinemann.

Fuld, G., Proctor, B., & Goldblith, S. (1957). Some microbiological aspects of resistance sterilization. *International Journal of Applied Radiation Isotopes* .

Gaze, J., Boyd, A., & Shaw, H. (2006). Heat inactivation of Listeria monocytogenes Scott A on potato surfaces. *Journal of Food Engineering* , **76,** 27-31.

Gianfreda, L., Marruci, G., Grizzuti, N., & Greco, G. (1984). Acid phosphatase deactivation by a series mechanism. *Biotechnology Bioengineering* , **26,** 518-527.

Goff, H. G. (1999) Food Preservation. In: *Wiley Encyclopaedia of Food Science and Technology*, pp. 953-959. Ed F. J. Francis. John Wiley & Sons: New York.

Griffiths, M., Phillips, J., & Muir, D. (1987). Effect of low-temperature storage on the bacteriological quality of raw milk. *Food Microbiology* , **4**, 285-291.

Grinberg, V., Dubovik, A., Kuznetsov, D., Grinberg, N., Grosberg, A., & Tanaka, T. (2000). Studies of the Thermal Volume Transition of Poly(N-isopropylacrylamide) Hydrogels by High-Sensitivity Differential Scanning Microcalorimetry. 2. Thermodynamic Functions. *Macromolecules* , **33,** 8685–8692.

Guiavarc'h, Y., Sila, D., Duvetter, T., Van Loey, A., and Hendrickx, M. (2003) Influence of sugars and polyols on the thermal stability of purified tomato and cucumber pectinmethylesterases: a basis for TTI development. *Enzyme and Microbial Technology* **33**, 544-555.

Guiavarc'h, Y. P., Van Loey, A. M., Zuber F.T., and Hendrickx, M. E. (2004a) *Bacillus licheniformis* α-amylase immobilized on glass beads and equilibrated at low moisture content: potentials as a time temperature integrators for sterilisation processes. *IFSET* **5**, 317-325.

Guiavarc'h, Y. P., Van Loey, A. M., Zuber F.T., and Hendrickx, M. E. (2004b) Development Characterization and use of a high-performance enzymatic time temperature integrator for control of sterilization process impacts. *Biotechnology and Bioengineering* **88**, 15-25.

Guiavarc'h, Y. P., Van Loey, A. M., and Hendrickx, M. E. (2005a) Extended study on the influence of z-value(s) of single and multicomponent Time Temperature Integrators on the accuracy of quantitative thermal process assessment. *Journal of Food Protection* **68**, 384-395.

Haentjens, T., Van Loey, A. M., Hendrickx, M. E., and Tobback, P. (1998) The use of α-Amylase at reduced water content to develop time temperature integrators for sterilization processes. *lebensm -Wiss u -Techno* **31**, 467-472.

Health, D. o. (1994). *Guidelines for the safe production of heat preserved foods.* Norwich, England: Her Majesty's Stationary Office.

Heinz. (n.d.). Retrieved March 1, 2009, from www.heinzsoup.co.uk

Hendrickx, M. E., Weng, Z., Maesmans, G., and Tobback, P. (1992) Validation of time temperature integrator for thermal processing of food under pasteurisation conditions. *International Journal of Food Science and Technology* **27**, 21-31.

Hendrickx, M., Maesmans, G., Decordt, S., Noronha, J., Van Loey, A., and Willockx, F. (1993) *Minimal Processing of Foods and Process Optimization.* CRC Press.

Hendrickx, M. E., Maesmans, G., De Cordt, S., Noronha, J., Van Loey, A. M., and Tobback, P. (1995) Evaluation of the integrated time temperature effect in thermal processing of foods. *Critical reviews in Food Science and Nutrition* **35**, 231-262.

Hiller, R., Zhou, Z., Adams, M., & Englander, S. (1997). Stability and dynamics in a hyperthermophilic protein with melting temperature close to 200°C. *Proc. Natl. Acad. Sci. USA* , **94**, 11329-11332.

Holdsworth, S. D. (1985) Optimisation of thermal processing -- A review. *J Food Eng* **4**, 89-116.

Holdsworth, S. D. (1993). Rheological models used for the prediction of the flow properties of food products. *Food Bioproducts Processing*, **71**, 139−179.

Holst, O., Manelius, A., Krahe, M., Markl, H., Raven, N., and Sharp, R. (1997) Thermophiles and fermentation technology. *Comparative Biochemistry and Physiology A-Physiology* **118,** 415-422.

Huber, H. and Stetter, K. O. (1998) Hyperthermophiles and their possible potential in biotechnology. *Journal of Biotechnology* **64,** 39-52.

Hugo, W. (1995). A brief history of heat, chemical and radiation preservation and disinfection. *International Biodeteriation and Biodegredation* , 197-217.

Ito, S. (1997) Alkaline cellulases from alkaliphilic Bacillus: Enzymatic properties, genetics, and application to detergents. *Extremophiles* **1,** 61-66.

Jaenicke, R. (1991). Protein stability and molecular adaptation to extreme conditions. *European Journal of Biochemistry* , **202,** 715-728.

Jaenicke, R. (1998) What ultrastable globular proteins teach us about protein stabilization. *Biochemistry-Moscow* **63,** 312-321.

Jaenicke, R., & Bohm, G. (1998). The stability of proteins in extreme environments. *Current Opinions in Structual Biology* , **8**, 738-748.

Jongsma, M., Bakker, P., & Stiekema, W. (1993). Quantitive determination of serine proteinase inhibitor activity using a radial diffusion assay. *Analytical Biochemistry* , **212**, 79-84.

Jorgensen, S., Vorgias, C., & Antranikian, G. (1997). Cloning, sequencing, characterisation, and expression of an extracellular a-amylase from the hyperthermophilic archaeon Pyrococcus furiosus in Escherichia coli and Bacillus subtilis. *Journal of Biological Chemistry* , **272** (26), 16335-16342.

Kang, S., Vieille, C., & Zeikus, J. (2005). Identification of Pyrococcus furiosus amylopullanase catalytic residues. *Applied Genetics and Molecular Biotechnology* , **66,** 408-413.

Kelly, R. M. and Deming, J. W. (1988) Extremely Thermophilic Archaebacteria - Biological and Engineering Considerations. *Biotechnology Progress* **4,** 47-62.

Kengen, S. W. M. and Stams, A. J. M. (1994) Growth and Energy-Conservation in Batch Cultures of Pyrococcus-Furiosus. *Fems Microbiology Letters* **117,** 305-309.

Kerry, J. P., O'Grady, M. N., and Hogan, S. A. (2006) Past, current and potential utilisation of active and intelligent packaging systems for meat and muscle-based products: A review. *Meat Sci* **74**, 113-130.

Koch, R., Spreinat, A., Lemke, K., and Antranikian, G. (1991) Purification and Properties of A Hyperthermoactive Alpha-Amylase from the Archaeobacterium Pyrococcus-Woesei. *Archives of Microbiology* **155,** 572-578.

Koch, R., Zablowski, P., Spreinat, A., and Antranikian, G. (1990) Extremely Thermostable Amylolytic Enzyme from the Archaebacterium Pyrococcus-Furiosus. *Fems Microbiology Letters* **71,** 21-26.

Krahe, M., Antranikian, G., and Markl, H. (1996) Fermentation of extremophilic microorganisms. *Fems Microbiology Reviews* **18,** 271-285.

Kujo, C., & Oshima, T. (1998). Enzymological characteristics of the hyperthermostable NAD-dependant glutamate dehydrogenase from the archaeon Pyrobaculum islandicum and effects of denaturants and organic solvents. *Applied Environmental Microbiology , 64*, 2152-2157.

Labuza, T., & Breene, W. (1989). Applications of "active packaging" for improvement of shelf-life and nutritional quality of fresh and extended shelf-life foods. *Journal of Food Processing and Preservation* , **13**, 1-69.

Laderman, K. A., Davis, B. R., Krutzsch, H. C., Lewis, M. S., Griko, Y. V., Privalov, P. L., and Anfinsen, C. B. (1993) The Purification and Characterization of An Extremely Thermostable Alpha-Amylase from the Hyperthermophilic Archaebacterium Pyrococcus-Furiosus. *Journal of Biological Chemistry* **268,** 24394-24401.

Lado, B. H. and Yousef, A. E. (2002) Alternative food-preservation technologies: Efficacy and mechanisms. *Microbes and Infection* **4**, 433-440.

Lee, H.-S., Shockley, K., Schut, G., Conners, S., Montero, C., Johnson, M., et al. (2006). Transcriptional and Biochemical Analysis of Starch Metabolism in the Hyperthermophilic Archaeon Pyrococcus furiosus. *Journal of Bacteriology* , **188**, 2115-2125.

Leisola, M., Ojamo, H., & Kauppinen, V. (1980). Measurement of alpha-amylase and gluco-amylase activities produced during fermentation. *Enzyme and Microbial Technology* .

Leuschner, C. and Antranikian, G. (1995) Heat-Stable Enzymes from Extremely Thermophilic and Hyperthermophilic Microorganisms. *World Journal of Microbiology & Biotechnology* **11,** 95-114.

Lim, W. J., Park, S. R., Cho, S. J., Kim, M. K., Ryu, S. K., Hong, S. Y., Seo, W. T., Kim, H., and Yun, H. D. (2001) Cloning and characterization of an intracellular isoamylase gene from Pectobacterium chrysanthemi PY35. *Biochemical and Biophysical Research Communications* **287,** 348-354.

Linden, A., Mayans, O., Meyer-Klaucke, W., Antranikian, G., & Wilmanns, M. (2003). Differential regulation of a hyperthermophilic apla-amylase with a novel (Ca, Zn) two metal centre by zinc. *Journal of Biological Chemistry* , **278**, 9875-9884.

Littlechild, J. (2002). Extremely versatile systems. *Trends in Biotechnology*, **20**, 359

Liu, D., Min, B., Angelidaki, I. (2008). Biohydrogen production from household solid waste (HSW) at extreme-thermophilic temperature (70 °C) – Influence of pH and acetate concentration. *International Journal of Hydrogen Energy*, **33**, 6985-6992

Lopez, A. A complete course in canning and related processes. 12th. (1987). Baltimore. The canning trade.

Lumry, R., & Eyring, H. (1954). Conformation changes of proteins. *Jounal of Physical Chemistry* , **58**, 110-120.

Lund, D. B. (1975) Heat Processing. In: *Principles of Food Science: Part 2*, p. 31. Ed O. R. Fennema. Marcel Dekker: New York.

Madigan, M. T. and Marrs, B. L. (1997) Extremophiles. *Scientific American* **276,** 82-87.

Maesmans, G., Hendrickx, M. E., De Cordt, S., Van Loey, A. M., Noronha, J., and Tobback, P. (1994) Combined use of the equivalent point method and a multi-component time temperature integrator in thermal process evaluation: Influence of kinetic characteristics and reference temperature. *Food Control* **5**, 249-256.

Maesmans, G., Hendrickx, M. E., De Cordt, S., and Tobback, P. (2005) Feasibility of the use of a time temperature integrator and a mathematical model to determine fluid to particle heat transfer coefficients. *Food Research International* **27**, 39-51.

Malik, B., Su, W. W., Wald, H. L., Blumentals, I. I., and Kelly, R. M. (1989) Growth and Gas-Production for Hyperthermophilic Archaebacterium, Pyrococcus-Furiosus. *Biotechnology and Bioengineering* **34,** 1050-1057.

Manas, P. and Pagan, R. (2005) Microbial inactivation by new technologies of food preservation. *Journal of Applied Microbiology* **98**, 1387-1399.

Manning, G. and Campbell, L. (1961) Thermostable alpha-amylase of Bacillus Stearothermophilus: Crystallization and Some General Properties. *Journal of Biological Chemistry* **236,** 2952.

Markl, H., Lechner, M., and Gotz, F. (1990) A New Dialysis Fermenter for the Production of High-Concentrations of Extracellular Enzymes. *Journal of Fermentation and Bioengineering* **69,** 244-249.

Marra, F. and Romano, V. (2003) A mathematical model to study the influence of wireless temperature sensor during assessment of canned food sterilization. *J Food Eng* **59**, 245-252.

Mehauden, K., Cox, P.W., Bakalis, S., Simmons, M.J.H., Tucker, G.S., Fryer, P.J., 2007. A novel method to evaluate the applicability of Time Temperature Integrators to different temperature profiles. *IFSET.* **8** (4), 507-514.

Mehauden, K., Bakalis, S., Fryer, P.J., Simmons, M.J.H., 2008. Use of time temperature integrators for determining thermal processing efficiency in agitated vessels. *IFSET*

Melasniemi, H. (1987) Characterization of Alpha-Amylase and Pullulanase Activities of Clostridium-Thermohydrosulfuricum - Evidence for A Novel Thermostable Amylase. *Biochemical Journal* **246,** 193-197.

Miller. (1959). Use of dinitrosalicylic acid reagent for determination of reducing sugar. *Analytical Chemistry* , **31**, 426–428.

Natrajan, N., & Sheldon, B. (2000). Inhibition of Salmonella on Poultry skin using protein--and polysaccharide--based film containing a nisin formulation. *Journal of Food Protection* , **63**, 1268-1272.

Niehaus, F., Bertoldo, C., Kahler, M., and Antranikian, G. (1999) Extremophiles as a source of novel enzymes for industrial application. *Applied Microbiology and Biotechnology* **51,** 711-729.

Nielsen, A., Pusey, M., Fuglsang, C., & Westh, P. (2003). Proposed mechanism for the thermal denaturation of a recombinant Bacillus halmapalus alpha-amylase - the effect of calcium ions. *Biochim. Biophys. Acta* , **1652**, 52-63.

Nipkow, A., Shen, G. J., and Zeikus, J. G. (1989a) Continuous Production of Thermostable Beta-Amylase with Clostridium-Thermosulfurogenes - Effect of Culture Conditions and Metabolite Levels on Enzyme-Synthesis and Activity. *Applied and Environmental Microbiology* **55,** 689-694.

Nury, S., & Meunier, J. (1989). Molecular mechanisms of the irreversible thermal denaturation of guinea-pig liver transglutaminase. *European Journal of Biochemistry* , **180**, 161-166.

Padgett, T., Han, Y., & Dawson, P. (2000). Effect of lauric acid addition on the antimicrobial efficiency and water permability of corn zein films containing nisin. *Journal of Food Processing and Preservation* , **24**, 423-432.

Perevalova, A. A., Svetlichny, V. A., Kublanov, I. V., Chernyh, N. A., Kostrikina, N. A., Tourova, T. P., Kuznetsov, B. B., and Bonch-Osmolovskaya, E. A. (2005) Desulfurococcus fermentans sp nov., a novel hyperthermophilic archaeon from a Kamchatka hot spring, and emended description of the genus Desulfurococcus. *International Journal of Systematic and Evolutionary Microbiology* **55,** 995-999.

Perkins, W., Ashton, D., & Evancho, D. (1975). Influence of the z value of Clostridium botulinum on the accuracy of process calculations. *Journal of food science* , **40**, 1189-1192.

Postec, A., Pignet, P., Cueff-Gauchard, V., Schmitt, A., Querellou, J., and Godfroy, A. (2005) Optimisation of growth conditions for continuous culture of the hyperthermophilic archaeon Thermococcus hydrothermalis and development of sulphur-free defined and minimal media. *Research in Microbiology* **156,** 82-87.

Pysz, M. A., Rinker, K. D., Shockley, K. R., and Kelly, R. M. (2001) *Continuous cultivation of hyperthermophiles*.

Randox (2006). Amylase ethylidene blocked-p-NPG7 manual. [AY1582].

Rao, J. L. U. M. and Satyanarayana, T. (2004) Amelioration in secretion of hyperthermostable and Ca2+-independent alpha-amylase of Geobacillus thermoleovorans by some polyamines and their biosynthesis inhibitor methylglyoxal-bis-guanylhydrazone. *Journal of Applied Microbiology* **97,** 1015-1020.

Raven, N., Ladwa, N., Cossar, D., and Sharp, R. (1992) Continuous Culture of the Hyperthermophilic Archaeum-Asterisk Pyrococcus-Furiosus. *Applied Microbiology and Biotechnology* **38,** 263-267.

Raven, N. D. H. and Sharp, R. J. (1997) Development of defined and minimal media for the growth of the hyperthermophilic archaeon Pyrococcus furiosus Vc1. *Fems Microbiology Letters* **146,** 135-141.

Reyes-De-Corcuera, J. I., Cavalieri, R. P., Powers, J. R., Tang, J., and Kang, D. H. (2005) Enzyme-electropolymer-based amperometric biosensors: An innovative platform for time-temperature integrators. *J Agric Food Chem* **53,** 8866-8873.

Richardson, P. (2001) *Thermal technologies in food processing*. Woodhead publishing limited: Cambridge.

Riesenberg, D. and Guthke, R. (1999) High-cell-density cultivation of microorganisms. *Applied Microbiology and Biotechnology* **51,** 422-430.

Robb, F. (1995). *Archaea: A Laboratory Manual.* Cold Spring Harbor Laboratory Press.

Robyt, J., & Whelan, W. (1968). The β-amylases. In J. Radley, *Starch and its Derivatives* (pp. 477-497). London: Academic Press.

Rooney, M. (1995). *Active food packaging.* London: Blackie Academic and Professional.

Rudiger, A., Ogbonna, J. C., Markl, H., and Antranikian, G. (1992) Effect of Gassing, Agitation, Substrate Supplementation and Dialysis on the Growth of An Extremely Thermophilic Archaeon Pyrococcus-Woesei. *Applied Microbiology and Biotechnology* **37,** 501-504.

Rudiger, A., Jorgensen, P., & Antranikian, G. (1995). Isolation and characterisation of a heat-stable pullanase from the hyperthermophilic archaeon Pyrococcus woeseo after cloning and expression of its gene in Escherichia coli. *AppliedEnvironmental Microbiology* , **61**, 567-575.

Ryan, C. (1967). Quantitative Determination Of Soluble Cellular Proteins By Radial Diffusion in Agar Gels Containing Antibodies. *Analytical Biochemistry* , **19**, 434-440.

Savchenko, A., Vieille, C., and Zeikus, J. G. (2001) *alpha-Amylases and amylopullulanase from Pyrococcus furiosus*.

Schafer, T. and Schonheit, P. (1992) Maltose Fermentation to Acetate, Co2 and H2 in the Anaerobic Hyperthermophilic Archaeon Pyrococcus-Furiosus - Evidence for the Operation of A Novel Sugar Fermentation Pathway. *Archives of Microbiology* **158,** 188-202.

Schicho, R. N., Ma, K., Adams, M. W. W., and Kelly, R. M. (1993) Bioenergetics of Sulfur Reduction in the Hyperthermophilic Archaeon *Pyrococcus-Furiosus*. *Journal of Bacteriology* **175,** 1823-1830.

Schillinger, U., Kaya, M., & Lücke, F.-K. (1991). Behaviour of Listeria monocytogenes in meat and its control by a bacteriocin-producing strain of Lactobacillus sake. *Journal of Applied Microbiology* , **70**, 473-478.

Schiraldi, C., Acone, M., Giuliano, M., Di Lernia, I., Maresca, C., Carteni, M., and De Rosa, M. (2001) Innovative fermentation strategies for the production of extremophilic enzymes. *Extremophiles* **5,** 193-198.

Schiraldi, C. and De Rosa, M. (2002) The production of biocatalysts and biomolecules from extremophiles. *Trends in Biotechnology* **20,** 515-521.

Schiraldi, C., Martino, A., Acone, M., Di Lernia, I., Di Lazzaro, A., Marulli, F., Generoso, M., Carteni, M., and De Rose, M. (2000) Effective production of a thermostable alpha-glucosidase from Sulfolobus solfataricus in Escherichia coli exploiting a microfiltration bioreactor. *Biotechnology and Bioengineering* **70,** 670-676.

Schut, G., Brehm, S., Datta, S., & Adams, M. (2003). Whole-genome DNA microarray analysis of a hyperthermophile and archaeon: *Pyrococcus furiosus* grown on carbohydrates or peptides. *Journal of Bacteriology* , **185**, 3935-3947.

Scott, W. (2003) M.Sc Thesis. Increased viablity of enzymatic-TTIs as a result of optimised hyperthermophilefermenters.

Sharma, R., & Bigelow, C. (1974). A comparison of the denatured states of alpha-lactalbumin and lysozyme. *Journal of Molecular Biology* , **88,** 247-257.

Sharp, R. J. and Munster, M. J. (1987) Biotechnological Implications for Micro-organisms for Extreme Environments. In: *Microbes in Extreme Environments*, pp. 215-296. Eds R. A. Herbert, G. A. Cobb. Academic Press: London.

Shaw, J. F., Lin, F. P., Chen, S. C., and Chen, H. C. (1995) Purification and Properties of An Extracellular Alpha-Amylase from Thermus Sp. *Botanical Bulletin of Academia Sinica* **36,** 195-200.

Snowden, L. J., Blumentals, I. I., and Kelly, R. M. (1992) Regulation of Proteolytic Activity in the Hyperthermophile Pyrococcus-Furiosus. *Applied and Environmental Microbiology* **58,** 1134-1141.

Stewart, E. M. (2004) Food preservation: New alternatives to old technologies. *Food Science and Technology* **18**, 30-32.

Stumbo, C., Murphy, J., & Cochran, J. (1950). Nature of thermal death time curves for PA 3679 and Clostridium botulinum. *Food Technology* .

Tanford, C. (1973). *The Hydrophobic Effect.* New York: Wiley.

Taoukis, P. S. and Labuza, T. P. (1989a) Reliability of time temperature indicators as food quality monitors under non isothermal conditions. *Journal of Food Science* **54**, 789-792.

Taoukis, P. S. and Labuza, T. P. (1989b) Applicability of Time-Temperature Indicators As Shelf-Life Monitors of Food-Products. *Journal of Food Science* **54,** 783-788.

Tucker, G.S., Lambourne, T., Adams, J. B., and Lach, A. (2002) Application of a biochemical time temperature integrator to estimate pasteurisation values in continuous food processes. *IFSET* **3**, 165-174.

Tucker, G., & Wolf, D. (2003). *Time-temperature integrators for food process analysis, modelling and control.* Chipping Campden: CCFRA.

Tucker, G.S., Cronje, M., and Lloyd, E. Evaluation of a time temperature integrator for mild pasteurisation processes. 215. (2005a). Camden & Chorleywood Food Research Association.

Tucker, G.S., Brown, H. M., Fryer, P. J., Cox, P. W., Poole, II, Lee, H. S., et al. (2007). A sterilisation Time–Temperature Integrator based on amylase from the hyperthermophilic organism *Pyrococcus furiosus*. *IFSET* **8**, 63−72.

Tyndall, J. (1897). Further experiments on the deportment and vital persistence of putrifactive and infective organisms from a physical point of view. *Philosophical Transactions of the Royal Society* , **167**, 149-206.

Valentas, K. J., Rotstein, E., and Singh, R. P. (1997) *Handbook of Food Engineering Practice*. CRC Press LLC: Boca Raton.

Van Loey, A. M., Hendrickx, M. E., De Cordt, S., Haentjens, T., and Tobback, P. (1996a) Quantitative evaluation of thermal processes using time temperature integrators. *Trends in Food Science & Technology* **7**, 16-26.

Van Loey, A. M., Hendrickx, M. E., Smout, C., Haentjens, T., and Tobback, P. (1996b) Recent advances in process assessment and optimisation. *Meat Sci* **43**, 81-98.

Van Loey, A. M., Arthawn, A., Hendrickx, M. E., Haentjens, T., and Tobback, P. (1997) The development and use of an α-amylase based time temperature integrators to evaluate in -pack pasteurisation processes. *lebensm -Wiss u -Techno* **30**, 94-100.

Vieille, C. and Zeikus, G. J. (2001) Hyperthermophilic enzymes: Sources, uses, and molecular mechanisms for thermostability. *Microbiology and Molecular Biology Reviews* **65,**

Violet, M., & Meunier, J. (1989). Kinetic study of the irreversible thermal denaturation of *Bacillus licheniformis* alpha-amylase. *Journal of Biochemistry , 263*, 665-670.

Welt, B. A., Sage, D. S., and Berger, K. L. (2003) Performance Specification of Time-temperature Integrators Designed to Protect Against Botulism in Refrigerated Fresh Foods. *Journal of Food Science* **68**, 2-9.

Weng, Z., Hendrickx, M. E., Maesmans, G., and Tobback, P. (1991) Immobilized peroxidase: A potential bioindicateur for evaluation of thermal processes. *Journal of Food Science* **56,** 567-570.

Woese, C. R., Kandler, O., and Wheelis, M. L. (1990) Towards A Natural System of Organisms - Proposal for the Domains Archaea, Bacteria, and Eucarya. *Proceedings of the National Academy of Sciences of the United States of America* **87,** 4576-4579.

Worthington, P., Hoang, V., Perez-Pomares, F., and Blum, P. (2003) Targeted disruption of the alpha-amylase gene in the hyperthermophilic archaeon Sulfolobus solfataficus. *Journal of Bacteriology* **185,** 482-488.

Zhao, H. M. and Arnold, F. H. (1999) Directed evolution converts subtilisin E into a functional equivalent of thermitase. *Protein Engineering* **12,** 47-53.

Appendix A

Matlab codes

A. Calculation diffusion co-efficents

```
function [t x u] = amylase(Deff)


H=20/1000;


global Deff


% H is the maximum radious Deff effective diffusivity
m = 1;
x = linspace(0,H,50);
t = linspace(0,100*60,60);
sol = pdepe(m,@mucus,@mucus_ic,@mucus_bc,x,t);
u = sol(:,:,1);


% figure;
% surf(x,t,u);
% title('Numerical solution computed with 41 mesh points.');
% xlabel('Distance x');
% ylabel('Time t');


conc = zeros(1,length(t));
flux = zeros(1,length(t));
iok = 2:length(t);
for j = iok
```

```
  % At time t(j), compute Du/Dx at x = 0.
  [conc(j),flux(j)] = pdeval(m,x,u(j,:),0);
end
clear global

%  figure;
%  plot(t(iok),conc(iok));

function [c,f,s] = mucus(x,t,u,DuDx)
global Deff
c = 1;
f = Deff*DuDx;
s = 0;

function u0 = mucus_ic(x)
if x<=2/1000
    u0 =5E-6;
else
    u0 = 0;
end

function [pl,ql,pr,qr] = mucus_bc(xl,ul,xr,ur,t)
pl = 0;
ql = 1;
pr = ur;
qr = 0;
```

B. Calculation diffusion fit

```
function ssq=amylase_min(Deff1)


[t x u]=amylase(Deff1);
mytimes=load('mytimes.txt');
rexp=mytimes(:,2);
texp=mytimes(:,1);
c_crit=0.05E-6;


    for k=1:length(mytimes)
        c(k,:) = interp1(t,u,texp(k));
        temp=find(c(k,:)>=c_crit);
        r(k)=interp1(c(k,temp(end):temp(end)+1),...
            x(temp(end):temp(end)+1),c_crit);
        clear temp;
end


ssq=sum(abs(rexp-r'*1000))



end
```

C. Plot halo radius vs. time

```
Deff1=2.42e-8
[t x u]=amylase(Deff1);
mytimes=load('mytimes.txt');
```

```
rexp=mytimes(:,2);

texp=mytimes(:,1);

tplot=linspace(0,texp(end),150);

c_crit=0.05E-6;


%loop to find the hallo radious
    for k=1:length(tplot)
        c(k,:) = interp1(t,u,tplot(k));
        temp=find(c(k,:)>=c_crit);
        r(k)=interp1(c(k,temp(end):temp(end)+1),...
            x(temp(end):temp(end)+1),c_crit);
        clear temp;
    end



    plot(tplot,r*1000);hold on;
    plot(texp,rexp,'o');hold off
```